Progress in Biochemistry and Biotechnology

# ADVANCES IN NANO AND BIOCHEMISTRY

## Environmental and Biomedical Applications

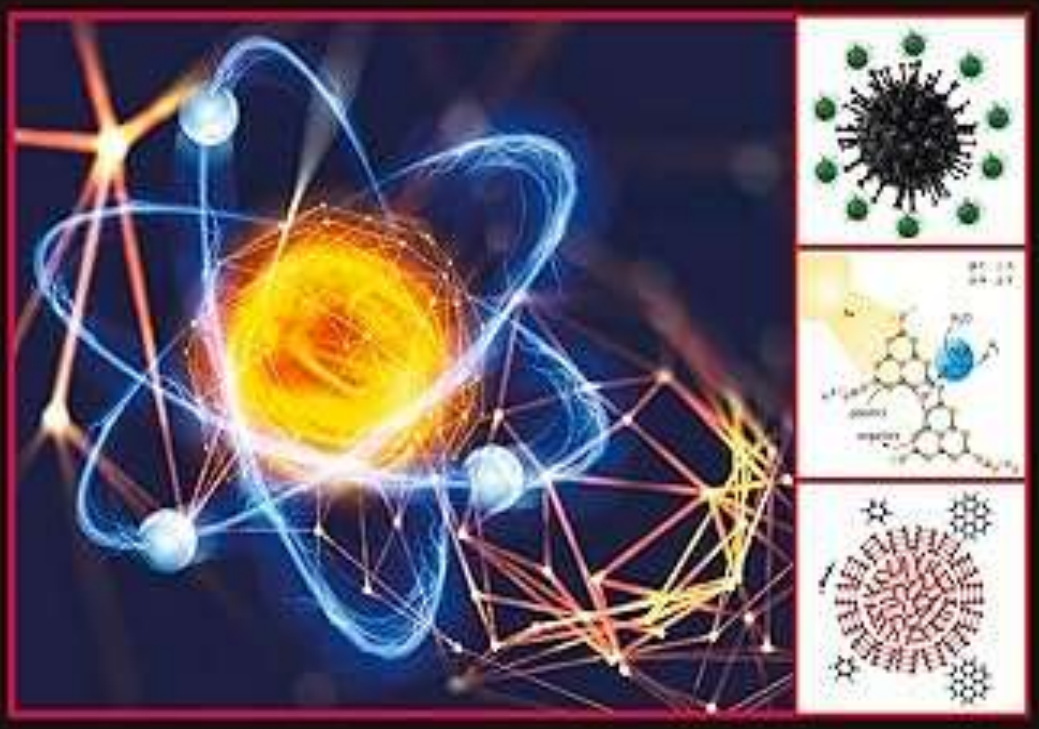

Edited by
**Pranay Pradeep Morajkar**
**Milind Mohan Naik**

No. of pages: 618

Language: English

Edition: 1

Published: May 12, 2023

Imprint: Academic Press

Paperback ISBN: 9780323952538

eBook ISBN: 9780323952545

Table of contents

14.5. Challenges and future prospects

# CHAPTER 12

# Biocompatible green-synthesized nanomaterials for therapeutic applications

**Maithili Majithia, PhD [1] and Delicia A. Barretto, PhD [2]**

[1]School of Biological Sciences and Biotechnology, School of Arts and Sciences, Ahmedabad University, Ahmedabad, Gujarat, India; [2]School of Chemical Sciences, Goa University, Taleigao plateau, Goa, India

## 12.1 Introduction

Nanoparticles (NPs) can be defined as materials or molecules that range in the size from 1 to 100 nm [1]. Nanotechnology has paved its way in various fields with applications ranging from medical to environmental technologies [2]. Although various strategies have been practiced for nanoparticle synthesis including physical and chemical methods, the use of toxic chemicals like organic solvents, stabilizers, reducing agents, and others for synthesis limits its application especially in clinical and biomedical fields owing to their potential hazards like cytotoxicity and carcinogenicity as well as environmental toxicity. To limit harmful chemical processes that could cause environmental damage and, moreover, to ensure that NPs have their utmost usage for human welfare, green synthesis of NPs has been explored and recommended as a possible alternative. This technology overcomes the hazardous nature of the chemically synthesized NPs, and is eco-friendly, biocompatible, and makes use of biological substances in synthesizing NPs [3]. The synthesis of these NPs is also cheap and easy and can be capped with agents of natural origin unlike that of chemical synthesis wherein postsynthetic coating step is a must and thus provides stable nanostructures for medical applications [4].

### 12.1.1 Green synthesis of nanoparticles

Green synthesis refers to an approach of NPs production that uses living entities such as bacteria, fungi, algae, viruses, plants, and animals as a replacement to harmful chemicals to yield NPs [5]. NPs made of metals such as copper, silver, gold, palladium, zinc oxide, magnetite, cobalt, platinum, etc., have been obtained using green synthesis. The process of using green synthesis is advantageous over the other physical and chemical methods by discarding the use of toxic and expensive chemicals, producing biocompatible products, more environmentally friendly and consumption of less energy [6]. The only known current disadvantage of using green synthesized NPs can be the choice of the living system and its associated bio toxic safety risks [7]. Three conditions should be focused on while selecting a biological material for green synthesis of NPs that are green or eco-friendly

*Advances in Nano and Biochemistry*
ISBN 978-0-323-95253-8, https://doi.org/10.1016/B978-0-323-95253-8.00012-7

solvent, a good reducing agent and a less toxic material for stabilization should be used for green synthesized NPs [8].

### 12.1.2 Green synthesis of nanoparticles using plants and microorganisms (bacteria, archaea, fungi, algae)

Certain microorganisms and plants have evolved to survive in heavy metal contamination areas. These properties of microorganisms have gained significance in NPs synthesis using biological sources. Microorganisms can detoxify toxic heavy metals by altering chemical nature of these toxic metals [3]. Microbes are used for their enzymes and other biomolecules, while plants have phytochemicals such as polyphenols that can find their use in green synthesis. Different microbial forms present different mechanisms for green synthesis of NPs. In a basic mechanism, metallic ions are adsorbed on the microbial cell surface or are absorbed inside the cell. Later these metallic ions are bioreduced into metal NPs mainly by certain enzymes of the microbial cell [9]. Enzymatic reactions, binding to proteins and peptides, efflux pump system, precipitation, interactions with biomolecules and organelles are some studied mechanisms for synthesizing NPs using microorganisms [10].

#### *12.1.2.1 Bacteria*

A wide variety of metal NPs and metal oxide NPs have been synthesized using bacterial cells owing to their advantages over chemical synthesis like cost-effectiveness, biocompatibility, limited usage of toxic chemicals, etc. [11,12]. Bacteria are considered one of the best sources for NPs synthesis due to their ability to reduce heavy metals [13,14]. The heavy metal reducing nature of these bacterial species results as a specific defense mechanism to quench heavy metals or metal ions toxicity [15]. Bacterial membranes are the most studied site for NPs synthesis. Enzymatic or biological reactions aid the NPs synthesis in bacteria either intracellularly or extracellularly. Despite the various mechanisms including detoxification of metals and energy-dependent efflux systems of the cell by membrane transporters like ATPase or as chemo-osmotic or proton antitransporters, the exact mechanism for biosynthesis of NPs using bacteria is not known. However, various mechanisms have been studied and accepted in different bacterial species like bio-reduction and bio-oxidation of toxic metals and metal ions, bacterial efflux systems, biosorption and bio-accumulation of metals, etc. [16].

#### *12.1.2.2 Archaea*

A few studies have been reported for green synthesis of NPs using archaea and mainly focused on extremely halophilic archaea. A study by Ref. [17] reported synthesis of silver NPs (AgNPs) using archaeal *Haloferax* sp. and *Halomonas* sp. and SeNPs (selenium NPs) using archaeal strain *Halogeometricum* sp. Ref. [18] reported SeNPs synthesis using halophilic strains including *Haloferax volcanii* BBK2, *Haloarcula japonica* BS2, and *Halogeometricum borinquense* E3 isolated from solar salterns of India. Ref. [19] reported AgNPs

synthesized using haloarchaeon *Halococcus salifodinae* BK6 that exhibited antibacterial properties.

#### 12.1.2.3 Fungi

Various genera of fungi have been widely explored for biological synthesis of metallic NPs as reducing and stabilizing agents due to their resistance and metal bioaccumulation ability. The simplicity with which fungi may be scaled up provides unique advantage of using them in NPs synthesis. Fungal species including yeasts can be used for biological synthesis of NPs and the NPs can be produced intracellularly or extracellularly [20]. Since fungi are exceptionally efficient secretors of extracellular enzymes and also other proteins that make them better sources of NPs synthesis over other microbial forms [21]. Economic viability and ease of handling biomass are also advantages of employing a fungal-mediated green technique for production of metallic NPs [22].

#### 12.1.2.4 Algae

Algae are recognized for their capacity to hyper-accumulate heavy metal ions and remodel them into more pliable forms. Algae have been proposed as model organisms for producing many types of nanomaterials, particularly metallic NPs, due to their appealing characteristics like large range of sizes and shapes [23]. When a precursor metal solution is incubated with algal extract, the biosynthesis of NPs begins. Antioxidants, pigments, phycobilins, chlorophylls, oils, minerals, carbohydrates, lipids, proteins, polyunsaturated fatty acids and other phytochemicals are among the biological molecules found in algae that help in the reduction of metal ion charge to zero valent state, thus considered as an appealing source for NPs synthesis [24]. Synthesis of NPs using algal forms is gaining importance owing to the properties like cost-effectiveness and environment-friendly production approaches [25]. The algae-mediated bio-reduction of metal ions takes place in three phases: activation phase, growth phase, and termination phase and is controlled by various factors such as temperature, pH, time, static conditions, substrate concentration, and stirring [26]. The activation phase comprises metal ion reduction and nucleation as result of enzymes released by algal cells, that can be observed by color change of the solution. In the growth phase, nucleated metal elements amalgamate with one another throughout, generating NPs of various sizes and forms that are thermodynamically stable. In the last phase that's the termination phase, NPs acquire their final morphology. Reducing agents like NADPH or NADPH-dependent reductase, which are produced during metabolic activities such as nitrogen fixation, photosynthesis, and respiration, are the enzymes aiding the NPs synthesis using algal nano-factories [27].

#### 12.1.2.5 Green synthesis of nanoparticles using plants

Plants have been studied for their metal bioaccumulation property since decades and have revealed the potentiality of certain plants to reduce metal ions on their surface as well as in

various tissues and organs thereby accumulating metals in their diverse parts [28]. Metals deposited in their parts were observed to be in the form of NPs, which paved a way for synthesis of NPs using plants [9]. Various parts of plants like stem, bark, root, seed, callus, leaves, peels, and fruits have been explored for green synthesis of NPs. Plants are known to produce a variety of secondary metabolites which have been explored for metallic NPs synthesis such as terpenoids, flavones, ketones, aldehydes, proteins, amino acids, vitamins, alkaloids, tannins, phenolics, saponins, and polysaccharides. These biomolecules act as reducing and stabilizing agents for NPs synthesis [29]. The extracts of whole plant or plant parts are used for NPs synthesis. Similar to algal-based NPs synthesis, the mechanism of NPs synthesis using plants and plant extracts takes place in three phases: the activation phase, growth phase, and termination phase. Synthesizing NPs using plant extracts have gained importance in recent decades due to various advantages like cost-effectiveness, feasibility, and efficacy of NPs synthesis [8,30].

### 12.1.3 Factors influencing green synthesis of nanoparticles

Several factors such as pH, amount of biomass, reactant concentration, reaction time, reaction temperature, and pressure have reported to have influential effects on the size, shape, and morphology of green synthesized NPs [3,31]. Ref. [32] observed that during the green synthesis of platinum NPs (PtNPs), the NP size co-related to the factors such as temperature, pH, and amount of plant extract in an indirect proportional fashion. When compared to physical and chemical procedures, production of NPs using microbes is a sluggish process (a few hours to a few days). This biosynthesis approach can be made more appealing if the synthesis time is reduced. The size of the NPs and their monodispersity are two crucial factors to consider while evaluating their synthesis. Therefore, efficient particle size and monodispersity management must be thoroughly researched. It may be possible to achieve sufficient control of particle size and monodispersity by varying parameters such as microorganism type, microbial cell growth stage (phase), growth medium, synthesis conditions, pH, substrate concentrations, temperature, reaction time, etc. Microbial cells are being manipulated at the genomic and proteomic levels as part of current research, to qualitatively and quantitatively improve NPs synthesis through short reaction times and high synthesis efficiency [33].

#### *12.1.3.1 pH*

The size and texture of green synthesized NPs have been reported to have been widely influenced by pH of the solution medium. For example, Ref. [34] showed that gold NPs (AuNPs) growth takes the form of clusters that aggregate in acidic conditions exhibiting dendritic morphology of NPs, however in contrast, in basic condition, core—shell structures of NPs formation occurred. Ref. [35] depicted that size of AgNPs synthesized using *Pistia stratiotes* extract increased in basic medium but decreased in acidic medium. A study

by Ref. [36] indicated that pH nine was optimum for synthesis of AgNPs using gallic acid as reducing and capping agent with smaller average size.

#### 12.1.3.2 Reactant concentration

Reactant concentration governs the synthesis of NPs using biological sources. It is attributed to the concentration of biomolecules available as reducing and capping agents for metallic NPs synthesis. Ref. [36] reported gallic acid concentration of 7 mM as optimum concentration of synthesis of AgNPs using gallic acid with larger number and smaller sizes of AgNPs with good stability. The concentration of the extract and salt both determine the success of NPs synthesis [37]. A study by Ref. [38] indicated 1 mM $AgNO_3$ was optimum concentration for the AgNPs synthesis using 20 mL extract of *Bacillus licheniformis*.

#### 12.1.3.3 Reaction time

The quality and quantity of green synthesized NPs is also determined by the reaction time. A study by Ref. [39] investigated the effect of reaction time on synthesis of AuNPs using aqueous extract of *Elaeis guineensis*. The study evaluated the influence of reaction time on rate of reduction (viz. reduction of Au precursor to form AuNPs), particle size, and stability of synthesized AuNPs. It was observed that the reaction mixture changed from yellow to light red after 8 min. The color intensity further increased and remained stable at 60 min showing wine red color indicating completion of reaction. Another study by Ref. [40] evaluated the effect of reaction time on synthesis of AgNPs using *Tithonia diversifolia* flower extract. Color change in the reaction mixture from green to brown was observed within 10 min which further intensified and stabilized at 90 min and thus 90 min was recorded as optimum reaction time for the synthesized AgNPs using *Tithonia diversifolia* flower extract.

#### 12.1.3.4 Reaction temperature

The temperature of reaction mixture also plays a significant role in determining the nature of the green synthesized NPs [31]. Effect of reaction temperature has been evaluated on AuNPs synthesis wherein it is observed that increase in reaction temperature, causes rapid nucleation process of NPs that increases the volume of NPs, and decreases the density of free electrons [41]. A study by Ref. [42] investigated the effect of reaction temperature on *Centella asiatica* flavonoids extract-mediated AuNPs synthesis. Rapid rate of reaction was observed for every 15°C rise in temperature and depicted better synthesis of NPs at temperatures 55 and 70°C in comparison to 25°C. A study by Ref. [43] evaluated the effect of temperature on synthesis of AgNPs using *Lawsonia inermis* extract and was observed that good amount and smaller sized AgNPs were synthesized at 45°C as compared to 35 and 25°C.

### 12.1.4 Biocompatibility of green synthesized nanoparticles

The term Biocompatibility refers to a material's ability to perform its intended function in relation to a medical therapy without causing any negative local or systemic impact on the recipient of the biomaterial [44]. The biocompatible material should also elicit the most suitable advantageous cellular or tissue response maximizing the clinically significant efficiency of that treatment [45]. The biomaterial should also carry out a desired function in a living system without causing any harmful and toxic effects such as immunogenic or carcinogenic reactions. Primarily biocompatibility of nanomaterials depends on the location of delivery in the body as the response varies in different parts of the body [46]. Biocompatibility of nanoparticles can be studied either in vitro or in vivo. Green synthesized NPs are considered safe and less toxic and thus are biocompatible in comparison to the chemically and physically synthesized NPs. The biocompatibility of green synthesized NPs is attributed to the biomolecules including bioactive molecules of biological origin that are used as capping and reducing agents during NPs synthesis [4,47]. A study by Ref. [48] depicted green synthesized NPs coated with biomolecules exhibit biocompatibility with high stability and are therefore beneficial for biomedical applications.

### 12.1.5 Therapeutic applications of green synthesized nanoparticles: antimicrobial, antioxidant, anticancer, antiinflammatory

Green synthesized NPs have varied applications as biomedical agents including antimicrobial (antibacterial, antifungal, and antiviral), antioxidant, antiinflammatory, anticancer, antidiabetic, anticoagulant and thrombolytic, etc. [49]. The term "Nanomedicine" is often used for the application of nanotechnology in biology and medicine. Most of the available therapeutic drugs/agents show varied disadvantages including various side effects, drug resistance in microbes, poor bioavailability, etc. The advent of nanomedicine has significantly curbed the disadvantages of the conventional drugs. NPs show easy interaction with proteins, cell surface receptors, and nucleic acids due to their sizes and thus are beneficial as therapeutic agents. Also, the biocompatibility of green synthesized NPs with reduced systemic toxicity makes them better source for nanomedicine [50]. A review by Ref. [51] reported that the green synthesized AuNPs exhibit antimicrobial and anticancer properties and thus can be used in drug delivery and as a biosensor for biomedical applications.

Several nanoparticle-based therapeutics are clinically approved and are commercially available as well. Abraxane is an albumin bound paclitaxel used intravenously for metastatic breast cancer manufactured by Abraxis Bioscience and AstraZeneca. The company Elan Nanosystems (San Francisco, CA, USA) produces oral therapeutics such as nanocrystalline aprepitant, nanocrystalline sirolimus, nanocrystalline fenofibrate under the trade names as Emend, Rapamune, and Tricor as antiemetic, immunosuppressant, and antihyperlipidemic, respectively. Micellular NP emulsion estradiol (MNPEE) is

commercially being produced by Novavax Inc. (Malvern, PA) under the name Estrasorb as a topical application for menopausal therapy. Several other NP-based drugs are under development and even at the various phases of clinical trials over varied platforms such as liposomal, polymeric, and so on [52].

#### 12.1.5.1 Antimicrobial activity

The increasing use of NPs in medicine owing to the various advantages over conventional drug therapies has led to increasing exploration of the synthesized NPs as potential antimicrobial agents. The increase in multi-drug resistance and extreme-drug resistance in microbes with conventional antimicrobial drugs has led to the shift in therapies using green synthesized NPs as antimicrobial agents. NPs have shown to inhibit biofilm formation which is an important aspect of a pathogen in microbial colonization and disease formation. Likewise, several ways of contact with microbes are employed while using NPs to achieve the antimicrobial nature of NPs including electrostatic attraction, receptor-ligand and hydrophobic interaction, van der Waals forces, etc. NPs employ diverse mechanisms to target and kill a specific microorganism that makes it suitable for combating drug resistant pathogens [53]. Once in contact with the target microbe, the NPs enter the cell and interfere with metabolic pathways in the target cell or alter the shape and function of the cell membrane and cell wall. NPs basically target the cellular components like nucleic acids, enzymes thereby causing oxidative damage, cell wall damage, cell membrane permeability, cytoplasmic leakage, enzyme inactivation/inhibition, alteration of protein machinery, etc. [51,54]. Several physicochemical properties of green synthesized NPs also play an important role in efficacy of NPs as antimicrobial agents such as size, charge, zeta potential, surface morphology, and crystal structure [55].

#### 12.1.5.2 Anticancer activity

Cancer is a major health issue world-wide leading to significant morbidity and mortality that needs special health care and attention. Cancer is a type of disease characterized by uncontrolled division or proliferation of cells as a result of disruption or dysfunction of regulatory cell signaling pathways. It can easily spread and invade other tissues and organs. Varied side effects and toxicity of available chemotherapy for cancer treatment have prioritized search for new drugs for cancer treatment with minimum side effects and high effectiveness [56]. The advancements in nanomedicine have led to the development of new anticancer therapeutic agents with minimum damage to normal cells and maximum damage to the cancer cells thereby providing higher therapeutic efficacy with minimum negative impacts. Nanomaterials are also used in cancer diagnosis apart from therapy as biosensors. Among the inorganic NPs, AgNPs have shown anticancer efficacy against several cancer cells like breast, ovary, brain, cervix, etc., and have been examined against cancer cell lines like Hep2, HT-29, Vero cell line, and breast cancer MCF-7. Green synthesized AgNPs target the cancer cells and cause cytotoxicity through

various mechanisms including impaired DNA replication upon uptake of AgNPs by cancer cells; oxidative stress due to generation of reactive oxygen species (ROS) and free radicals and cell membrane damage [57]. Recently AuNPs have shown anticancer activity against liver cancer cell lines (HepG2) and lung cancer cell lines (A549) [3,58]. NP-based drug delivery system has studied the effect of NP-based drug carriers including organic molecules like liposomes, dendrimers, and inorganic NPs including metal oxides and metals like ZnO, iron oxide, $TiO_2$, Au, AgNPs, etc., for cancer therapy and also for drug delivery [59]. Green synthesized NPs acting as carriers or nanocarriers for the drug delivery system for targeting cancer cells can be designed with well-defined properties like size, surface charge, and surface chemistry of the NPs to efficiently improve their cellular uptake by the target cancer cells that lower incidence of adverse effects on noncancerous or nontarget cells and increases the therapeutic efficacy of an anticancer agent. The nanocarrier can be used to transport more than one anticancer drug per NP that increases the efficacy of the anticancer agent through synergistic effect [60].

#### 12.1.5.3 Antioxidant activity

The increased incidence of degenerative diseases has proven the role of oxidative stress that generates surplus free radicals causing damage to the cellular components like nucleic acid, proteins, and lipids. Long-term effect of these oxidants has been interpreted for pathophysiology of diseases like diabetes, atherosclerosis, high blood pressure, cancer, and some neurodegenerative diseases like Parkinson's and Alzheimer's disease. To combat the effect of the oxidants generated (reactive oxygen species), antioxidants have been assessed that are known to delay, control, and prevent oxidative processes of the biomolecules in very low concentrations [61]. The antioxidant molecules are reported to decrease the oxidative damage by directly reacting with generated free radicals or by indirect ways by producing intracellular antioxidant enzymes or inhibiting free radical generating enzymes [62]. Various green synthesized NPs have been assessed for their antioxidant nature and are often found associated with free radical trapping activities with the help of various intracellular enzymes including superoxide dismutases and catalases [63]. Plants are known to be a rich source of antioxidants like phenolic, vitamins, enzymes, carotenoids, etc., and the antioxidant activity of these phytoconstituents can further be enhanced by using these biological sources in NPs production. A study by Ref. [64] reported that melanin NPs can be used for antioxidative therapy and further to treat Ischemic stroke in rat model. The success of using green synthesized NPs in antioxidative therapy is also dependent on several factors like NPs nature, composition, size, surface charge, etc. [65].

#### 12.1.5.4 Antiinflammatory activity

Inflammation is body's defense mechanism against infection, internal injury, hormonal imbalance, etc., that restores cellular homeostasis and tissue environment post infection

or injury. Long-term inflammatory response predisposes body to various illnesses like rheumatoid arthritis (RA), inflammatory bowel syndrome (IBS), cancer, etc. Owing to the harmful effects of commercially available nonsteroidal antiinflammatory drugs (NSAIDs), search for novel antiinflammatory drugs is need of the hour [66]. Increasing research on NPs has evolved the efficacy of green synthesized NPs including AgNPs, AuNPS, ZnONPs, $TiO_2$NPs, and SeNPs as antiinflammatory agents. Various mechanisms are adopted by these NPs for antiinflammatory process. Some of the common mechanisms involved include scavenging of ROS, inhibiting the NF-κB (nuclear factor-κB) and COX-2 (cyclooxygenase-2) pathways and blocking of proinflammatory cytokines, which are inflammation-enhancers and also blocking inflammation-assisting enzymes [67]. These NPs can easily be phagocytosed during the uptake by a cell by forming a protein corona around themselves [68]. A study by Ref. [69] reviewed the antiinflammatory mechanisms of green synthesized ZnONPs and observed that various modes of actions were used by green synthesized NPs as antiinflammatory agents. The most common mechanisms include suppression of expression of inflammatory marker genes including IL-6, IL-1β, IL-10, and TNF-α, also downregulation of expression of COX-2 enzyme and inhibition of NF-κB pathway.

#### *12.1.5.5 Antidiabetic activity*

Diabetes is a health condition observed as high levels of glucose in human blood and arises from imbalance of insulin production. People with diabetes are prone to various health complications including heart diseases, stroke, kidney failure, blindness, premature death, delay in wound healing, etc. It is a serious health issue worldwide and thus development of new drugs with higher antidiabetic efficacy but minimal side effects are challenging parts for the field of nanomedicine. Various plant extracts have been researched as antidiabetic agents and with the advent of nanomedicine, it is observed that the antidiabetic potency of the green synthesized NPs has enhanced the antidiabetic activity of the plant extracts [70]. Various mechanisms are reported for antidiabetic nature of green synthesized NPs. A common mechanism includes inhibition of carbohydrate digesting enzymes (α-glucosidase and α-amylase) that prevents the breakdown of carbohydrates into monosaccharides. As the monosaccharide glucose is a main cause of increase in blood glucose level, inhibiting the production of this sugar can become a useful way to manage diabetes [71]. Some other mechanisms include stimulation of insulin signaling pathway; enhancing insulin receptors, etc. [72].

Apart from these biological activities for biomedical applications, green synthesized NPs have gained interest in other therapeutic applications like for wound healing [73], antiarthritic agents [74]; anticoagulants that can help in treating thrombosis-related diseases [75]; thrombolytic for treatment of thrombosis that dissolves thrombi which causes vascular blockage [76]; etc. The green synthesized NPs are also employed in drug and gene delivery system and in diagnostics [26,49].

## 12.2 Fundamental principles of techniques and instrumentation/ methods/procedures involved

NP synthesis can be achieved by various biological and physicochemical pathways. These can be achieved by two classes of techniques namely bottom-up approach and top-down approach. The bottom-up approach is employed for NPs synthesis using biological forms or green synthesized NPs [8].

### 12.2.1 Techniques in green synthesis of nanoparticles: bio-reduction and biosorption

Nanoparticle production by green synthesis is carried out by two major ways:

**Bio-reduction:** This approach uses bio-reducing agents like enzymes, bioactive molecules including flavonoids, terpenoids, etc., from biological sources to chemically reduce metal ions into a physiologically stable state. The metal salts are first reduced to metallic NPs by the bio-reducing agent, which further undergoes growth phase. Finally, the NPs undergo stabilization by capping agents thus, producing stable and inert NPs [77]. Various NPs can be synthesized using bio-reduction procedures. During synthesis of NPs using plant extracts, the phytochemicals in plants like alcohols, terpenes, phenols, alkaloids, saponins, and proteins are involved in the bio-reduction and stabilization of green synthesized NPs. While synthesizing NPs using microbial cells or extracts, microbial enzymes like NADH-dependent enzymes (nitrate reductase), acetyl xylan esterase, cellobiohydrolase D, glucosidase, β-glucosidase, laccases, etc., act as reducing and stabilizing agents [78].

**Biosorption:** This is a novel technique of NPs manufacturing in which metal cations in aqueous media are allowed to bound with the cell wall of an organism by electrostatic interaction, resulting in the generation of stable NPs due to cell wall and protein peptide contact [79]. Ref. [80] demonstrated green synthesis of CuONPs using *Eucalyptus globulus* leaf extract by biosorption methods.

The biogenic methods employed for NP synthesis bear varied advantages over nonbiogenic methods. In the nonbiogenic methods, an additional step referred to as functionalization wherein polymers and surfactants are coated on NP surfaces to facilitate anchoring of desired substances is involved. However, in biogenic method, no additional step is required as the capping occurs simultaneously using biomolecules from biological form during NPs formation. Capping agents play pivotal role in governing size and morphology of the synthesized NPs. During synthesis of NPs using biological material, certain bioreducing agents also act as capping agents like amino acids (L-histidine, glutamic acid), polysaccharides (dextran, fructose), phytochemicals (flavonoids, alkaloids, polyphenols, quinones, etc.) that makes it suitable for biomedical applications [81–83]. Capping provide stability to NPs and prevent agglomeration and aggregation [22].

### 12.2.2 Techniques in biological synthesis of nanoparticles using microorganisms

Microorganisms are explored as biofactories for NPs synthesis by green approach owing to the various advantages like easy culturing, high growth rate, easy scale-up, manageable optimum conditions, cost-effective, etc. Not all microorganisms synthesize NPs and the fate of synthesis by microbial forms depends on presence of enzymes especially the ones participating in bio-reduction mechanism. Various NPs like Ag, Au, CuO, Zn, $TiO_2$, Pd, Pt, and Ni can be produced using microbes. The synthesis of NPs using microbes can be achieved intracellularly and extracellularly. During intracellular synthesis, microbial cells cultured in appropriate growth media under ambient conditions. The biomass is then harvested and washed to remove impurities and media. The microbial cells are then incubated with metal salt solution of desired concentration for NPs synthesis. During extracellular approach, microbial cells are first cultured in desired media and optimum growth conditions and the cell-free supernatant is used for NPs synthesis. Cell-free supernatant is incubated with metal salt for NPs synthesis. The synthesized NPs are harvested by centrifugation [84]. The brief procedure for NPs synthesis using microbes is given (insert Fig. 12.1). Table 12.1 gives information regarding various microbial forms and plant extracts used for NPs synthesis and their possible mode of synthesis.

### 12.2.3 Techniques in biological synthesis of nanoparticles using plants

Similar to the microbial forms for NPs synthesis, green approach for synthesizing NPs using plant extract has been widely explored. Plant extracts containing phytochemical constituents implore reducing and stabilizing properties for NPs synthesis. Plant material is dried and subjected for extraction procedures in aqueous or organic solvents. Solvent

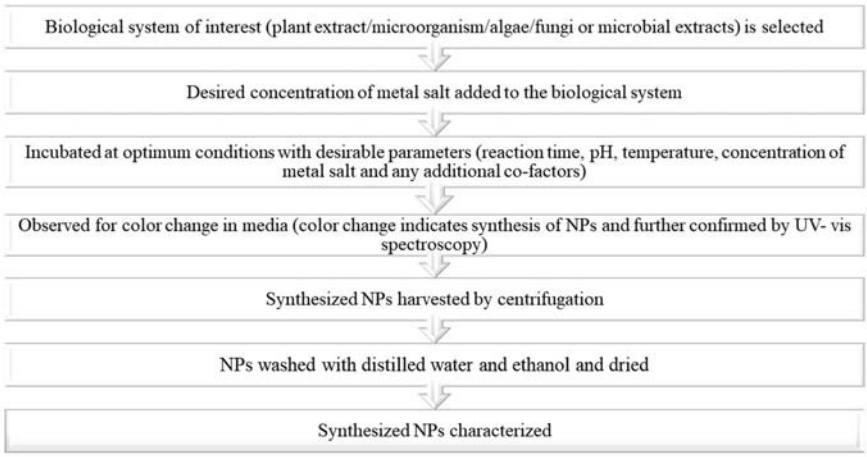


**Figure 12.1** Procedural steps for green synthesis of nanoparticles using desired biological system.

**Table 12.1** Green synthesized NPs from biological forms and their mode of synthesis.

| NPs | Organism | Mode of synthesis | References |
|---|---|---|---|
| ***Bacteria-based NPs*** | | | |
| AgNPs | *Bacillus subtilis* | Proteinaceous molecules and enzymes like nitrate reductase present in the cell free supernatant helps in synthesizing and stabilizing AgNPs from $AgNO_3$ (1 mM). | [85] |
| | *Bacillus anthracis* PFAB2 | $AgNO_3$ (1 mM) solution was used for synthesizing AgNPs using the bacterial EPS 1 mM solution. Functional groups like carboxylic and phosphoric groups present in the EPS provide acted as reducing and capping agents. | [86] |
| | Lactic acid bacteria including *Lactobacillus plantarum, Lactobacillus brevis*, and *Lactobacillus bulgaricus* | Enzymes mainly nitrate reductase present in the cell free culture supernatant played an essential role in bio-reduction of $AgNO_3$ (2 mM) to AgNPs, other enzymes include nicotinamide adenine dinucleotide (NADH) and NADH-dependent enzyme also participated in AgNPs synthesis. Apart from the enzymes, aldehydic groups belonging to polysaccharides from *Lactobacillus* spp. were also responsible for the reduction of $Ag^+$ to AgNPs. The enzymes also acted as stabilizing agents. | [87,88] |
| | *Cytobacillus firmus* | Functional groups of bacterial secondary metabolites like alcohols, amines, sulfonamide present in the cell free supernatant were associated with metal reduction, stabilization, and capping of AgNPs from $AgNO_3$ (5 mM). | [89] |

**Table 12.1** Green synthesized NPs from biological forms and their mode of synthesis.—cont'd

| NPs | Organism | Mode of synthesis | References |
|---|---|---|---|
| | *Pseudomonas aeruginosa* 25W | Bacterial siderophores pyoverdine and pyocyanin were used for synthesizing AgNPs and AuNPs. The functional groups of pyoverdine like amine and hydroxyl groups and that of pyocyanin like methyl groups were involved in reduction and stabilization of the NPs. | [90,91] |
| | *Streptomyces hirsutus* strain SNPGA-8 | Biomolecules present in the cell free supernatant including alcohols, phenols, bromide, iodine, chlorides, and sulfate were associated with the reduction, stabilization and capping of AgNPs with 1 mM $AgNO_3$ solution. | [92] |
| | *Pseudoduganella eburnea* MAHUQ-9 | Functional groups of biomolecules present in the cell free supernatant including alcohols, amines, alkanes, carbonyls and ether and enzymes like reductases (nitrate reductase) were associated with synthesis and stabilization of AgNPs with 1 mM $AgNO_3$ solution. | [93] |
| AuNPs | *Delftia acidovorans* | AuNPs were formed bound to delftibactin, a small ribosomal peptide. | [7,94] |
| | *Pseudomonas fluorescens* 417 | Secondary metabolites present in the cell free supernatant provided functional groups like hydroxyl, carbonyl and aromatic groups for synthesis and stabilization of AuNPs. | [95] |
| | *Gordonia amarae* | Glycolipid was associated with synthesis and stabilization of AuNPs from $HAuCl_4$ (2 mM). | [96] |
| | *Streptomyces* sp. Strain NH-27 | Proteins present in the cell free supernatant participated in | [97] |

*Continued*

**Table 12.1** Green synthesized NPs from biological forms and their mode of synthesis.—cont'd

| NPs | Organism | Mode of synthesis | References |
|---|---|---|---|
| | | AuNPs synthesis $HAuCl_4$ (3 mM). | |
| | *Paracoccus haeundaensis* | Extracellular AuNP were synthesized by reducing gold ions to AuNPs using the proteins, enzymes and other metabolites present in the cell free culture supernatant. | [98] |
| | *Bacillus flexus* GPI-1 | Enzymes mainly nitrate reductase and others like NADPH-dependent reductase helped in bio-reduction of gold ions ($Au^{3+}$) to elemental gold ($Au^0$) NPs. Also, the functional groups like carboxylic acids, primary amines, alkyl group helped in synthesizing AuNPs. | [99] |
| Palladium NPs (PdNPs) | *Pseudomonas* sp. | The enzyme hydrogenlyase participated in the formation of PdNPs that is Pd(II) to Pd(0). | [100,101] |
| | *Geobacter sulfurreducens* | Soluble Pd (II) was reduced to Pd (0); $Pd^0$ NPs synthesized extracellularly predominantly in the EPS surrounding the bacterial cells. | [102] |
| | *Desulfovibrio desulfuricans* | Hydrogenases in the periplasmic space of the bacteria played an important role in Pd (II) reduction for synthesizing PdNPs using hydrogen as electron donor. | [103] |
| | *Bacillus benzeovorans* | PdNPs were synthesized in the S-layer protein of the bacterial cell anaerobically with formate as electron donor probably by formate dehydrogenases. | |
| CuNPs | *Shewanella loihica* PV-4 | CuNP synthesized extracellularly by Cu(II) bioreduction by the means of cytochrome C that used cytoplasm components such as vitamins, organic acids | [104] |

**Table 12.1** Green synthesized NPs from biological forms and their mode of synthesis.—cont'd

| NPs | Organism | Mode of synthesis | References |
|---|---|---|---|
| | | and NADH/NADPH that acted as electron donors through soluble proteins to reduce Cu(II) to CuNPs with the help of enzymes. Proteins secreted by the bacteria provided stability to CuNPs. | |
| | *Shigella flexneri* SNT22 | Copper resistant strain was used for CuNP synthesis and biomolecules with functional groups of alcohol and others were involved in synthesizing and capping CuNPs. | [105] |
| | *Pseudomonas silesinsis* strain A3 | Copper reductase played an important role in synthesizing CuNPs present in cell-free extract with 1 mM $CuSO_4$. | [106] |
| | Bacterial consortium *(Marinomonas, Rhodococcus, Pseudomonas, Brevundimonas,* and *Bacillus)* | Bacterial consortium associated with antarctic ciliate *Euplotes focardii* was used for CuO NPs synthesis. Bacterial biomolecules or functional groups like carbonyl and NH groups present in the supernatant were associated with reduction of $CuSO_4$ to CuO NPs and also for stabilization of NPs. | [107] |
| | *Morganella morganii* | Synthesized CuO NPs with the help of bacterial biomolecules. | [108] |
| ZnNPs | *Pseudochrobactrum* sp. C5 | ZnO NPs synthesized extracellularly with the help of secondary metabolites from the bacterial cells. | [109] |
| | *Lactococcus lactis* NCDO1281(T) and *Bacillus* sp. PTCC 1538 | ZnO NPs synthesized extracellularly. Presence of amino and carbonyl functional groups were observed in the cell free culture supernatant that are associated with NADH-dependent reducing enzyme | [110] |

*Continued*

**Table 12.1** Green synthesized NPs from biological forms and their mode of synthesis.—cont'd

| NPs | Organism | Mode of synthesis | References |
|---|---|---|---|
| | | mainly nitrate reductase which is involved in reducing zinc nitrate into ZnO NPs. | |
| $TiO_2$ NPs | *Streptomyces* sp. HC1. | Functional groups present in the cell free supernatant like hydroxyl groups were involved in reducing and stabilizing $TiO_2$ NPs from $TiO(OH)_2$. | [111] |
| | *Halomonas elongata* IBRC-M 10214 | $TiO_2$ NPs synthesized using $TiO(OH)_2$ solution. Functional groups including alcohol, alkyne, alkene and alkyl halide of biomolecules participated in $TiO_2$ NPs formation. | [112] |
| Uranium NPs (UNPs) | *Bacillus sphaericus* JG-A12 | Binding of uranium to the phosphate and carboxyl groups of the S-layer protein of bacteria caused synthesis of UNPs. | [113] |
| ***Fungi-based NPs*** | | | |
| AgNPs | *Trichoderma harzianum* | AgNPs synthesized by stirring silver nitrate solution in mycelia free cell filtrate. Biomolecules such as secondary metabolites (naphthoquinones and anthraquinones) and various hydrolytic enzymes present in the cell filtrate participated as reducing and stabilizing agents. | [114] |
| | *Trichoderma longibrachiatum* | AgNPs were synthesized extracellularly using the cell filtrate containing proteins (enzymes) as reducing and stabilizing agent. | [115] |
| | *Fusarium oxysporum* | AgNPs were synthesized by stirring silver nitrate solution in mycelia free cell filtrate that contains nitrate reductase enzyme. | [116] |
| | *Rhizopus stolonifera* | Aqueous mycelial extract was used for synthesis of AgNPs wherein proteins present in | [117] |

**Table 12.1** Green synthesized NPs from biological forms and their mode of synthesis.—cont'd

| NPs | Organism | Mode of synthesis | References |
|---|---|---|---|
| | | the extract acted as reducing capping agents. | |
| | *Aspergillus fumigatus* BTCB10 | Cell free extract was used for synthesis that provided biomolecules with amide, cysteine, and carboxyl functional groups for reducing and capping of AgNPs. | [118] |
| | *Rhizoctonia solani* | Fungal extract containing biomolecules with functional groups that of amide linkages of proteins and carbonyl and hydroxyl functional groups in alcohols and phenol derivatives with optimum parameters were used for AgNPs synthesis and stabilization. | [119] |
| | *Penicillium oxalicum* | Cell free culture supernatant with nitrate reductase was used for AgNPs synthesis. | [120] |
| | *Penicillium duclauxii* | Biomolecules in the cell supernatant were involved in synthesis and stabilization of AgNPs from $AgNO_3$ solution (1 mM). | [121] |
| | *Aspergillus sydowii* | AgNPs synthesized extracellularly using the culture supernatant containing biomolecules for AgNPs synthesis and stabilization. | [122] |
| | *Letendraea* sp. WZ07 | Mycelial filtrate containing biomolecules as reducing and capping agent was used for AgNPs synthesis. | [123] |
| | *Talaromyces purpureogenus* | Cell free supernatant containing secondary metabolites like terpenoids and phenols showed reducing and stabilizing property for synthesis of AgNPs. | [124] |
| AuNPs | *Cladosporium cladosporioides* | Fungus isolated from seaweed *Sargassum wightii* as an | [125] |

*Continued*

**Table 12.1** Green synthesized NPs from biological forms and their mode of synthesis.—cont'd

| NPs | Organism | Mode of synthesis | References |
|---|---|---|---|
| | | endophyte; AuNPs synthesized extracellularly with NADPH-dependent reductase (nitrate reductase) and phenolic compounds as reducing and capping agents. | |
| | *Fusarium solani* | Fungus isolated as an endophyte from roots of *Chonemorpha fragrans*. Cell free supernatant containing biomolecules with amide functional groups of proteins participated in the AuNPs synthesis as reducing and capping agents. | [126] |
| | *Rhizomucor pusillus* ATCC 42,782, *Sporotrichum thermophile* ATCC 36,347, *Termoascus thermophilus* ATCC 26,413 and *Termomyces lanuginosus* ATCC 46,882 | Fungi-originated metabolites including primary and secondary metabolites, enzymes, DNA and RNA fragments, etc. were used for synthesis of AuNPs as reducing and capping agents present in the culture supernatant/autolysate liquid/debris-free liquid from mycelial disruption. | [127] |
| ZnNPs | *Fusarium oxysporum* | ZnO NPs synthesized extracellularly with cell free supernatant rich in polyphenols such as terpenoids and flavanoids acting as bio-reducing agents and proteins as both stabilizing and reducing agents. | [128] |
| | *Phanerochaete chrysosporium* | ZnO NPs synthesized extracellularly using biomolecules present in cell free supernatant. Further, ZnO NPs—cellulose composite synthesized by amending sugarcane bagasse-extracted cellulose where cellulose acted as capping agent. | [129] |
| CuNPs | *Aspergillus niger* | Nitrate reductase present in the fungal extract led to the | [130] |

**Table 12.1** Green synthesized NPs from biological forms and their mode of synthesis.—cont'd

| NPs | Organism | Mode of synthesis | References |
|---|---|---|---|
| | | reduction of $Cu^{2+}$ ions into CuNPs with NADPH acting as a reducing agent and phenolic and alcoholic functional groups in the extract as capping agents. | |
| | *Penicillium olsonii* | Biomolecules mainly proteins present in the fungal extract reduced copper sulfate to CuNPs and also acted as capping agents | [131] |
| | *Trichoderma harzianum* | Enzymes and various other proteins present in the cell free extract caused reduction from $Cu^{+2}$ to $Cu^{0}$ producing CuO NPs and further stabilizing the CuO NPs. | [132] |
| PtNPs | *Neurospora crassa* | Proteins in cell free extract were involved in synthesis and stabilization of PtNPs intracellularly. | [133] |
| | *Fusarium oxysporum* | Bioactive functional groups present in the fungal extract caused reduction of hexachloroplatinic acid into PtNPs. | [134] |
| $TiO_2$ NPs | *Aspergillus flavus* | Fungal extract containing bioactive compounds like oxidoreductases and quinones acted as reducing and capping agents. | [135] |
| | *Aspergillus* sp. TK4 | Fungal extracellular enzymes were involved in $TiO_2$ NPs synthesis. | [136] |
| | *Fomitopsis pinicola* | Secondary metabolites from the mushroom extract like polyphenols and flavonoids acted as reducing and capping agents. | [137] |
| Pd NPs | *Agarics bisporus* | Bioactive molecules like phenolic compounds (hydroxyl group), terpenoids, amine groups, and flavonoids were involved in the reduction | [138] |

*Continued*

**Table 12.1** Green synthesized NPs from biological forms and their mode of synthesis.—cont'd

| NPs | Organism | Mode of synthesis | References |
|---|---|---|---|
| | | process for synthesis of PdNPs and polysaccharides and phenolic acids as capping agents. | |
| ***Algae-based NPs*** | | | |
| AgNPs | *Caulerpa racemosa* | Peptides in the seaweed extract played important role for the reduction of $AgNO_3$ into AgNPs and further stabilization of AgNPs. | [139] |
| | *Cylindrospermum stagnale* | Biomolecules like proteins, enzymes, sugars, and lipids present in the algal extract acted as reducing and stabilizing agents. | [140] |
| | *Chlorella vulgaris* | Extracted polysaccharide form the microalga was used for AgNPs synthesis wherein the reducing sugars in the polysaccharides acted as reducing and capping agents. | [141] |
| | *Amphora* sp. (IMMTCC-46) | Pigment fucoxanthin extracted from the diatom was used for AgNPs synthesis wherein the pigment provided functional groups (hydroxyl, epoxy, carbonyl, and carboxyl moieties) for reducing $Ag^+$ ion to $Ag^0$ and stabilization of AgNPs. | [142] |
| | *Oscillatoria limnetica* | Proteins, enzymes, metabolites like flavonoids present in the cyanobacterial extract provided functional groups as reducing and capping agents for AgNPs synthesis. | [143] |
| | *Sargassum muticum* | Polysaccharide fraction of brown macroalga acted as reducing and stabilizing agent for AgNPs. Phenolic compounds also helped in reducing $Ag^+$ to AgNPs. | [144] |

**Table 12.1** Green synthesized NPs from biological forms and their mode of synthesis.—cont'd

| NPs | Organism | Mode of synthesis | References |
|---|---|---|---|
| | *Sargassum myriocystum* | Phyco-molecules in the algal aqueous extract like phenolic compounds (notably polyphenols and tannins) provided reducing and capping agents for AgNPs synthesis. | [145] |
| AuNPs | *Turbinaria conoides* and *Sargassum tenerrimum* | Aqueous extracts of brown algae were able to reduce Au(III) ions to AuNPs with the help of various secondary metabolites in the extract such as amino acids, alkaloids, carbohydrates, flavonoids, saponins, sterols, tannins, proteins and phenolic acids and also had the potential to stabilize them. | [146] |
| | *Galaxaura elongata* | Secondary metabolites from the algal extract like Andrographolide, Alloaromadendrene oxide, glutamic acid, hexadecanoic acid, oleic acid, 11-eicosenoic acid, stearic acid, gallic acid, epigallocatechin catechin, and epicatechin gallate were observed that acted as reducing, stabilizing, and capping agent for AgNPs. | [147] |
| | *Arthrospira platensis* | Algal exopolysaccharides were used for synthesis of AuNPs and stabilization. | [148] |
| | *Nitzschia* sp. | The diatom carried out AuNPs synthesis intracellularly wherein biomolecules like diatom proteins and polysaccharides caused reduction, and stabilization of AuNPs. | [149] |
| CuNPs | *Botryococcus braunii* | Proteins, polysaccharides, amides, and long-chain fatty acids were involved in | [150] |

*Continued*

**Table 12.1** Green synthesized NPs from biological forms and their mode of synthesis.—cont'd

| NPs | Organism | Mode of synthesis | References |
|---|---|---|---|
| | | bioreduction, capping, and stabilization of CuNPs. | |
| | *Corallina officinalis* Linnaeus and *Corallina mediterranea* | Biomolecules present in the seaweed aqueous extract like proteins, carboxylic acids, complex carbohydrates acted as reducing agents from copper sulfate to CuNPs and also stabilization agents. | [151] |
| | *Macrocystis pyrifer* | Separated protein fractions from the aqueous extract of the brown alga were used as reducing and capping agents for CuO NPs synthesis. | [152] |
| ZnNPs | *Arthrospira platensis* | Biomolecules like polysaccharide, proteins, and enzymes (NADPH-dependent reductase) present in the extract played essential role as reducing and stabilizing agents for ZnO NPs synthesis. | [153] |
| | *Chlorella* sp. | Biomolecules present in the microalgal extract acted as reducing and capping agents for ZnO NPs. | [154] |
| | *Sargassum muticum* | ZnO NPs synthesized using algal extract. | [155] |
| PdNPs | *Padina boryana* | Various secondary metabolites like polyols (terpenoids, tannins, saponins, etc.) in the extract played role in bio-reduction and bio-capping of Pd-NPs. | [156] |
| PtNPs | *Padina gymnospor* | Presence of various functional groups (associated with carbohydrates and proteins) in the aqueous seaweed extract must have served as reducing and capping agents of the PtNPs. | [157] |
| $TiO_2$ NPs | *Chlorella pyrenoidosa* | Phytochemicals like carboxyl, amino, and hydroxyl groups present in the biomolecules of the green alga acted as | [158] |

**Table 12.1** Green synthesized NPs from biological forms and their mode of synthesis.—cont'd

| NPs | Organism | Mode of synthesis | References |
|---|---|---|---|
| | | both reducing and capping agent for $TiO_2$ NPs synthesis. $TiO_2$-GO nanocomposite was further synthesized using the graphene oxide. | |
| ***Plants-based NPs*** | | | |
| AgNPs | *Carya illinoinensis* | Functional groups like phenolic compounds, aliphatic amines, and alkanes in leaf extract at ambient temperature were used as reducing and capping agents for AgNPs. | [159] |
| | *Tectona grandis* | Proteins and other functional groups in the seed extract used for bio-reduction and stabilization of AgNPs. | [160] |
| | *Adathoda vasica* | Ag@$Fe_2O_3$ nanoparticles synthesized; Vasicine/quinazoline alkaloids present in the leaf extract were responsible for the stability of the nanoparticles. | [161] |
| | *Spondias mombin* | Secondary metabolites from leaf extract including enzymes, polysaccharides, alkaloids, tannins, phenols, terpenoids and vitamins helped synthesizing AgNPs with 1 mM $AgNO_3$ solution and organic components like flavonoids and terpenoids from the leaf extract helped to stabilize the AgNPs. | [162] |
| | *Medicago sativa* | AgNPs were synthesized using the chlorophyll pigment extracted using ethanol solvent from the alfalfa leaves. | [163] |
| | *Malva sylvestris* | Biomolecules such as proteins and terpenoids in the flower extract acted as reducing and capping agents for AgNPs. | [164] |

*Continued*

**Table 12.1** Green synthesized NPs from biological forms and their mode of synthesis.—cont'd

| NPs | Organism | Mode of synthesis | References |
|---|---|---|---|
| | *Calotropis gigantea* | The phytochemical constituents in the flower extract like alkaloids, glycosides, flavanols, tannins, saponins, sterols, and triterpenoids carried out reduction and stabilization of AgNPs. | [165] |
| | *Bauhinia purpurea* | Bioactive molecules in the flower extract acted as reducing and capping agents. | [166] |
| | *Annona muricata* | Phytochemical constituents mainly lactone present in leaves, stems, and skin extract served as reducing and capping agent for AgNPs. | [167] |
| AuNPs | *Chamaecostus cuspidatus* | AuNPs synthesized from the insulin plant leaf extract containing bioactive molecules for reducing and stabilization of AuNPs. | [168] |
| | *Capsicum chinense* | Metabolites such as proteins, flavonoids, amino acids, polyphenols, and reducing sugars in the leaf extract acted as reducing and stabilizing agents for AuNPs synthesis. | [169] |
| | *Solanum lycopersicum* | Lycopene extracted using benzene solvent from tomato was used for AuNPs synthesis that served as reducing and stabilizing agent. | [170] |
| | *Hevea brasiliensis* | Latex extracted from the plant was used for bio-reduction and stabilization of AuNPs. | [171] |
| | *Citrus lanatus* | Watermelon rind extract was used for synthesis of AuNPs with phenolic compounds, flavonoids, and lycopene as | [172] |

**Table 12.1** Green synthesized NPs from biological forms and their mode of synthesis.—cont'd

| NPs | Organism | Mode of synthesis | References |
|---|---|---|---|
| | | reducing agents and proteins/peptides as stabilizing agents. | |
| ZnNPs | *Cassia alata* | Leaf extract with the phytochemicals groups like phenolic groups, amines, ether, carboxylic acid and a hydroxyl group acted as reducing and capping agent for the synthesis of ZnO NPs. | [173] |
| | *Passiflora caerulea* | The functional groups including amines and alkanes belonging to secondary metabolites such as terpenoids, flavonoids, alkaloids, etc., present in the leaf extract served as reducing and stabilizing agents for ZnO NPs. | [174] |
| | *Rubus fairholmianus* | The presence of phytochemical compounds (polyphenolics, flavonoids, tannins, glycosides, saponins, and gallic acids) in the root extract acted as reducing and stabilizing agent for ZnO NPs. | [175] |
| CuNPs | *Malus domestica* | The functional groups of phytochemicals in the leaf extract served as capping and reducing agents for CuO and Ag−CuO NPs synthesis. | [176] |
| | *Cissus vitiginea* | Phytochemicals (carbohydrates, proteins, flavonoids, saponins, alkaloids, polyphenol, anthraquinone, steroids, terpenoids, and tannins) present in aqueous plant extract carried out synthesis of CuNPs from $CuSO_4$ (10 mM). | [177] |

*Continued*

**Table 12.1** Green synthesized NPs from biological forms and their mode of synthesis.—cont'd

| NPs | Organism | Mode of synthesis | References |
|---|---|---|---|
| $TiO_2$ NPs | *Piper betel* | The plant biomolecules like proteins, tannins, carbohydrates, and polyols in the leaf extract acted as capping and reducing agent for $TiO_2$ NPs. | [178] |
| | *Carum copticum* | Aqueous extract of seeds with bioactive molecules was used for $TiO_2$ NP synthesis. | [179] |
| | *Azadirachta indica* | Biologically active phytoconstituents in leaf extract including flavonoids, alkaloids, terpenoids, and polyphenols served as reducing and capping agents $TiO_2$ NP synthesis. | [180] |
| PdNPs | *Rosmarinus officinalis* | Leaf extract was used for synthesis of PdNPs which was rich in biomolecules as flavonoids, proteins, enzymes, polysaccharides, alkaloids, terpenoids, aldehydes, carboxylic acids, etc., that provided reducing and stabilizing agents. | [181] |
| | *Basella alba, Allium fistulosum, and Tabernaemontana divaricate* | Biomolecules present in the aqueous extracts were associated with PdNPs synthesis from 2 mM aqueous palladium acetate solution. | [182] |
| | *Moringa oleifera* | Peel extract with biomolecules was used for reducing and capping PdNPs. | [183] |
| PtNPs | *Ononis spinosa* L | Phytochemical constituents in the plant extract like flavonoid derivatives, sterols, terpenes, phenolic acids, essential oil, and isoflavonoids served as reducing and capping agents for PtNPs synthesis. | [184] |

is evaporated and the dried sample is dissolved in water or desired solvent (ensure that the solvent is not cytotoxic to normal cells). The sample is mixed with desired metal salt solution and incubated under optimum conditions. Color change of the solution indicates the synthesis of NPs. NPs synthesis using plant extract involves three main phases: the activation phase where the metal ions get reduced, growth phase wherein more metal ions get reduced, and termination phase wherein reduced ions assemble to a definite morphology [185].

### 12.2.4 Techniques in characterization of green synthesized nanoparticles

NPs are characterized based on their size, shape, dispersity nature, and surface area. The unique characteristics determines the biomedical potentiality and application of an NP. Analytical techniques for identifying, isolating, or quantifying NPs, as well as studying their physical properties are widely employed for characterization of green synthesized NPs. Microscopy, spectroscopy, calorimetry, gravimetry, light or radiation scattering, chromatography, and other chemical and material science measurements are among them.

#### *12.2.4.1 Microscopy-based techniques for characterization of green synthesized NPs*

Optical microscopy allows the observation of materials at a micron scale with a good degree of resolution. Further resolution in optical microscopes is challenging due to aberrations and wavelength limitations. As a result, additional imaging methods such as AFM, SEM, and TEM have evolved in their ability to identify materials with submicron dimensions. Although the fundamentals of the approach vary, they all generate a substantially enlarged image. These imaging methods can be used to observe NPs.

##### 12.2.4.1.1 Atomic force microscopy (AFM)

Surface sensing is used in AFM microscopes, which use an incredibly sharp tip on a micro-machined silicon probe. Although the approach differs drastically between operating modes, this tip is used to photograph a sample by raster sweeping across the surface line by line. The length, width, and height and other physical properties like texture and morphology of the NPs can be determined using AFM [186]. By this microscopic technique, high resolution and good quality images can be captured of the green synthesized NPs.

##### 12.2.4.1.2 Scanning electron microscopy (SEM)

SEM (scanning electron microscopy) is an advanced microscopy technique that produces high-resolution three-dimensional images of the green synthesized NPs at nanoscale features as small as 1−100 nm. Instead of a light beam, as in an optical microscope, an electron beam is directed at the object in SEM that scans the surface of NPs to produce image

giving surface landscape and matter composition. SEM analysis determines the size, shape, texture, surface morphology, and crystalline structure of green synthesized NPs [187].

Field emission—scanning electron microscopy (FE-SEM) is a more sophisticated technique than SEM, which helps to determine the size and morphology of green synthesized NPs. It captures images of surface morphology that gives detailed structures of organic matter. Irregular, bubble-like, elliptical and faveolate shaped pores are observed in organic-rich matter, whereas limited and isolated pores are observed in organic poor matter [188].

#### 12.2.4.1.3 Scanning electron microscopy—energy dispersive X-ray analysis (SEM-EDX)

SEM-EDX uses distinctive X-rays to infer elemental compositions. In this technique, EDX is coupled to SEM, backscattered electrons are also employed to create the picture wherein electron beam moves across the material that develops image of each element in the synthesized NPs sample. This technique allows determination of chemical composition of green synthesized NPs. It also helps determine size and shape of NPs. This technique employed by Ref. [169] indicated homogeneous size distribution of the AuNPs-leaf and quasi-spherical morphologies for AuNPs synthesized using *Capsicum chinense* leaf extract.

#### 12.2.4.1.4 Transmission electron microscopy (TEM)

Transmission electron microscopy is a high-magnification imaging method that visualizes the transmission of an electron beam through a material. TEM imaging offers a substantially greater resolution than light-based imaging methods because it employs electrons to illuminate the sample rather than light. The sample thickness (the quantity of material that the electron beam must travel through) and the sample material both influence the amplitude and phase changes in the transmitted beam, which give imaging contrast. Drying NPs on a copper grid covered with a small coating of carbon prepares samples for imaging. Materials with much greater electron densities than amorphous carbon are easily photographed. Most metals (e.g., Ag, Au, Cu, Al), most oxides (e.g., silica, aluminum oxide, titanium oxide), and other particles (e.g., polymer nanoparticles, carbon nanotubes, quantum dots, and magnetic nanoparticles) are examples of these materials. To directly evaluate the particle size, grain size, size distribution, and shape of NPs, TEM imaging is the preferable approach with accuracy of sizing within 3% of the actual value. Using TEM, it is possible to analyze high-resolution imagery with diameters as tiny as 0.2 nm. The electron diffraction technique is helpful for phase identification, determining structure and symmetry, measuring lattice parameters, and identifying disorder and defects. As no metallic staining is required, TEM is thought to be a good choice for structural imaging of organic materials. It is feasible to see the crystalline lattice

directly. It provides details like shape, size, and provides 2-dimensional morphology of green synthesized NPs [185].

#### 12.2.4.1.5 High-resolution transmission electron microscopy (HRTEM)

This technique is an advanced TEM imaging technique that develops images of the crystallographic structure of green synthesized NPs at an atomic level. High-resolution property of this technique allows detection of defects in crystal structure and atoms while imaging the crystal structure [189]. Selected area electron diffraction (SEAD) technique makes use of advanced TEM technique (high-resolution transmission electron microscopy (HRTEM)) that helps analyze crystalline and noncrystalline properties [190].

#### 12.2.4.1.6 Scanning tunneling microscopy (STM)

STM works based on the principle of tunneling that produces surface images with an atomic scale lateral resolution and helps to characterize NPs [191].

### *12.2.4.2 Spectroscopy-based techniques for characterization of green synthesized NPs*

#### 12.2.4.2.1 UV/visible spectrophotometry

UV/visible spectroscopy is a method for determining how much light is absorbed and dispersed by the specimen. It works on the Beer Lambert's law. As various green synthesized NPs give representative peaks at varied absorption, this technique is widely employed for the detection of synthesized NPs. The increase in particle size shifts the absorption spectra of NPs toward longer wavelength [192]. This technique provides information regarding the size, structure, stabilization, and aggregation of nanoparticles based on surface plasmon resonance (SPR). Ag and AuNPs show absorption at 400−450 and 500−560 nm, respectively, within the visible range as a result of function of SPR [191].

#### 12.2.4.2.2 Fourier transform infrared spectroscopy (FTIR)

FTIR is a technique for obtaining an infrared spectrum of a solid, liquid, or gas's absorption or emission. An FTIR spectrometer obtains high-resolution spectral data over a large spectral range (4000−400 $cm^{-1}$). FTIR is a helpful tool for chemical identification as each molecule has its own imprint and a variation in the material composition is readily shown by changes in the absorption band pattern [193]. FTIR is a widely employed technique for characterizing green synthesized NPs to determine the type of functional groups and their participation in synthesizing NPs and stabilizing synthesized NPs through their bio-reduction process [93]. In this spectroscopy method, FTIR spectra from green synthesized NPs and that of the extract of plant or microorganisms is compared and analyzed to evaluate the functional groups participating in bioreduction. The analysis of FTIR data helps determine the functional groups on the surface of the synthesized NPs in the presence of functional groups of biomolecules like

proteins, hydroxyl, carbonyl groups which are involved in bio-reduction process [194]. A study by Ref. [195] reported the green synthesis of AgNPs using *Citrus reticulate Blanco* (Kinnow) peel extract. The FTIR spectra depicted major peaks at 1641.8 $cm^{-1}$ related to C—N and C—C stretching and also at 3251.0 $cm^{-1}$ attribute to functional groups like O—H in water, alcohol, and phenols, 2917.9 $cm^{-1}$ corresponding to C—H groups in alkanes, 1738.4 $cm^{-1}$ for carbonyl groups of an acid and 1068.7 $cm^{-1}$ that attribute to functional groups with ether and C-stretching. These results depicted that the functional groups of the biomolecules present in the Kinnow fruits extract provides capping agents for the green synthesis of AgNPs and also in stabilizing the NPs. Another study by Ref. [148] synthesized AuNPs using the algal *Arthrospira platensis* exopolysaccharides (EPS) and depicted the bio-reduction and capping of AuNPs by the functional groups present in the algal EPS. The major peaks in the FTIR spectra were observed related to OH groups of the algal polysaccharide. Similarly, peaks were observed that could be attributed to the carbonyl groups, amide groups, sugar moieties, etc., of the algal polysaccharide participating in the reduction and capping of the AuNPs. The study of biomolecules participating in bio-reduction is beneficial in developing novel pathways for NPs via green synthesis [49].

#### 12.2.4.2.3 Raman spectroscopy

Raman spectroscopy is a spectroscopic technique that studies the rotational, vibrational, and other modes of a system by using Raman scattering or inelastic scattering of monochromatic laser light. Stimulated Raman spectroscopy, surface enhanced Raman spectroscopy, and resonance Raman spectroscopy are examples of advanced Raman spectroscopy [191]. Similar to that of FTIR spectroscopy, Raman spectroscopy is also used for vibrational characterization of NPs [196]. A study by Ref. [197] studied the structural and compositional characteristics of SeNPs synthesized using *Azospirillum thiophilum*. The Raman spectral peaks obtained can be attributed to amorphous elementary selenium. The study also concluded that combination of FTIR and Raman spectroscopy is highly informative in analyzing the structural and compositional nature of the synthesized NPs. Another study by Ref. [198] studied the vibrational and structural polarity of ZnONPs synthesized using *Elaeagnus angustifolia* leaf extracts by Raman spectroscopy technique. A study by Ref. [199] used Raman spectroscopy for the identification and quantification of amorphous and crystalline phases of $TiO_2$ NPs synthesized by gum arabic (*Acacia senegal*).

#### 12.2.4.2.4 Zeta potential

The zeta potential (also known as the electrokinetic potential) assesses the charge stability of colloidal NPs by measuring the "effective" electric charge on the NPs surface. The difference in potential between the main fluid in which a particle is disseminated and the layer of fluid containing oppositely charged ions that is associated with the NPs

surface is measured by the zeta potential. Positively charged particles bond with negatively charged surfaces, and vice versa. Higher magnitude potentials show enhanced electrostatic repulsion and hence improved stability, whereas lower magnitude potentials show decreased electrostatic repulsion and thus decreased stability. It is vital to remember that the size of the charge on the NPs surface is affected by the pH of the solution. In fact, at a certain pH, known as the isoelectric point, the surface charge can be decreased to zero. Particle speed is monitored at various voltages, and the zeta potential is calculated using this information [200]. This technique determines the nature of the materials encapsulated inside the NPs, its stability, and surface charge [186].

#### *12.2.4.3 X-ray–based characterization techniques*

##### 12.2.4.3.1 X-ray diffraction (XRD)

For characterizing crystalline materials, X-ray diffraction (XRD) is a strong nondestructive method. Structures, phases, preferred crystal orientations (texture), and other structural data such as average grain size, crystallinity, strain, and crystal defects can be evaluated by this technique [191]. XRD is yet another widely employed characterization technique for green synthesized NPs. It is used to assess the crystallinity of the synthesized NPs. The peaks obtained in the XRD determine whether the synthesized NPs is crystalline or amorphous in nature. Higher peak height indicates crystalline and lower peak height indicates amorphous NPs [185]. However, powder XRD gives detailed information about phase character, degree of crystallinity, and NPs structure [201]. Ref. [202] reported green synthesis of AgNPs from *Juniperus procera* plant extract and confirmed the crystalline nature of the synthesized AgNPs by XRD technique. The XRD diffractogram showed intense diffractions that can be attributed to the crystallinity of the synthesized AgNPs. The peaks corresponding to 111, 200, 220, 311, and 222 indicated the expected face-centered cubic (FCC) structure of the synthesized AgNPs. Similarly, XRD analysis of green synthesized AuNPs using *Barbarea verna* extract by Ref. [203] exhibited diffraction peaks corresponding to crystalline gold atomic planes that confirmed the expected FCC structure of the green synthesized AuNPs.

##### 12.2.4.3.2 X-ray photoelectron spectroscopy (XPS)

XPS is a quantitative spectroscopic technique that carries out analysis of material irradiated with X-rays under ultra-high vacuum conditions. This technique assesses the elemental composition of a material and can be used for characterization of green synthesized NPs that provides information regarding shells and coatings and also indicates the contamination of synthesized NPs [204].

#### *12.2.4.4 Dynamic light scattering (DLS)*

Hydrodynamic particle size and distribution in a range of sizes can be analyzed using dynamic light scattering (DLS). Light interference is measured by DLS using the Brownian

motion of NPs in suspension and the correlation of their speed (the diffusion coefficient) with their size based on Stokes–Einstein equations. Polydispersity index (PDI) provides information on particle size distribution ranges which is an output of the autocorrelation function. In the PDI assessment, values range from 0 to 1, where one corresponds to the very heterogeneous population and 0 to the highly homogeneous population. In order to be able to determine size accurately, the dispersity is the major factor limiting correlation. Due to the fact that there is no absolute control over the synthesis process, and a chemical reaction isn't homogenous, NPs can't be created uniformly and thus dispersity is a limiting factor. DLS is used in characterizing green synthesized NPs that determine the particle size and distribution during NP synthesis [205,206]. A study by Ref. [207] evaluated the mean size and size distribution of AgNPs synthesized using *Aloe vera* gel extract with size 82 nm and PDI value of 0.134. A study by Ref. [208] indicated the mean particle size between 10 and 20 nm for the green synthesized silver oxide nanoparticles ($Ag_2O$ NPs) that were synthesized using *Bergenia ciliata* rhizome extract.

### 12.2.5 Methods for therapeutic applications of green synthesized nanoparticles

#### *12.2.5.1 Antimicrobial activity of green synthesized nanoparticles*

##### 12.2.5.1.1 Diffusion methods

**A) Agar disk-diffusion methods**

Agar disk-diffusion method commonly referred to as Kirby–Bauer disk diffusion assay is widely employed by researchers evaluating the antibacterial/antifungal properties of molecules. Sterile disks of 6 mm diameter impregnated with the compound of choice with desired concentrations is placed on the agar plate swab inoculated with the test microorganism. An antibiotic containing disk is kept for reference/control. The petriplates are then incubated at 37°C for 24 h for bacteria and at 27°C for 48 h for fungi [209]. Upon incubation, zones of inhibition are observed and measured for the NPs in mm. This antimicrobial technique has been reported by Ref. [210] that evaluated the antibacterial activity of green synthesized AgNPs using turmeric extracts. Antimicrobial activity of AgNPs synthesized using a tree extract *Lysiloma acapulcensis* is assessed by Ref. [211] by disk-diffusion method. In this study, Gram-positive and Gram-negative bacteria as well as fungi were used as test pathogens (insert Fig. 12.2).

**B) Agar well-diffusion methods**

This technique is one among the widely implemented antimicrobial techniques as per Clinical and Laboratory Standards Institute [212]. Briefly, mid-log phase cultures of test bacteria or fungi are swab inoculated on Mueller–Hinton media for bacteria and potato dextrose agar for fungi. Wells/holes are bored into the media with diameter size of 6 mm. Various concentrations of the synthesized NPs are added into the wells. Antibiotics with known concentration can be used as positive control and the solvent used for diluting the synthesized NPs can be used as negative control. Also, the microbial or plant extract used

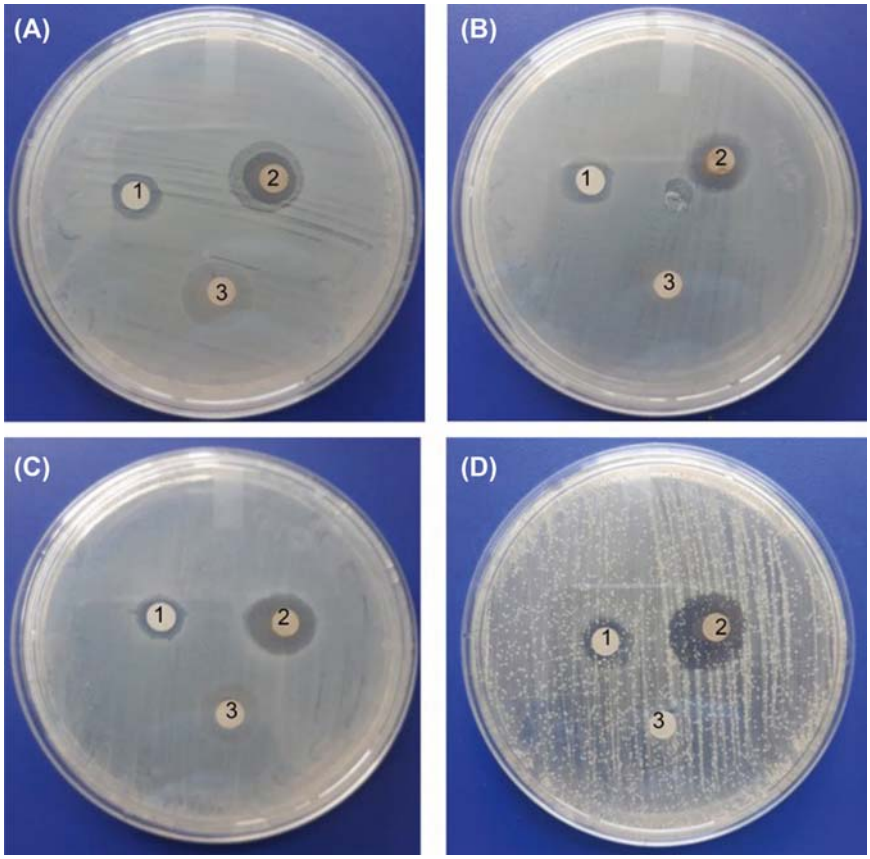


**Figure 12.2** Antimicrobial activity of NPs by disk diffusion method. Test pathogens (A) *E. coli*, (B) *P. aeruginosa*, (C) *S. aureus*, (D) *C. albicans*. Disks impregnated with: (1) $AgNO_3$ solution, (2) AgNPs synthesized using *L. acapulcensis* aqueous extract, (3) *L. acapulcensis* aqueous extract. The zones of inhibition seen as clearance around the wells indicate the antimicrobial activity of the synthesized NPs and is observed to be greater for the NPs as compared to $AgNO_3$ solution and *L. acapulcensis* aqueous extract. *(Figure reproduced from D. Garibo, H.A. Borbón-Nuñez, J.N.D. de León, E. García Mendoza, I. Estrada, Y. Toledano-Magaña, et al., Green synthesis of silver nanoparticles using* Lysiloma acapulcensis *exhibit high-antimicrobial activity, Sci. Rep. 10 (1) (2020) 1–11 with permission from Scientific Reports and Springer nature publishers.)*

for synthesizing NPs and the metal salt solution used for NPs synthesis can also be tested for the antimicrobial activity to compare the antimicrobial activity of green synthesized NPs to the starting material used for synthesis. The plates should be incubated at 4°C for 20 min for prediffusion of NPs. The plates are then incubated at 37°C for 24 h for bacteria and 27°C for 48 h for fungi followed by observing and measuring the zones of inhibition in mm. A study by Ref. [159] showed antibacterial activity by agar well diffusion method for the AgNPs synthesized using *Carya illinoinensis* leaf extract. This technique is

also reported by Ref. [178] for antibacterial activity of titanium dioxide ($TiO_2$) NPs synthesized using *Piper betel* leaf extract.

In another study, Ref. [213] evaluated antimicrobial activity of gadolinium doped titanium dioxide (GdT) NPs using *Piper betel* leaf extract by agar well diffusion method with slight modification while NPs sample preparation for antimicrobial activity (insert Fig. 12.3). In this study, the synthesized NPs were subjected to UV radiation (365 nm) for 12 h and then various concentrations of the preirradiated NPs were added into the wells. NPs without preirradiation were used as control. It was observed that UV irradiated GdT NPs showed higher zones of inhibition as compared to the NPs that were not UV irradiated.

#### 12.2.5.1.2 Dilution methods

**A) Broth dilution methods**

Broth dilution method is the widely used antimicrobial technique for determining the minimum inhibitory concentration (MIC) of compounds, according to the Clinical and Laboratory Standards Institute [214] guidelines [212]. This technique can be carried out in two ways: Macro-dilution broth and Micro-dilution broth method. Microdilution method is more accurate than the macrodilution method in determining MIC value. Briefly, antimicrobial agent is subjected to twofold dilutions in a liquid growth media (sterile Mueller–Hinton broth for bacteria and potato dextrose broth for fungi) in tubes with minimum 2 mL capacity (macro-dilution) or in 96 well microtitre plate

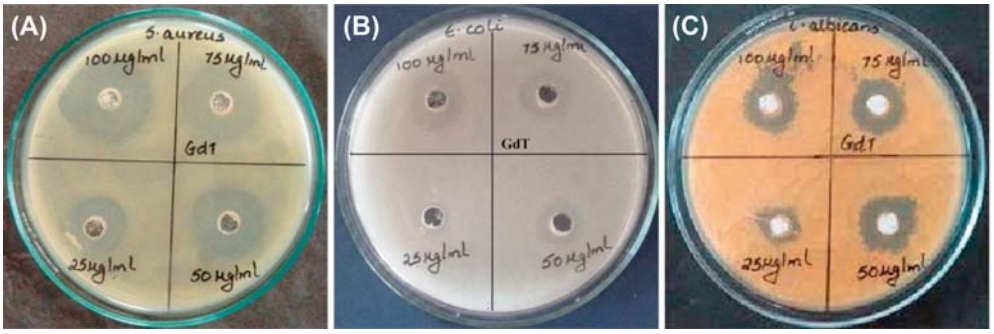


**Figure 12.3** Antimicrobial activity of various concentrations (25, 50, 75, and 100 μg/mL) of gadolinium doped titanium dioxide (GdT) NPs synthesized using *Piper betel* leaf extract against pathogens under UV irradiated condition by Agar well diffusion method (A) *S. aureus*, (B) *P. aeruginosa*, (C) *C. albicans*. The zones of inhibition seen as clearance around the wells indicate the antimicrobial activity of the NPs and is observed that antimicrobial activity increased with increase in concentration. *(Figure reproduced from publication, S.M. Hunagund, V.R. Desai, D.A. Barretto, M.S. Pujar, J.S. Kadadevarmath, S. Vootla, A.H. Sidarai, Photocatalysis effect of a novel green synthesis gadolinium doped titanium dioxide nanoparticles on their biological activities, J. Photochem. Photobiol. Chem. 346 (2017) 159–167, Copyright Elsevier (2017).)*

(microdilution). Each tube/well is inoculated with mid log phase culture of test microorganism that is diluted with same medium used for antimicrobial compound dilution to get a desired microbial cell suspension adjusted to 0.5 McFarland scale. Upon thorough mixing, the tubes/plates are incubated under suitable conditions. MIC values were determined as the lowest dilution of NPs inhibiting visible microbial growth. This technique is reported by many researchers for determining the MIC values of synthesized NPs. Ref. [160] reported the MIC value for AgNPs synthesized from *Tectona grandis* seed extract and has shown antimicrobial activity against bacteria *Bacillus cereus*, *S. aureus*, and *E. coli* showing MIC values 5.2, 2.6, and 2.0 μg/mL, respectively. A study by Ref. [161] has evaluated the MIC value of multifunctional Ag@$Fe_2O_3$ NPs synthesized by *Adathoda vasica* leaf extract and depicted antimicrobial activity against *S. aureus*, *E. coli*, and *Candida albicans*. The MIC values observed were evaluated as $15.33 \pm 4.62$ and $12.67 \pm 4.32$ μg/mL for *S. aureus* and *E. coli*, respectively, by macro-dilution broth method.

Minimum bactericidal concentration (MBC) is a confirmatory technique for MIC plates/tubes. 100 μL culture from the microtitre well/tube from the micro-/macro-dilution broth method is taken and inoculated onto agar media by spread plate technique. The plates were incubated for 24 h at 37°C for bacteria and for 48 h at 27°C for fungi with MBC calculated as the lowest concentration at which no colonies formed or 99.9% of the bacterial population is killed. Ref. [215] depicted the use of MBC technique for antimicrobial activity of AgNPs synthesized using banana peel extract.

Ref. [4] has reported the antimicrobial activity of AgNPs synthesized using Actinobacterial strain SF23 which showed the MIC of 8, 32, 8, and 128 μg/mL, respectively, for *E. coli*, *K. pneumoniae*, *P. aeruginosa*, and *S. aureus*. Furthermore, the synthesized AgNPs showed the MBC values 32, 64, 64, and 256 μg/mL for *E. coli*, *K. pneumoniae*, and *P. aeruginosa* and *S. aureus*, respectively.

#### 12.2.5.1.3 Thin-layer chromatography (TLC)-bioautography methods

This method for antibacterial activity of NPs is reported by Ref. [216] in which the NPs solution was spotted on silica-coated TLC plates and the spots identified in iodine chamber after running the chromatography technique with 3:7 methanol and chloroform as solvents. The Rf values were calculated. The developed TLC plate was placed in a sterile petriplate and sterile molten nutrient agar was poured in a thin layer ensuring that the TLC plate is covered with media and then allowed to solidify. 18 h old culture of a test bacteria was swab inoculated onto the solidified nutrient agar plate and incubated at 37°C for 24 h. The zones of inhibition for the test bacteria were observed at the spots developed on TLC.

#### 12.2.5.1.4 Flowcytometry methods

The antimicrobial activity by flowcytometry analysis is done for evaluating the minimum membrane disruptive concentration (MDC) of a compound. The advantage of MDC over MBC and MIC assays is that it directly measures compound/microbe interactions and lysed cell numbers rather than microbial survival. The microbial cell suspension is prepared in the respective media (NB or MHB for bacteria and PDB or SB for fungi) to 0.5 McFarland standard. Test compounds (NPs) diluted to get desired concentration and mixed with 100 μL microbial cell suspension each in microtitre plate and incubated at 37°C for bacteria or 27°C for fungi for 90 min. MDC was then studied after the incubation period by Flow cytometry method. Briefly, the LIVE/DEAD BacLight Bacterial viability kit is used for the analysis, according to the manufacturer's instructions. 150 μL of bacterial/fungal suspension was stained with 5 μL SYTO9 and propidium iodide (PI). This was incubated for 15 min at room temperature (RT) under dark conditions. Flow cytometric measurements were performed using the flow cytometer instrument. The fluorescence signals are displayed for live cells as green and dead cells as red fluorescence. Results are expressed as the percentage of dead microbial cells [217]. The flow cytometry technique for antimicrobial analysis of green synthesized AgNPs using *Aloe arborescens* as reducing, stabilizing, and capping agent has been reported by Ref. [218] against human pathogens that revealed increased cell death of bacteria treated with the NPs through cell membrane damage (insert Fig. 12.4). A study by Ref. [219] also employed the flow cytometry method antibacterial activity of green synthesized AgNPs and has reported the death of multidrug resistant bacterial forms.

#### 12.2.5.1.5 Microscopy methods

**A) AFM analysis**

AFM technique can be used to evaluate cell integrity disruption of target microbial cells as a measure of antimicrobial property of test compound. This technique is reported by Ref. [220] for Catechin-CuNPs in which the sample is prepared by treated known microbial cell load with desired concentration of test compound. 200 μL treated cell suspension is taken in a microcentrifuge tube and cells harvested by centrifuging and the cell pellet is washed twice in ice cold Tris-HCl (pH 8.0, 2 mmol/L) and then resuspended in Tris-HCl. The cell suspension was placed on freshly cleaved mica substrate and dried under $N_2$ gas for 3 min. The image of sample is taken using AFM instrument and the topographic analysis of the bacteria with and without NPs was carried out for observing morphological changes. The parameter of surface roughness [mean roughness (Ra) and root-mean-square roughness (Rq)] was calculated using the software. The increase in surface roughness of treated cells as compared to untreated cells attributes to the membrane damage of the treated microbial cells.

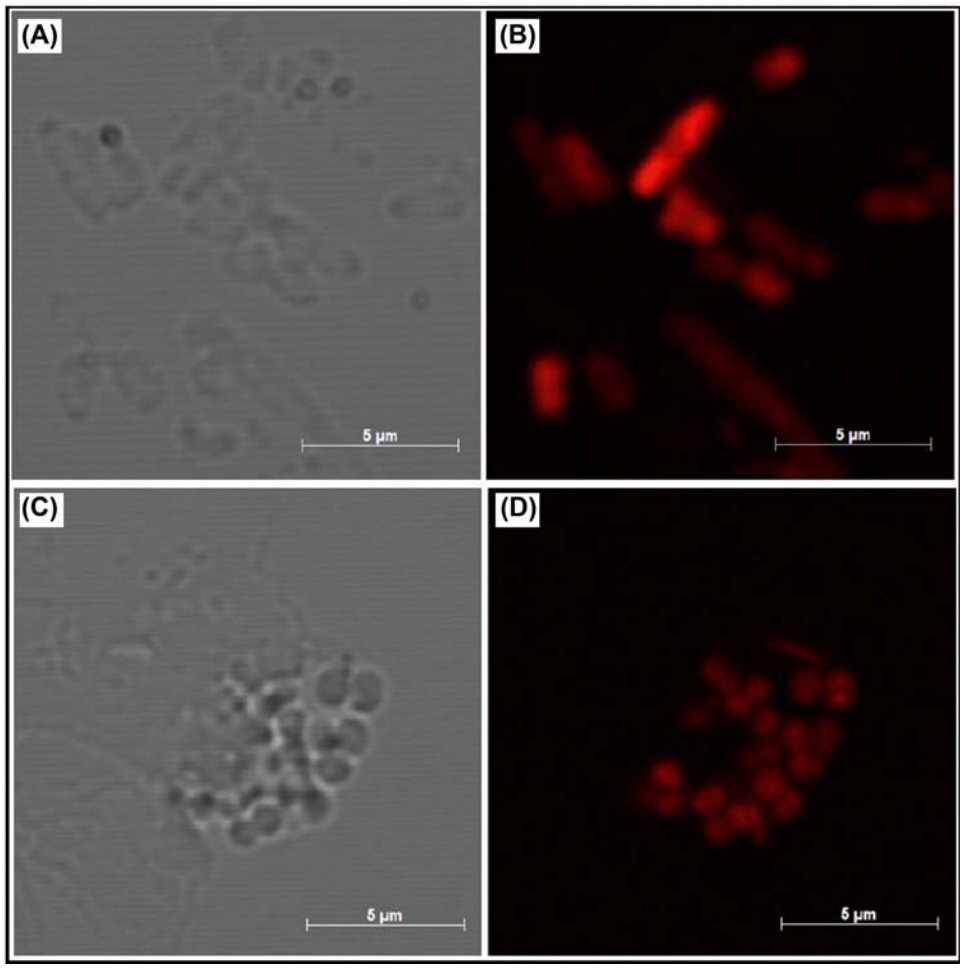


**Figure 12.4** Antimicrobial activity of NPs evaluated by flow cytometry technique using thiazole orange (TO) and propidium iodide (PI) stains wherein to stains live cells and PI stains dead cells. (A) Bright field image of *P. aeruginosa*, (B) fluorescence image of *P. aeruginosa*, (C) bright field image of *S. aureus*, (D) fluorescence image of *S. aureus*. These images indicate severe damage to the bacterial cells thus killing them when treated with AgNPs synthesized using *A. arborescens* leaf sap extract. Images (B) and (D) indicates cells stained with PI captured by fluorescence microscope. *(Figure reproduced from publication, S.S.D. Kumar, N.N. Houreld, E.M. Kroukamp, H. Abrahamse, Cellular imaging and bactericidal mechanism of green-synthesized silver nanoparticles against human pathogenic bacteria, J. Photochem. Photobiol. B Biol. 178 (2018) 259–269, Copyright Elsevier (2018).)*

### B) SEM analysis

SEM analysis is a technique applied to visualize the effects of antimicrobial agents and gives a visual insight of the membrane disruption and microbial cell killing effects of the antimicrobials. In this technique, mid log phase microbial cells are diluted in respective

culture media and desired concentration of test antimicrobial (synthesized NPs) is added to it and incubated under suitable temperature for 1 h. Untreated microbial cells are used as control. After incubation, the cells harvested by centrifugation at 3000 g for 5 min and then washed with sterile PBS twice. 2.5% glutaraldehyde in PBS (phosphate buffered saline) solution is added to the cells at room temperature for cell fixation for 2 h. The fixed cells are then collected and filtered through 0.2 μm filter. The filtered cells are then rinsed with PBS for 15 min twice and then dehydrated in ethanol solutions of increasing concentrations (30%, 50%, 70%, 80%, and 100%) for 10 min at each concentration. The cells are then dried by covering with hexamethyldisilazane as a drying agent. The cells are then sputtered with gold and analyzed and imaged with SEM instrument. Treated and untreated microbial cells are observed for cell morphology [221]. Ref. [222] reported the antimicrobial activity of AgNPs synthesized using *Aloe vera* plant extract using SEM analysis. Changes in the NPs treated bacterial cells were observed particularly in cell membrane displaying pores and thinning of the membrane. Ref. [223] carried out green synthesis of Ag and AuNPs stabilized with gum acacia (GA-AgNPs and GA-AuNPs) which were further loaded with two citrus fruits flavonoids Hesperidin (HDN) and Naringin (NRG) (GA-AgNPs-HDN and GT-AuNPs-NRG). The synthesized NPs were tested against human pathogens MRSA (methicillin-resistant *S. aureus*) and *E. coli* K1 by SEM analysis. It was observed that GA-AgNPs-HDN were bactericidal at 50 μg/mL against MRSA and 0.5 μg per mL against *E. coli* K1. However, GT-AuNPs-NRG did not show antibacterial activity at 50 μg/mL against the test pathogens (insert Fig. 12.5).

**C) TEM analysis**

TEM analysis is a microscopic technique applied in evaluating the antimicrobial nature of a compound by observing the effect of antimicrobial compound on the microbial cell and their probable bioaccumulation. Similar to sample preparation for SEM analysis, the target microorganism is treated with the desired concentration of the antimicrobial and incubated at suitable temperature conditions for 1−2 h. The cells are then harvested by centrifugation washed with PBS and fixed with 2% glutaraldehyde and the with 1% $OsO_4$ and then dehydrated and infiltrated in Spurr's resin. The samples are then sectioned (100 nm) with an ultramicrotome and slides mounted on mesh grids. The cells are then imaged and analyzed by TEM instrument [224]. Ref. [225] examined the antibacterial effect of synthesized AgNPs using aqueous extract of turmeric powder against pathogens *E. coli* O157:H7 and *Listeria monocytogenes* using TEM imaging (insert Fig. 12.6). It was observed that untreated cells were smooth and undamaged having regular cell walls with homogeneous cytoplasmic contents, whereas the AgNPs treated pathogen cell membranes showed abnormalities and protrusions. In many cells, cell membranes appeared fragmented and numerous gaps and pits were seen. The damage to the cell wall and cell membrane caused leaching out of cytoplasmic matter and thus caused death of the

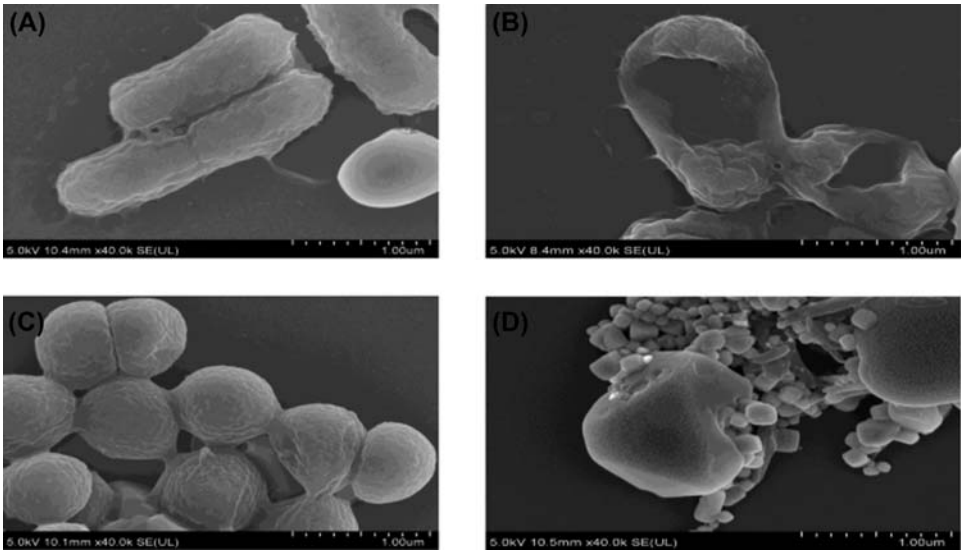


**Figure 12.5** Antimicrobial activity of synthesized NPs (AgNPs synthesized using gum acacia and further loaded with flavonoids Hesperidin viz. GA-AgNPs-HDN) against bacterial pathogens by SEM analysis: (A) *E. coli* K1 control cells (untreated cells), (B) *E. coli* K1 cells treated with NPs (0.5 μg/mL of GA-AgNPs-HDN), (C) MRSA control cells (untreated cells), (D) MRSA cells treated with NPs (50 μg/mL of GA-AgNPs-HDN). The NPs treated bacterial cells show cellular damage but the control cells appear undamaged with integrated cell membranes thus confirming the antibacterial nature of the NPs. *(Figure reproduced from A. Anwar, A. Masri, K. Rao, K. Rajendran, N.A. Khan, M.R. Shah, R. Siddiqui, Antimicrobial activities of green synthesized gums-stabilized nanoparticles loaded with flavonoids, Sci. Rep. 9 (1) (2019) 1–12 with permission from Scientific Reports and Springer nature publishers.)*

bacterium. Dense AgNPs precipitates were observed around the damaged cells, within the cytoplasm and even inside the cytoplasm of the damaged cells.

#### 12.2.5.1.6 DNA damage assays

Antimicrobial activity of the synthesized NPs can also be evaluated by DNA cleavage study that determines the effect of green synthesized NPs on the DNA of target microbe. A study by Ref. [176] has reported the DNA cleavage study of green synthesized CuO and Ag–CuO NPs prepared using *Malus domestica* leaf extract (insert Fig. 12.7). NPs solution of desired concentration was prepared and mixed with a target plasmid DNA (*E. coli* pBR322) and incubated at 37°C for 2 h. DNA was then electrophoresed using agarose gel electrophoresis technique. Untreated DNA was used as control. The DNA bands were visualized by Gel documentation instrument. It was observed that the NPs treated DNA lane showed smearing indicating the damage to the target bacterial DNA, whereas the untreated bands were intact. DNA damage assay of green synthesized AgNPs using cell-free filtrate of fungus *Macrophomina phaseolina* is demonstrated by

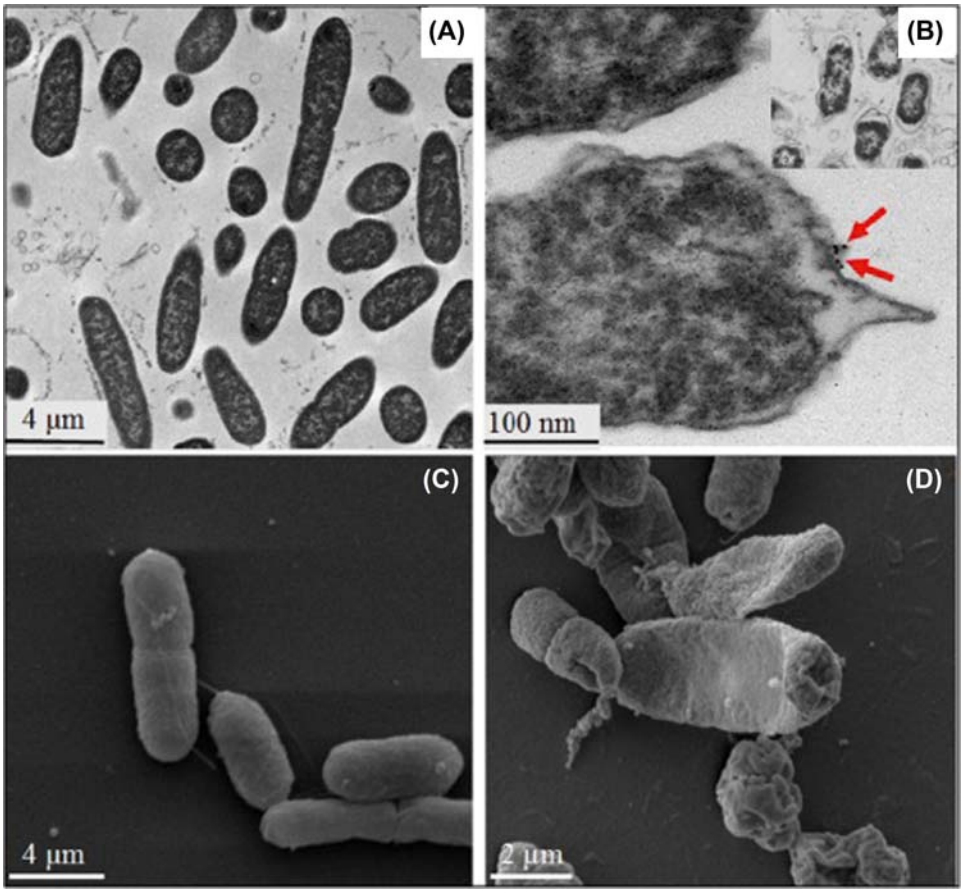


**Figure 12.6** Antimicrobial activity of synthesized AgNPs synthesized using aqueous extract of turmeric powder against bacterial pathogens *E. coli* O157:H7 and *Listeria monocytogenes* by TEM analysis: (A) *L. monocytogenes* control cells (untreated cells), (B) *L. monocytogenes* cells treated with AgNPs, (C) *E. coli* O157:H7 control cells (untreated cells) (D) *E. coli* O157:H7 cells treated with AgNPs. The AgNPs treated bacterial cells showed cellular damage and shrinkage but the control cells appear undamaged with integrated cell membranes. *(Figure reproduced from publication, F.K. Alsammarraie, W. Wang, P. Zhou, A. Mustapha, M. Lin, Green synthesis of silver nanoparticles using turmeric extracts and investigation of their antibacterial activities, Colloids Surf. B Biointerfaces 171 (2018) 398–405, Copyright Elsevier (2018).)*

Ref. [226] using the plasmid DNA pZPY112 (plasmid isolated from *E. coli* DH5α containing pZPY112 vector). The plasmid DNA treated with varied concentrations of synthesized NPs showed DNA strand breaks in a dose-dependent manner confirming its genotoxicity toward the target bacteria.

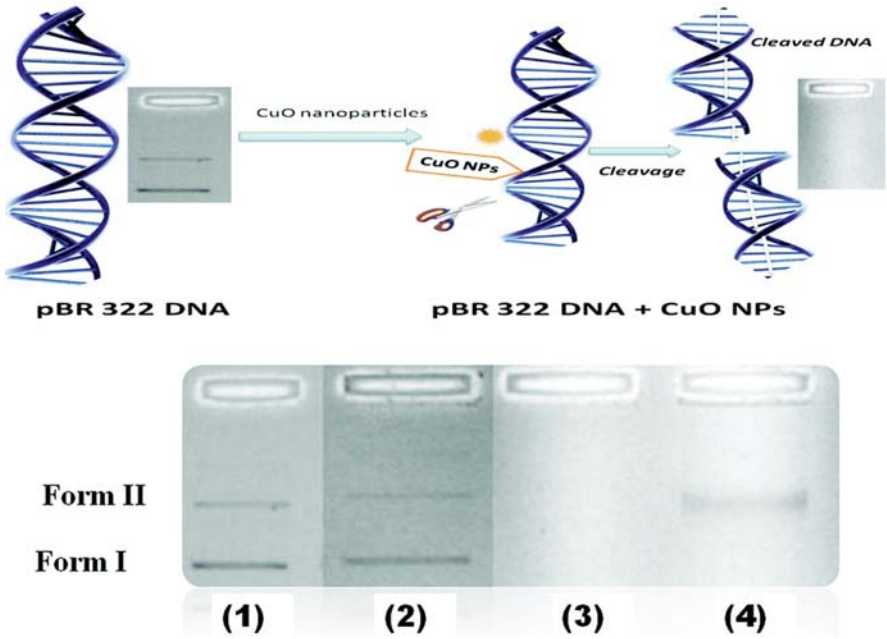


**Figure 12.7** DNA cleavage activity for determining antimicrobial activity of NPs: (1) lane 1: pBR322 DNA (untreated DNA); (2) lane 2: pBR322 DNA + *Malus domestica* leaf extract; (3) lane 3: pBR322 DNA + CuO NPs synthesized using *M. domestica* leaf extract; (4) lane 4: pBR322 DNA + Ag—CuO NPs synthesized using *M. domestica* leaf extract. Lane three and four shows complete shearing of DNA than lane two indicating antibacterial nature of the synthesized NPs that cleaves/denatures bacterial DNA observed as smearing of DNA band but *M. domestica* leaf extract did not show any effect on bacterial DNA. *(*Figure reproduced from M.S. Jadhav, S. Kulkarni, P. Raikar, D.A. Barretto, S.K. Vootla, U.S. Raikar, Green biosynthesis of CuO & Ag—CuO nanoparticles from* Malus domestica *leaf extract and evaluation of antibacterial, antioxidant and DNA cleavage activities, New J. Chem. 42 (1) (2018) 204—213 with permission from the Center National de la Recherche Scientifique (CNRS) and the Royal Society of Chemsitry.)*

### *12.2.5.2 Anticancer activity of green synthesized nanoparticles*

#### 12.2.5.2.1 In vitro anticancer studies

##### 12.2.5.2.1.1 Cytotoxicity assays

**A) MTT and MTS assay**

The preliminary anticancer activity of a compound is mainly assessed by in vitro cytotoxicity assays using 3-(4,5-dimethylthiazol-2-yl)-2,5-diphenyltetrazolium bromide (MTT) and 3-(4,5-dimethylthiazol-2-yl)-5-(3-carboxymethoxyphenyl)-2-(4-sulfophenyl)-2H-tetrazolium inner salt (MTS). These assays are most economic, easy to use, reliable, rapid, and convenient methods and also possess great sensitivity and specificity. These assays consider the colorimetric methods based on the reduction of tetrazolium salt MTT which is yellow colored to blue colored product formazan. The tetrazolium salt is

bio-reduced by mitochondrial dehydrogenase in the metabolically active cells forming formazan crystals that are further dissolved using solvents. In MTS assay, the bioconversion takes place by the same enzyme mitochondrial dehydrogenase that produces NADH or NADPH thereby reducing the colorless MTS salt to colored aqueous formazan. An electron coupling reagent phenazine ethosulfate or PES is added that generates a water-soluble formazan product, unlike MTT assay that needs solvents to dissolve formazan crystals. The quantity of the colored product which is measured colorimetrically reflects the metabolic rate of treated cells and is directly proportional to the number of live cells in the culture [56]. The MTT assay is performed by the method described by Ref. [227]. Briefly, cancerous cells to be tested against are cultured in RPMI-1640 medium with 10% fetal bovine serum or respective medium in 96 well microtitre plates. The cells are then treated with increasing concentrations of the NPs for various time intervals (0—48 h), while the controls received only DMSO (DMSO is widely used as a solvent in anticancer activities due to its low cytotoxicity, high stability, and membrane penetrating potential). Cells can also be treated with a standard drug as a reference molecule to check the efficacy of the synthesized NPs in comparison to the standard drug. 10 μL of MTT solution (5 mg/mL MTT stock solution prepared by dissolving in PBS buffer and then filter sterilized through 0.22μ syringe filter) is added to 100 μL of cell suspension in 96 well culture. The plates are incubated at 37°C for 48 h in $CO_2$ incubator. MTT containing medium is discarded and the cells washed with 200 μL PBS. The insoluble blue formazan crystals formed in the wells are then dissolved by adding 100 μL DMSO. The colorimetric estimation is performed on the micro-ELISA reader at 570 nm. The inhibitory concentration-50 ($IC_{50}$) values of the synthesized NPs calculated from the readings recorded. Noncancerous cell lines can also be tested for the cytotoxicity assays that will also evaluate the biocompatibility of the synthesized NPS.

Cytotoxicity percentage can be determined using the following equation:

$$\text{Viability\%} = \frac{\text{Test OD}}{\text{Control OD}} \times 100 \tag{12.1}$$

$$\text{Cytotoxicity\%} = 100 - \text{Viability\%} \tag{12.2}$$

A study by Ref. [228] depicted anticancer activity of AuNPs synthesized using marine bacteria *Enterococcus* sp. by MTT assay. The synthesized NPs showed anticancer activity against HepG-2 and lung cancer cell (A549) lines. The lowest inhibitory of 10 μg action was observed against A549 cell lines. A study by Ref. [229] depicted the anticancer activity of AgNPs synthesized using pigment phycocyanin extracted from *Nostoc linckia*. The synthesized NPs were tested against mammary gland breast cancer (MCF-7) cell line and % cytotoxicity was calculated by MTT assay. The synthesized AgNPs depicted good cytotoxicity to the cancer cell lines tested and the results disclosed similar

cytotoxicity values for the standard drug 5-FU (5-flurouracil as standard commercially available anticancer drug) used in the study. $IC_{50}$ of cell inhibition for synthesized AgNPs for cancer cell lines was observed at $27.79 \pm 2.3$ μg/mL and at $31.78 \pm 2.2$ and $32.97 \pm 1.7$ μg/mL for noncancerous cell lines tested against human lung fibroblast (WI38) and human amnion (WISH) cell lines, respectively, indicating the biocompatibility of the synthesized AgNPs. Cytotoxic effect of the synthesized AgNPs using a marine algae *Chaetomorpha linum* extract was reported by Ref. [230] against colon cancer cell lines HCT-116 by MTT assay. The green synthesized AgNPs were also compared for cytotoxicity against the same cell lines for $AgNO_3$ and *C. Linum* extract and observed that green synthesized AgNPs exhibited significant cytotoxicity with cytotoxic concentration ($CC_{50}$) of $48.84 \pm 0.78$ and $32.75 \pm 1.02$ μg/mL after 24 and 48 h, respectively, but the cytotoxicity was higher for $AgNO_3$ with $125.23 \pm 1.21$ and $102.57 \pm 1.09$ μg/mL and *C. Linum* extract with $135.09 \pm 2.51$ and $119.26 \pm 0.48$ μg/mL after 24 and 48 h, respectively. A study by Ref. [231] reported anticancer potential of AgNPs synthesized using *Abelmoschus esculentus* (L.) pulp extract as reducing and a stabilizing agent for the synthesis using MTT assay. Anticancer activity is tested against Jurkat cell line or Human T-cell lymphoma and depicted $IC_{50}$ value of AgNPs as 16.15 μg/mL. The dose-dependent cytotoxicity study indicated that at 10, 25 and 50 μg/mL the cell viability decreased by 52.6, 85.4 and 91.6% respectively. The study also revealed that the pulp extract alone does not bear anticancer property and the anticancer property is due to synthesized AgNPs.

**B) Trypan blue dye exclusion assay**

The dye exclusion assay in another type of in vitro cytotoxicity assay that determines the number of viable cells. A cell suspension is mixed with trypan dye and the cells are observed to analyze whether the cells have taken up the dye or not. Live cells exclude the dye due to their intact cell membranes but dead cells take up the dye and thus live cells show clear cytoplasm, whereas dead cells show cytoplasm stained blue. The cytotoxicity assay for evaluation of anticancer potential of green synthesized NPs was reported by Ref. [170] wherein AgNPs, FeNPs, and AuNPs were synthesized using lycopene extracted from tomato against colorectal and cervical cancer cell lines HT-29 cells, COLO320DM, and HeLa cell lines. Briefly, 50 μL of each cell lines were taken in three different microcentrifuge tube and incubated for 3 min. 50 μL of synthesized NPs (100 μg/mL) was added to each tube and incubated in $CO_2$ incubator for 3 min. After incubation, 50 μL Tryphan blue dye (0.4%) was added in each tube and incubated for 3 min in $CO_2$ incubator and analyzed for total viable cells and nonviable cells by using Neubauer's slide. The results indicated inhibition % of $79.44 \pm 0.4967$, $64.8 \pm 0.4172$ and $83.45 \pm 0.4694$ for AgNPs, FeNPs and AuNPs respectively against COLO320DM; $88.05 \pm 0.1870$, $67.86 \pm 0.2661$ and $80.72 \pm 0.8134$ % for AgNPs, FeNPs and AuNPs respectively against HT29, and $65.47 \pm 0.4766$, $64.76 \pm 0.4115$ and $57.51 \pm 0.4805$% for AgNPs, eNPs and AuNPs respectively against HeLa cell lines.

The results indicated viability % of 21.28 ± 0.2902, 33.93 ± 0.6697 and 16.31 ± 0.3922 for AgNPs, FeNPs and AuNPs respectively for COLO320DM; 12.08 ± 0.0946, 30.76 ± 0.7734 and 18.74 ± 0.4422 % for AgNPs, FeNPs and AuNPs respectively for HT29, and 36.05 ± 0.7071, 35.5 ± 0.4215 and 42.4 ± 6191% for AgNPs, eNPs and AuNPs respectively for HeLa cell lines.

**C) Morphology studies by Cell imaging**

The morphological changes in the cancer cells treated with an anticancer agent can be observed by microscopy. Target cancer cells should be treated for 24 h using previously established $IC_{50}$ doses of synthesized NPs. Morphology changes can be assessed by phase contrast microscopy. Images of NPs treated cancer cells as well as non-NP-treated control cells are taken at the end of the experiment and analyzed. The images should notably depict reduction in size and abnormally shrunken NPs treated cancer cells as compared to non-treated cancer cell lines and also non-cancer cell lines [232]. A study by Ref. [161] depicted the anticancer activity of $Fe_2O_3$/Ag@$Fe_2O_3$ nanocomposites synthesized using *Adathoda vasica* leaf extract against MB-231 human adenocarcinoma cell lines (insert Fig. 12.8). The cells upon MTT cytotoxicity assay were taken and observed using phase contrast microscope and imaged. The untreated cancer cells show damage and abnormalities as compared to synthesized AgNPs treated cell lines.

**D) Cell lactate dehydrogenase (LDH) leakage**

The effect of anticancer compound on the growth of the cancer cells can be determined by quantification of cancer cell death, based on the measurement of LDH activity released from the cytosol of damaged cells into the supernatant. LDH is a stable cytosolic enzyme and its leakage indirectly defines the weak or damaged cell membrane integrity which is commonly associated with necrosis. The released enzyme reacts with the iodonitrotetrazolium violet to form a red formazan product which is then measured at 490 nm by colorimetric methods. The intensity of color is directly proportional to the number of lysed cells. LDH leakage assay is reported by Ref. [4] for AgNPs synthesized using Actinobacterial strain SF23 for evaluation of anticancer nature of the synthesized AgNPs against RAW 264.7 macrophages and MCF-7 breast cancer cells. Cells were cultured in a 96-well microtitre plate in 100 μL of the appropriate culture medium for 24 h at 37°C and 5% $CO_2$. The medium was replaced with medium containing various concentration of synthesized AgNPs. 50 μL of supernatants were transferred to the new wells of 96-well plate. 50 μL of freshly prepared CytoTox 96 Reagent (Promega) or the particular reagents is added and mixed thoroughly and incubated for 30 min at RT in the darkness and absorbance measured at 490 nm with plate reader. The results showed $IC_{50}$ values 102.3 and 76.2 μg/mL for RAW 264.7 and MCF-7 cells, respectively.

#### 12.2.5.2.1.2 In vitro cell proliferation assay

**A) Clonogenic assay:**

Clonogenic assay, an in vitro cell proliferation assay, is performed to investigate the effect of anticancer compounds by studying the inhibition of colony formation of cancer cells. As the cancer cells have the potential to grow in colonies showing cell to cell

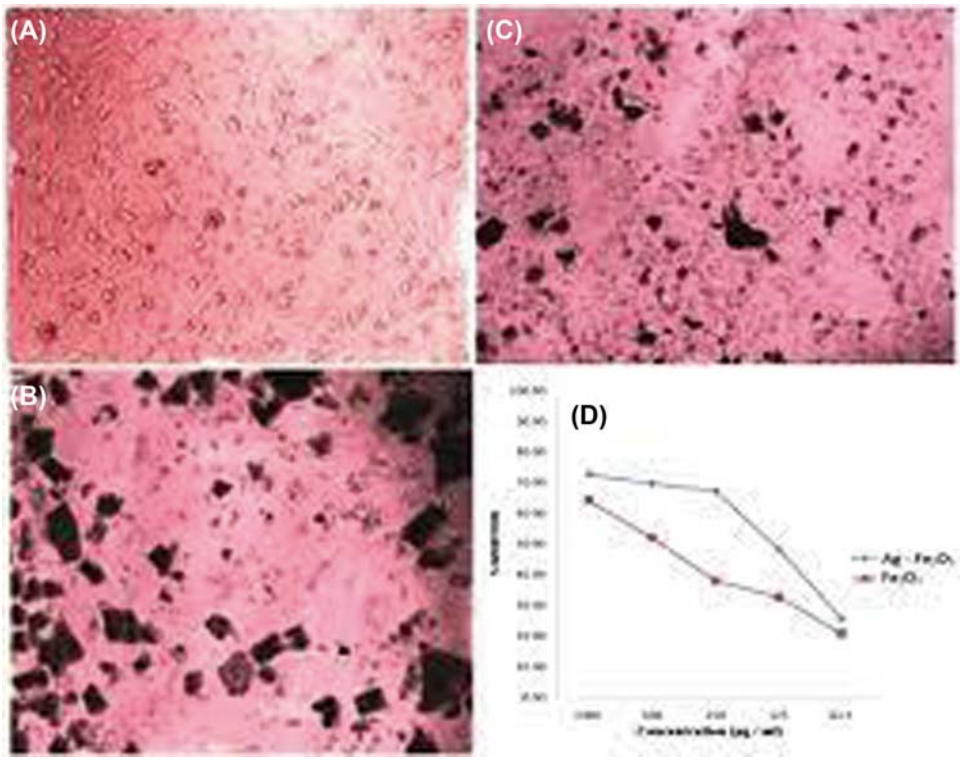


**Figure 12.8** In vitro anticancer activity by MTT assay for NPs. (A) control cells (MDA-MB-231 human adenocarcinoma cell line); (B) MDA-MB-231 cell line treated with $Fe_2O_3$ NPs synthesized using *Adathoda vasica* leaf extract; (C) MDA-MB-231 cell line treated with Ag@$Fe_2O_3$ NPs synthesized using *Adathoda vasica* leaf extract. Ag@$Fe_2O_3$ showed better cytotoxic effect against the breast cancer cells as compared to $Fe_2O_3$ NPs. *(Figure reproduced from S. Kulkarni, M. Jadhav, P. Raikar, D.A. Barretto, S.K. Vootla, U.S. Raikar, Green synthesized multifunctional Ag@$Fe_2O_3$ nanocomposites for effective antibacterial, antifungal and anticancer properties, New J. Chem. 41 (17) (2017) 9513–9520 with permission from the Center National de la Recherche Scientifique (CNRS) and the Royal Society of Chemsitry.)*

contact with the adjacent cells. Anticancer agents have the tendency to break the cell to cell contact with the neighboring cells and thus can result in the cancer cell death thereby inhibiting the cancer cell proliferation. In this experiment, test cells are seeded (500 cells/mL) in a 12 well microtitre plate in a respective medium and incubated under optimum conditions for 24 h or until the doubling time for the cell growth. Cells are treated with various concentrations of the anticancer compounds and incubated at desired conditions for 48 h. The medium is discarded and fresh medium is added to the wells containing the treated cells and incubated for 1 week or more based upon the size and number of cell colonies. The medium needs to be replaced every third days while incubation. The incubation should be terminated once the colonies in the untreated wells are of optimum size and are not mixed with neighboring colonies. The medium is removed and the cells

washed with PBS and then the cells are fixed with 500 μL 100% ice cold methanol and incubated at −20°C for 15−20 min. The cells are again washed with PBS after discarding the methanol. The cells are stained with 500 μL Coomassie blue or Giemsa or Crystal violet or trypan blue stain (0.5% in $H_2O$) to cover the cells completely and incubated for 15−30 min and then washed with PBS twice. The plates are then air dried and images are captured. The number of colonies in each well is counted under the microscope [233]. The relative cell surviving fraction can be calculated from plating efficiency (PE) as follows:

$$\text{Plating efficeincy (PE)}\% = \frac{\text{No. of colonies formed}}{\text{No. of cells seeded}} \times 100 \tag{12.3}$$

$$\text{Surviving fraction (SF)}\% = \frac{\text{No. of colonies formed after treatment}}{\text{No. of cells seeded}} \times \text{PE} \tag{12.4}$$

A study by Ref. [234] depicted in vitro cell proliferative activity of AgNPs synthesized using aqueous extracts of *Ginkgo biloba* leaves by Clonogenic assay against cervical cancer cells and observed through microscopic imaging that the green synthesized AgNPs significantly decreased cellular attachments in HaLa and SiHa cells that were treated with AgNPs as compared to untreated cancer cells indicating that the synthesized AgNPs suppressed the cancer cell proliferation. Ref. [235] indicated the anticancer nature of magnetic iron oxide nanoparticles (MNPs) synthesized using *Albizia adianthifolia* leaf extract against human breast carcinoma cell AMJ-13 and MCF-7 using Clonogenic assay and observed that synthesized NPs significantly reduced the number of colonies of AMJ-13 and MCF-7 cells.

#### 12.2.5.2.1.4 Gel electrophoretic assays

**A) Comet assay**

Comet assay also termed as single cell gel electrophoresis (SCGE) assay measures transient genetic damage. It detects any single or double stranded breaks in the DNA. This assay can be conducted via both approaches in vitro using cell lines and in vivo using cell suspension from tissues. The comet assay was first described by Ref. [236] and is widely used to study genotoxicity of various compounds to both cancer and non-cancer cells. In this assay, when a cell suspension with damaged DNA is electrophoresed, the damaged DNA migrates away from the nucleoid body with undamaged DNA and thus resembles the structure of a comet. In this technique, the undamaged DNA in nucleoid is referred to as head and the trailing damaged DNA as tail like that of the comet structure. The analysis of Comet assay is then done by a method reported by Ref. [237] which calculates the Arbitrary Unit (AU) to express the extent of DNA damage. Based on the extent of DNA migration, the cells are classified in five categories as class 0 (undamaged), class 1 as very little damage, class 2 as moderate damage, class 3 as high damage, and class 4 as ultrahigh damage.

A study by Ref. [238] has employed Comet assay for evaluating the anticancer nature of carbon-based NPs or carbon dots synthesized using *Nerium oleander* leaves extract against human breast adenocarcinoma cell line (MCF7). It was observed that higher DNA damage was observed in the NPs treated cancer cell lines as compared to untreated cancer cells thus indicating the genotoxicity of synthesized NPs to cancer cells.

The comet assay is also widely used to determine the genotoxicity of various test compounds. In vitro genotoxicity of the AuNPs synthesized using latex from *Hevea brasiliensis* was assessed by Ref. [171] against non-cancerous cells. Briefly, cells (Chinese hamster ovarian (CHO-K1) cells) were seeded in a 12-well microtitre plate with Dulbecco's Modified Eagle's Medium/F10 Ham (1:1) media supplemented with 10% fetal bovine serum. Cells were then treated with desired concentrations of the synthesized NPs and incubated under optimum conditions for a period of 24, 48, or 96 h. After incubation, cell suspension was used for comet assay. It was observed through this study that lowest concentration and lower time did not show DNA damage and hence are not toxic to cells at lower concentration and thus are biocompatible. To evaluate the genotoxicity of synthesized AgNPs using *Streptomyces roseolus* was reported by Ref. [239] by Comet assay. Cells (Peripheral Blood Lymphocytes normal cells) were seeded with RPMI-1640 medium and treated with various concentrations of the synthesized NPs and incubated at desired conditions. The cells were then washed with PBS and seeded in 1% low dissolving agarose and then overlayered on 1% typical agarose and allowed to solidify. The slides are then placed in lysis buffer overnight at 40°C and then in unwinding buffer at 40°C for 40 min. The slides were then electrophoresed and finally neutralized using 0.4 M Tris buffer. The slides were then stained with ethidium bromide (EtBr) and observed using UV light. The tail intensity (%), head intensity, and tail moment were then assessed. It was observed in this experiment that no tail formation and no DNA fragmentation was seen thus indicating the safe use or consumption of these NPs in therapy.

**B) DNA fragmentation assay**

Apoptotic pathways are well studied in cancer research. Apoptosis caused a number of distinctive changes in the cancer cells including fragmentation of DNA, cell shrinkage, and plasma membrane blebbing. The DNA fragmentation is one of the widely studied consequences of apoptosis and is performed by the enzyme caspase-activated DNase (CAD) which is activated by the caspase cascade. This enzyme cleaves the DNA at specific sites (internucleosomal linker sites) thereby generating DNA fragments of ~200 base pairs which are referred to as DNA ladders. Through agarose gel electrophoretic technique, these DNA ladders can be examined. The DNA fragmentation technique was explored by Ref. [240] for AuNPs synthesized using marine macroalgae, *Padina gymnospora*. The apoptosis was studied using two cancer cells lines, Human hepatocellular liver carcinoma (HepG2) and Human lung adenocarcinoma epithelial cell line (A549). Briefly, cells were seeded in 96-well microtitre plates with Dulbecco's modified Eagle medium (DMEM) and incubated at specific conditions for 48 h. The medium discarded

from each well and washed twice with the DMEM. Cells were exposed to varied concentrations of the synthesized AuNPs prepared in DMEM while the control (untreated cells) wells received 0.25% DMSO. The plates were again incubated for 48 h under optimum conditions. The AuNPs treated and untreated cells were subjected for DNA isolation by following the DNA extraction procedures for animal cells. The isolated DNA samples were subjected to Agarose gel electrophoresis technique with 1% Agarose gel containing EtBr. The gel was then observed and imaged under a UV transilluminator or using a Gel-doc instrument. The results indicated that the cancer cells treated with the synthesized NPs exhibited higher DNA ladder smearing appearance as compared to the untreated cells thereby confirming apoptosis in AuNPs treated cancer cells.

**12.2.5.2.1.4 Flow cytometry for cell cycle and apoptosis analysis** The apoptosis induction of anticancer agents on cancer cells can be confirmed by flow cytometry technique for Apoptosis assay using annexin V-FITC (Annexin-V-Fluorescein-5-isothiocyanate) and PI (propidium iodide) staining method. The cancer cells treated with the synthesized NPs for 48 h were harvested for the assay. For the cell cycle assay, the cells are suspended in PBS and fixed in ice-cold 70% ethanol at −20°C for 12 h. The fixed cells are further incubated for 15 min with staining buffer containing 50 μg/mL PI and 10 μg/mL DNase-free RNase. The cells are then analyzed by Flow cytometry. In order to perform the apoptosis assay, the cells were rinsed with PBS. The rinsed cells were suspended in annexin V-FITC and PI buffer for 15 min in dark and then apoptotic cells are counted using a Flow Cytometer system [241]. The anticancer potency by flow cytometry for Apoptosis was depicted by Ref. [242] for green synthesized AgNPs using *Enteromorpha compressa* against Human Colon Cancer Cell HCT-116 and observed that the cancer cells treated with the synthesized NPs induced and increased early and late apoptosis in comparison to the untreated cancer cells. The Annexin-fluorescein-5-isothiocyanate (FITC)-phycoerythrin (PE) staining was performed in this assay. Ref. [243] reported cell cycle analysis of AgNPs synthesized using *Nepeta deflersiana* against Human Cervical Cancer Cells (HeLA) by flow cytometry. It was observed that HeLa cells exposed to synthesized AgNPs treatment showed increased apoptosis as compared to the untreated cells. Increased apoptotic SubG1 peak was observed suggesting cells were arrested at subG1 at 50 μg/mL AgNPs and did not undergo G2 and thus G2/M transition was affected.

### 12.2.5.2.2 In vivo anticancer activity

**A) In vivo cytotoxicity assays**

The procedure for in vivo cytotoxicity assay for evaluation of anticancer potential is reported by Ref. [229] for AgNPs synthesized using a proteinaceous pigment phycocyanin extracted from *Nostoc linckia* as reducing agent. Albino adult Swiss male mice with 20−25 g weight were used as animal model and were maintained under controlled environment in the laboratory conditions. The researchers used Ehrlich ascites carcinoma

(EAC) cells for cancer induction in the animal model. The experiment was carried out in four groups with group I as negative control which received only physiological saline (0.9% NaCl) on day 0; group II were injected with EAC cells on day 0 and served as positive control; group III were injected with EAC cells on day 0 and 5-FU after 24 h of EAC injection and served as positive control; group IV were injected with EAC cells on day 0 and AgNPs (5 mg/kg body weight) after 24 h of EAC injection and served as test. The inoculation process was repeated for 10 days and half of the mice in each group were kept on fasting state and were weighed individually and sacrificed at 24 h of the last dose. Blood estimation including RBC count, WBC count, and hemoglobin estimation was performed from each group upon blood collection from the sacrificed mice. The tumor cell volume and their count were also estimated upon collecting the ascetic fluid from the peritoneal cavity of the mice. Trypan blue staining was carried out for the tumor cells for counting the viable and nonviable cells by centrifuging part of the ascetic fluid and packed cell volume was measured from the remaining ascetic fluid by centrifuging the ascetic fluid in a graduated centrifuge tube at 1000 rpm for 5 min. Body weights of the mice were recorded both in the treated and control groups from day 0 to day 11. It was observed through this study that the hemoglobin content and RBC count in group II had reduced significantly being developed cancer as compared to group I. The Hb content and RBC count in group IV was similar to group I and slightly lesser in group III in comparison to group IV. WBC count was observed to have increased in group II in comparison with group I. WBC count was lesser in group IV than group III as compared to group II. Also, decrease in tumor cell count, body weight, and tumor volume was observed in group IV than in group II. The results indicated that the synthesized AgNPs were significant in fighting the cancer cells than the standard drug 5-FU. (Note: Ethical clearance statement needs to be submitted after approval from the Research ethics committee if working with animal models. The experiments should be performed as the guidelines and regulations provided by the committee.)

#### *12.2.5.3 Antioxidant activity of green synthesized nanoparticles*

The methods for evaluating antioxidant activities fall in three categories: spectrometry methods, electrochemical assays, and chromatography methods [244]. Among these in vitro methods, spectroscopic methods are widely employed for evaluating the antioxidant potential of green synthesized NPs and thus are discussed below:

##### 12.2.5.3.1 In vitro spectrometry methods

A number of tests can be performed under this category for evaluation of in vitro antioxidant property. The tests are as listed below:

**A) ORAC (Oxygen radical absorption capacity):**

This test is used to report the inhibition of oxidation of peroxyl radical. It uses azo-compounds (e.g., 2,2′-azobis(2-amidinopropane) dihydrochloride (AAPH)) for the generation of peroxyl radical, the generated peroxyl radical further reacts with fluorescent

molecule (fluorescein or phycoerythrin) that leads to loss of fluorescence. A study by Ref. [245] evaluated the antioxidant activity of AgNPs synthesized using aqueous extract of *Solanum mammosum* and also compared the antioxidant activity of synthesized AgNPs with *S. mammosum* aqueous leaves extract by ORAC-fluorescence method. Briefly, various concentrations of samples (synthesized AgNPs and leaves extract) to be analyzed for antioxidant activity were added to the 96-well microtiter plate and incubated with 150 μL of fluorescein solution (40 nM) at 37°C for 5 min. 25 μL of AAPH solution (18 mmol/L) was added. The fluorescence was recorded using microplate reader every 2 min for 2 h at 37°C with an emission filter of 528/20 and excitation wavelength of 485/20 nm. The results were expressed as μmol/L Trolox equivalent/gram (TE/g) of sample. A Trolox calibration curve was used with a concentration range between 3 and 20 μmol/L. However, in this study the antioxidant activity of synthesized AgNPs was observed to be 637.5 ± 14.8 μM TE/g of sample which was comparatively reduced as compared to that of leaf extract which showed 3944 ± 112 μM TE/g of sample.

**B) HORAC (Hydroxyl radical antioxidant capacity): HORAC (Hydroxyl radical antioxidant capacity):**

This method is based on the principle that hydroxyl radicals oxidize fluorescein by a classic hydrogen atom transfer mechanism. The hydroxyl (·OH) radicals are first generated by $H_2O_2$ that further quench the fluorescence of fluorescein over time. The fluorescence generated is then measured by fluorometry. This assay can also be performed by colorimetry using salicylic acid. In this method, ·OH radicals are generated by Fenton' reaction. The ·OH radicals further attack salicylate producing major oxidation products like 2,3-dihydroxybenzoate, 2,4-dihydroxybenzoate, and 2,5-dihydroxybenzoate that can be measured colorimetrically. A Study by Ref. [246] reported the hydroxyl radical antioxidant capacity for AgNPs synthesized using *Brassica oleracea* leaf extract. The reaction mixture was prepared with 1 mL of salicylic acid (9 mM), 1 mL ferrous sulfate (9 mM), and 1 mL $H_2O_2$, mixed thoroughly and 1 mL of various concentrations of synthesized AgNPs were added to respective tubes. The tubes were incubated for 60 min at 37°C in boiling water bath. The hydroxyl radical activity was recorded as 71% at 200 μg/mL synthesized AgNPs concentration and was comparatively lesser than the standard ascorbic acid (98% at 200 μg/mL).

**C) TRAP (Total peroxyl radical trapping antioxidant parameter):**

This assay measures the potency of antioxidant compound to inhibit the reaction between peroxyl radicals and a target molecule. AAPH and peroxidase are generally used as peroxyl radical generators and target molecules as fluorescein, dihydrofluorescein diacetate (DCFH-DA) or luminol. In the assay involving chemiluminescence, luminol-enhanced chemiluminescence is used in monitoring the reactions. The chemiluminescence signal is driven by the production of luminol-derived radicals resulting from the thermal decomposition of AAPH. By this method, TRAP value is calculated from the duration of the time period during which the sample quenches the

chemiluminescence signal. TRAP procedure by chemiluminescence can be carried out as described by Ref. [247] that used 2,2-azo-bis-2amidinopropane hydrochloride (ABAP) as peroxyl radical generator. Briefly, the reaction was carried out by mixing 475 μL of PBS (100 mM, pH 7.4), 50 μL of 10 mM luminol in 100 mM borate buffer (pH 7.4), and 20 μL of a sample and incubated at 37°C for 10 min in a temperature-controlled carrousel of the luminometer. 50 μL of 400 mM ABAP were added to start peroxyl radical generation. The TRAP value was then determined from the period of time, during which the samples quenched the chemiluminescence signal due to the antioxidants present in the NPs sample. Trolox (8 nM) was used as a reference/standard compound.

**D) CUPRAC (Cupric reducing antioxidant power) assay:**

This test measures the reducing power of cupric ($Cu^{2+}$) to cuprous ($Cu^{+}$) ions. Neocuproine (Nc; 2,9-dimethyl-1,10-phenanthroline) is a commonly employed ligand in CUPRAC assay for the formation of copper–ligand complex to facilitate the measurement of absorbance. A study by Ref. [248] demonstrated the antioxidant potential of green synthesize AgNPs using *Morinda lucida* plant extracts by CUPRAC method. In this method the reaction mixture was prepared with 0.25 mL $CuCl_2$ solution (0.01 M), 0.25 mL ethanolic neocuproine solution ($7.5 \times 10^{-3}$ M), and 0.25 mL acetate buffer (1 M) and further 0.25 mL samples (synthesized NPs/crude extract/standard) were added and mixed thoroughly in, respectively, labeled tubes. The reaction mixture was diluted with distilled water to get total reaction volume 2 mL. The test tubes were incubated at room temperature (RT) for 30 min and the absorbance was measured at 450 nm. Trolox was used as the standard. Increased absorbance indicated greater reduction potential, which was represented as Trolox equivalent (TEAC). It was observed that synthesized AgNPs showed higher antioxidant capacity of $65.62 \pm 1.07$ mg TE/g sample that was 40% higher than the crude extract which was estimated as $28.63 \pm 1.03$ mg TE/g sample.

**E) FRAP (Ferric reducing antioxidant power):**

This test evaluates the antioxidant property of compounds based on the reduction of ferric ions to ferrous ions. The antioxidants bind to $Fe^{3+}$ ions linked to a ligand (e.g., tripyridyltriazine (TPTZ) or ferrozine) in acidic environments reducing it to intense blue ($Fe^{2+}$)-complex which is then determined colorimetrically at 593 nm. Increased absorbance at 593 nm is related to better antioxidant efficacy. The experiment can be performed as follows: 0.75 mL of various concentrations of NPs is mixed with 0.75 mL phosphate buffer 0.2 M, pH 6.6, and 0.75 mL of 1% potassium hexacyanoferrate [$K_3Fe(CN)_6$]. The reaction mixture is incubated at 50°C in a water bath for 20 min. 0.75 mL trichloroacetic acid (10%) is added to stop the reaction. The solution is then centrifuged at 3000 r/min for 10 min and 1.5 mL supernatant and mixed equal volume of distilled water and finally 0.1 mL of 0.1% ferric chloride ($FeCl_3$) is added and incubated for 10 min at RT and absorbance recorded at 700 nm as the reducing power. Ascorbic

acid was used as a standard. Increased absorbance indicates higher reducing power. Ref. [249] reported the antioxidant nature of AgNPs synthesized using *Acanthospermum australe* (Loef.) leaves extract by FRAP assay. The results depicted that the green synthesized AgNPs possessed higher ferric reducing power (596 ± 10) than the leaf extracts (279 ± 1) and no activity for $AgNO_3$ used for synthesis. Ref. [250] reported the antioxidant activity of AgNPs synthesized from the aerial parts of *Lippia nodiflora* by FRAP method. The synthesized AgNPs exhibited the reducing power of 0.115 at concentration 500 μg/mL, which was found to be higher as compared to that of the standard BHT (butylated hydroxyl toluene) used in this study which was estimated as 0.095 at concentration 500 μg/mL.

**F) PFRAP (Potassium ferricyanide reducing power):**

Similar to FRAP assay, PFRAP determines either the reduction of ferric ions to ferrous ions or reduction of ferricyanide to ferrocyanide by antioxidants. In this test potassium ferricyanide is used as the ferric reagent. The resulting Prussian blue colored complex is the result of binding of $Fe^{2+}$ to ferricyanide or binding of free $Fe^{3+}$ ions available upon reduction of ferricyanide to ferrocyanide. The antioxidant activity of AgNPs synthesized using methanolic leaf extract of *Blighia sapida* was explored by Ref. [251] using PFRAP method. Various concentrations of synthesized NPs were mixed with 2.5 mL phosphate buffer (0.2 M, pH 6.6) and 2.5 mL of 1% potassium ferricyanide and incubated at 50°C for 20 min. 2.5 mL of 10% trichloroacetic acid was added and then centrifuged for 10 min at 3000 rpm. 2.5 mL of supernatant was mixed with 2.5 mL distilled water and 0.5 mL of 0.01% $FeCl_3$. Ascorbic acid was used as the standard. The absorbance was measured at 700 nm. The results indicated a maximum reducing capability of 53.52% at 150 μg/mL for synthesized AgNPs which was lower than that of standard ascorbic acid which was 70.19%.

**G) ABTS (2,2′-azinobis-(3-ethylbenzothiazoline-6-sulfonic acid) radical scavenging percentage:**

This test is based on the neutralizing capacity of $ABTS^{\cdot+}$ (a stable radical cation) by antioxidants. $ABTS^{\cdot+}$ is a blue-green chromophore that is formed in the presence of powerful antioxidant from ABTS. $ABTS^{\cdot+}$ gives maximum absorption at 734 nm but the neutralizing power of antioxidants causes discolouration of the blue-green chromophore leading to a drop in absorbance. A study by Ref. [71] reported the antioxidant activity of AgNPs synthesized using *Punica granatum* leaf extract by ABTS method. ABTS salt (7.0 μM) was mixed with potassium persulphate (2.45 μM) and incubated in the dark at 25°C for 16 h to generate $ABTS^{\cdot+}$. Some volume of $ABTS^{\cdot+}$ solution was mixed with 80% ethanol to get the absorbance between 0.700 ± 0.005 at 734 nm. 0.2 mL of various concentrations of synthesized AgNPs were added to 2 mL diluted $ABTS^{\cdot+}$ solution and mixed thoroughly. Absorbance was read at 734 nm. Ascorbic acid was used as a standard. The results were expressed as the $IC_{50}$ values. The following equation is used for the calculation and was observed that $ABTS^{\cdot+}$ radicals scavenging percentage of the

green synthesized AgNPs increased with increasing concentration and showed the $IC_{50}$ value of 52 μg/mL

$$\text{Free radical scavenging } (\%) = \frac{A_0 - A_1}{A_0} \times 100 \tag{12.5}$$

where $A_0$ is absorbance of control and $A_1$ as absorbance of the test sample.

**H) DPPH ([2,2-di(4-tert-octylphenyl)-1-picrylhydrazyl]) free radical scavenging activity (%):**

This test alike ABTS determines the neutralizing effect of antioxidants. A π-radical DPPH· is formed from DPPH that produces deep purple coloration and maximum absorbance at 517 nm. The neutralizing effect of antioxidants leads to drop in absorbance due to discolouration and forms a deep yellow colored solution. DPPH· radical shows similarity with peroxyl radicals ROO· and hence is widely used. Ref. [176] demonstrated antioxidant activity of CuO and Ag—CuO NPs synthesized using *Malus domestica* leaf extract by DPPH free radical scavenging activity and calculated the $IC_{50}$ values as 45.90 and 52.78 μg/mL for CuO and Ag—CuO, respectively. Briefly, 2 mL DPPH solution (0.1 mM in methanol) was added to 1 mL of desired concentrations of synthesized NPs and incubated at RT for 30 min. Ascorbic acid was used as standard. Absorbance was recorded at 517 nm after incubation. The % DPPH free radical scavenging activity was calculate using Eq. (12.5).

**I) Nitric oxide radical-scavenging assay:**

In this assay, the nitric oxide radicals generated from sodium nitroprusside are measured by Greiss reagent. The nitric oxide radicals formed are scavenged by antioxidants and thus absorbance decreases. A study by Ref. [252] reported the nitric oxide scavenging activity of AuNPs synthesized from marine seaweed extract *Acanthophora spicifera*. Concisely, various concentrations of synthesized NPs were prepared with sodium nitroprusside solution (10 mM) and incubated at 25°C for 150 min. 1 mL Griess reagent (1% sulfanilamide in 5% o-phosphoric acid and 0.1% 1-naphthylethylenediamine dihydrochloride in water) was added and incubated at 25°C for 30 min. The absorbance was read at 540 nm. The nitric oxide radical scavenging activities were calculated using Eq. (12.5). Ascorbic acid was used as a standard. *A. spicifera* extract was also tested for antioxidant activity. It was observed that the highest scavenging effect of $NO_2$ for the synthesized AuNPs was 59.2% at the concentration of 500 μg/mL. The $NO_2$ radical scavenging activity for *A. spicifera* extract was found to be 39.8% at the concentration of 500 μg/mL, thus the synthesized AuNPs showed better antioxidant activity as compared to that of the extract.

**J) Superoxide anion radical-scavenging assay:**

Superoxide anions are one of the strongest ROS generated that directly or indirectly damage biomolecules. In the superoxide radicals scavenging assay, superoxide radicals are generated in Phenazine methosulfate-Nicotinamide adenine dinucleotide (PMS/

NADH) system. The generated radicals reduce nitro blue tetrazolium (NBT) to purple formazan (nitroblue tetrazolium). The antioxidants carry out quenching of the generated radicals thereby inhibiting the reduction of NBT. The test can be performed taking 1 mL of sodium phosphate buffer (100 mM, pH 7.4), 1 mL of NBT (150 μM) solution, 1 mL NADH (468 μM) solution, and various concentrations of synthesized NPs. 1 mL PMS (60 μM) solution is added to start the reaction and incubated at 25°C for 5 min. Absorbance is measured at 560 nm. The superoxide radical scavenging in % can be calculated using Eq. (12.5).

This test was performed by Ref. [246] for AgNPs synthesized using *Brassica oleracea* leaves extract. Ascorbic acid was used as a standard for the assay. It was observed that the superoxide radical scavenging potential of the synthesized AgNPs was slightly lower as compared to the standard ascorbic acid. The $IC_{50}$ value of AgNPs was estimated as 50.37 μg/mL and that of ascorbic acid as 44.10 μg/mL.

**K) Total antioxidant assay (Phosphomolybdenum method):**

Phosphomolybdenum method is based on the property of antioxidants to reduce phosphomolybdate ion. Mo(IV) ions are reduced to Mo(V) by antioxidants that results in subsequent formation of a green phosphate/Mo(V) complex at acidic pH. A study by Ref. [253] reported the antioxidant power of AgNPs synthesized using *Bergenia ciliata* extracts by Phosphomolybdenum assay. 500 μL synthesized AgNPs solution was added to 4.5 mL reagent solution [ammonium molybdate (4 mM), sodium phosphate (28 mM), and sulfuric acid (0.6 M)] and incubated at 95°C for 1.5 h and cooled. The absorbance was recorded at 695 nm. Ascorbic acid was used as a standard. The antioxidant potential of green synthesized NPs was compared with that of *Bergenia ciliata* extract. It was observed that synthesized NPs showed higher power of 60.48 ± 2.2 as compared to extract that showed 38.8 ± 1.08 AAE (ascorbic acid equivalent).

#### *12.2.5.4 Antiinflammatory activity of green synthesized nanoparticles*

##### 12.2.5.4.1 In vitro antiinflammatory activity

**A) Inhibition of protein denaturation assay**

Inhibition of protein denaturation is one of the important properties of antiinflammatory compounds as protein denaturation is a marker for various inflammatory response and degenerative diseases. Proteins denature in the presence of strong acid or base, heat, and organic solvents. Therefore, inhibition of protein denaturation assay can be performed using egg albumin or bovine serum albumin (BSA) as the protein source for denaturation.

A study by Ref. [254] reported the antiinflammatory activity of AgNPs synthesized using mangrove plant extracts from *Avicennia officinalis* (leaf extracts) and *Xylocarpus granatum* (bark extracts) by protein denaturation assay using egg albumin as the protein source. Briefly, 0.2 mL of egg albumin (from fresh hen's egg) was mixed with 2.8 mL of PBS (pH 6.4). Various concentrations of NPs were added and incubated at 37°C

for 15 min. The reaction mixture was further heated at 70°C for 5 min and absorbance was recorded at 660 nm upon cooling the solution. The inhibition of protein denaturation was calculated using Eq. (12.5). The results of the investigation showed antiinflammatory activity of AgNPs from both the plant extracts but AgNPs synthesized using *A. officinalis* showed better activity with $IC_{50}$ value of 0.17 mg/mL as compared to the other. Aspirin was used as a standard for the assay that showed $IC_{50}$ value of 0.41 mg/mL which was comparable to the synthesized NPs.

The inhibition of protein denaturation assay for evaluation of antiinflammatory activity using BSA as the protein source was reported by Ref. [74] for AgNPs synthesized using *Cissus quadrangularis* extract. Briefly, 2 mL of 1% BSA (prepared in PBS) was mixed with various concentrations of synthesized NPs and incubated at 37°C for 20 min and absorbance was recorded at 255 nm. The antiinflammatory activity as % inhibition of protein denaturation was calculated as in Eq. (12.5). The study indicated 85% inhibition of BSA (protein) denaturation at 500 μg/mL in a dose-dependent manner and was higher than the standard used (Diclofenac sodium) with ~75% at 500 μg/mL.

**B) Cytokine secretion assay by LPS-induced inflammation**

Lipopolysaccharides (LPS) are a type of pathogen-associated molecular patterns (PAMPs) present in the outer membrane of Gram-negative bacteria. Exposure of macrophages to LPS induces phagocytotic response by initiating the production of proinflammatory cytokines required to immune response. Ref. [67] assessed antiinflammatory activity of AgNPs synthesized from *Cotyledon orbiculata* aqueous extract by Cytokine secretion assay. Briefly, the human monocytic leukemia cell line (THP-1) was differentiated into macrophages using PMA (phorbol 12-myristate 13-acetate). The differentiated macrophages were stimulated with 1 μg/mL LPS (LPS from *E. coli* 0111: B4) for 6 h in 24 well microtitre plate. LPS was removed from the cell culture and stimulated macrophage cells THP-1 were treated with various concentrations of synthesized AgNPs at 37°C for 24 h. Control well only received LPS and no AgNPs. Cell supernatants were centrifuged at 1500 rpm for 10 min. The production levels of the cytokines, IL-1β, IL-6 and TNF-α were determined using cytokine enzyme-linked immunosorbent assay (ELISA) kits available commercially. The findings of this study indicated that the proinflammatory cytokines (TNF-α, IL-6, and IL-1β) increased in untreated cells but reduction was observed in AgNPs treated cells.

**C) Erythrocyte membrane stabilization assay and hemolysis assay**

RBC membrane resembles lysosomal membrane and stabilization of lysosomal membrane is essential in inhibiting inflammatory response by preventing the release of initiated neutrophils. The enzymes released from lysosomes after membrane disruption can further lead to inflammation and thus, the antiinflammatory agent should inhibit the membrane disruption and help in membrane stabilization of lysosomes. The HRBC (human red blood cell) membrane stabilization assay is therefore used to evaluate the antiinflammatory activity of compounds by inhibiting the membrane damage and stabilize

the membrane [255]. A study by Ref. [256] demonstrated the antiinflammatory activity of AgNPs using *Solanum khasianum* leaf extract. Concisely, blood was collected in sterile vials with anticoagulants. The humans who did not take any NSAIDs for 2 weeks before the start of the experiment were chosen for the test. The blood sample was centrifuged at 3000 rpm for 15 min to precipitate the RBC pellet and washed with iso-saline solution thrice. 10% HRBC was prepared with iso-saline solution. Various concentrations of synthesized NPs were mixed with 1 mL Phosphate buffer, 2 mL hypo-saline solution, and 0.5 mL HRBC suspension and incubated at 37°C for 30 min. It was centrifuged at 3000 rpm for 10 min and Hb content was estimated form the supernatant at 560 nm. Blank was prepared without NPs and diclofenac sodium was used as standard. The hemolysis % was calculated using the following equations considering percentage of hemolysis of control as 100%:

$$\text{Hemolysis } (\%) = \frac{A_t}{A_c} \times 100 \tag{12.6}$$

$$\text{Protection } (\%) = \left(100 - \frac{A_t}{A_c}\right) \times 100 \tag{12.7}$$

where $A_c$ is absorbance of control and $A_t$ as absorbance of the test sample.

It was observed through this study that green synthesized AgNPs showed decreased hemolysis from 37.4% to 15.26% between 200 and 1000 μg/mL and that was similar to diclofenac sodium. The membrane stabilization or protection % was found to be 62.6%−84.74% at 200−1000 μg/mL in a dose dependent manner.

**D) 5-LOX (5-lipoxygenase) inhibition assay**

Leukotrienes are inflammatory molecules metabolized by 5-LOX from arachidonic acid. Therefore, inhibition of 5-LOX serves the purpose of antiinflammatory compounds. Ref. [257] reported antiinflammatory activity of AgNPs synthesized using *Lonicera japonica* leaf extract by 5-LOX inhibition assay. Concisely, various concentrations of AgNPs were treated with 80 μL 5-LOX (0.575 U/μL, prepared in Tris-HCl) and incubated at 25°C for 15 min in microtitre plates. 10 μL of linoleic acid (140 μmol/L, prepared in anhydrous ethanol and diluted with Tris-HCl buffer) was added and incubated at 25°C for 10 min. Finally, 100 μL FOX reagent (ferrous oxidation-xylenol orange) was added and incubated at 25°C for 10 min and absorbance was recorded at 590 nm using microtitre plate reader. The well with 5-LOX, linoleic acid and FOX reagent without AgNPs served as the control with 100% enzyme activity. This procedure is based on the principle that linoleic acid generates linoleic acid peroxide which is further catalyzed by 5-LOX which further oxidises $Fe^{2+}$ to $Fe^{3+}$. $Fe^{3+}$ combines with xylenol orange to form stable complex. 5-LOX inhibition in % can be calculated using Eq. (12.5). The study indicated % inhibition of 5-LOX by the green synthesized AgNPs with $IC_{50}$ value as 5.08 μg/mL.

#### 12.2.5.4.2 In vivo antiinflammatory activity

**A) Carrageenan-induced rat paw edema assay**

Ref. [258] demonstrated the antiinflammatory activity of AgNPs synthesized using *Selaginella myosurus* aqueous extract in vivo following carrageenan-induced rat paw edema procedures. Briefly, five groups of experimental animals were taken for this study. Group I was taken as control which received only inflammatory inducing agent (0.1 mL of carrageenan (1% carrageenan suspended in 0.9% NaCl) was injected in the right paw of the animal models (rats) as inflammatory inducing agents) on day 0; group II were injected with inflammatory inducing agent and standard drug (indomethacin (10 mg/kg) on day 0 and served as standard; group III, IV, and V were injected with inflammatory inducing agent on day 0 and desired concentrations of synthesized AgNPS after 24 h of the injection and served as tests. Paw size was measured immediately before and 30 min, 1, 2, 3, 4, and 5 h after the carrageenan injection. The antiinflammatory activity was determined as inhibition of edema (%) in each treated group as compared to control using the following equation:

$$\text{Inhibition } (\%) = \frac{(V_t - V_0)\ \text{control} - (V_t - V_0)\text{treated}}{(V_t - V_0)\ \text{control}} \times 100 \qquad (12.8)$$

$V_t$ is the average diameter for each group after treatment and $V_0$ is the average diameter for each group before any treatment.

The results obtained for the assay indicated significant inhibition of paw edema for the rats treated with synthesized AgNPs orally as compared to the untreated ones. 60.50% inhibition was observed at 5 h for the AgNPs treated rat at 0.4 mg/kg of AgNPs.

### *12.2.5.5 Antidiabetic activity of green synthesized nanoparticles*

#### 12.2.5.5.1 In vitro antidiabetic activity of green synthesized nanoparticles

**A) Alpha-amylase Inhibition Assay:**

Starch is partially digested by salivary amylase in humans upon food ingestion that results in degradation of polymeric substrate starch into shorter oligomers which are further hydrolyzed by pancreatic α-amylases into maltose, maltotriose and small malto-oligosaccharides which are furthermore hydrolyzed by α-amylases into glucose prior absorption. Therefore, by inhibiting α-amylase, reduction in post prandial hyperglycemia can be achieved in diabetic condition. The in vitro antidiabetic activity can be performed using 3,5-Dinitro salicylic acid (DNSA) method. Briefly, various concentrations of antidiabetic test compound are preincubated with 1% α-amylase (in 20 mM sodium phosphate buffer pH 6.9) for 30 min and is considered as test. The control is taken as various concentrations of antidiabetic test compound (synthesized NPs) untreated with α-amylase. Then 1 mL starch solution (1%) is added and incubated at 37°C for 10 min. 1 mL DNSA reagent is added. All the reaction tubes are boiled for 5 min and absorbance is recorded at 540 nm. Metformin or acarbose can be used as a standard

drug [259]. The inhibition of α-amylase is calculated using Eq. (12.5). The in vitro antidiabetic activity can also be performed by starch-iodine method wherein 10 μL of α-amylase solution (0.025 mg) mixed with 390 μL of phosphate buffer (0.02 M containing 0.006 M NaCl, pH 7.0) containing desired concentrations of synthesized NPs. After incubation at 37°C for 10 min, 100 μL of 1% starch solution be added, and the mixture re-incubated for 1 h. Next, 0.1 mL of 1% iodine solution be added, and finally mixed with 5 mL distilled water. The absorbance to be taken at 565 nm. The inhibition of alpha-amylase is calculated using Eq. (12.5).

A study by Ref. [260] depicted in vitro antidiabetic activity of green synthesized starch NPs using *Gymnema sylvestre* extracts by α-amylase inhibition assay. Antidiabetic activity was found to be highest at 100 μg/mL with 58.56 ± 0.44% α-amylase inhibition activity and $IC_{50}$ value was estimated as 80.98 μg/mL. In vitro antidiabetic activity of ZnO NPS were reported by Ref. [70] synthesized using various plant extracts *Azadirachta indica, Hibiscus rosa-sinensis, Murraya koenigii, Moringa oleifera*, and *Tamarindus indica*. It was observed that among the green synthesized NPs, ZnONPs synthesized using *T. indica* exhibited highest α-amylase inhibition activity in comparison to others with 89% inhibition at 100 μg/mL.

**B) α-glucosidase inhibition assay:**

α-glucosidase carries out digestion of carbohydrates thereby increasing postprandial glucose level in diabetic patients. α-glucosidase inhibitors (AGIs) are developed as therapeutic agents for treating diabetes mellitus that inhibits α-glucosidase activity that further decreases the release of α-glucose thereby retarding glucose absorption in small intestine [261]. The α-glucosidase inhibition assay was reported by Ref. [71]. Briefly, α-glucosidase (1U/L α-glucosidase in 150 μL of 0.1 M sodium phosphate buffer (pH 6.9)) was preincubated at 37°C for 10 min with various concentrations of synthesized AgNPs. 50 μL of p-nitrophenyl-α-D-glucopyranoside (2 mM in sodium phosphate buffer) was added and incubated at 37°C for 20 min. 50 μL sodium carbonate (0.1 M) was added to terminate the reaction and absorbance recorded at 405 nm. Tube with enzyme but without NP samples served as control and Acarbose was taken as a standard compound. The inhibition of α-glucosidase is calculated using the formula in Eq. (12.5). The $IC_{50}$ value was found to be 53.8 μg/mL for AgNPs. Ref. [262] depicted the in vitro antidiabetic activity of AgNPs synthesized using *Lonicera japonica* leaf extract using α-glucosidase inhibition assay and reported the $IC_{50}$ value of 37.86 mg/mL.

## 12.3 Latest research and development in the field

### 12.3.1 Green synthesis of NPs using enzymes

Enzymes are thought to be the most important players in the reduction and stabilization of metals in microorganisms during NPs synthesis, via redox processes that take place either in their intracellular or extracellular spaces and frequently serve as nucleation sites.

Metal capture, enzymatic reduction, and capping are all involved in the intracellular technique, whereas secreted or membrane-bound enzymes/proteins are used in the extracellular method. The process also involves shuttle quinones such as anthraquinones, naphthoquinones, and hydroquinones [10]. Certain enzymes like α-amylase, bromelain, laccases, cellulase, nitrate reductase, keratinase, lysozyme are used for green synthesis of various NPs like AgNPs, AuNPs and $TiO_2$NPs and have shown antimicrobial properties [263]. A study by Ref. [264] depicted the synthesis of AuNPs using xylanases isolated form *Aspergillus niger* and *Trichoderma longibrachiatum*. The synthesized NPs showed biological activities like antimicrobial, antioxidant, anticoagulant, and thrombolytic activities.

### 12.3.2 Microwave-assisted green synthesis of NPs

Traditional heating methods employed for the green synthesis of NPs are laborious, inefficient, and time-consuming taking hours to days for NPs synthesis. Also, these methods make use of solvents for NPs synthesis increasing the solvent waste disposal issue. With the advent of microwave-assisted synthesis methods in green chemistry, these limitations have been solved. Microwave-assisted green synthesis of NPs has been advantageous over the conventional heating methods for synthesis wherein microwave radiations are absorbed by the metallic ions and reducing biological forms in a reaction mixture. Microwave radiations easily enters the material causing uniform distribution of temperature between surface and material. The reaction takes place in very short duration in minutes or even seconds under solvent free conditions using minimum energy. The green synthesized NPs are reported with maximum stability, minimum particle size and size distribution by microwave-assisted methods. Several factors like pH, temperature, reaction time, microwave power, stirring rate, etc., determine the synthesis process [265–267]. Microwave-assisted green synthesis method has been employed in recent decade by several researchers and various types of NPs have been synthesized and studied for biomedical application. Ref. [267] synthesized CuONPs from Indian bael (*Aegle marmelos*) juice via Microwave-assisted route and showed potent antibacterial and antioxidant properties of synthesized NPs. Ref. [268] depicted antimicrobial activities of pectin-based AgNPs by microwave-assisted green synthesis method. The antimicrobial and noncytotoxic activities of AgNPs synthesized from *Rosa santana* (rose) petals extract by Microwave-assisted green synthesis method was reported by Ref. [269]. A study by Ref. [266] reported synthesis of SeNPs using *Theobroma cacao* L. bean shell extract as a stabilizing and capping agent and indicated its antioxidant nature using this microwave-assisted synthesis process. Microwave-assisted synthesis for $TiO_2$NPs were reported by Ref. [270] from *Wrightia tinctoria* leaf extract that depicted antioxidant and antibacterial nature of green synthesized NPs. Ref. [271] showed antibacterial and antioxidant activities of AgNPs synthesized using *Cyanthillium cinereum* leaf extract and also described its potential as a biosensor in diagnostics. Ref. [272] reported the antibacterial

activity of gold coated iron NPs (Fe@AuNPs) against *Helicobacter pylori* synthesized using extract solution of olive oil, licorice root and coconut oil. Microwave-assisted NPs synthesis was reported for NiONPs formulated using *Andrographis paniculata* leaf extract by Ref. [273] with anticancer activities. The reports suggest that microwave-assisted green synthesis of NPs is a significant approach for green synthesis of NPs for their use in biomedical applications.

### 12.3.3 Bio-based green synthesis of NPs

#### *12.3.3.1 Polymer-based NPs synthesis*

These are synthesized from natural or synthetic polymers and are researched for biomedical applications. Mainly drug delivery system makes use of encapsulated polymers in chemotherapeutics. Nonbiodegradable polymers such as poly(methyl methacrylate) (PMMA), polyacrylamide, polystyrene and polyacrylates were the first polymers used for synthesis of polymeric NPs. Recently, biodegradable polymers including synthetic polymers such as poly(D,L-lactide) (PLA), poly(D,L-glycolide) (PLG), co-polymer poly(-lactide-co-glycolide) (PLGA), polyalkylcyanoacrylates, poly-ϵ-caprolactone and natural polymers including chitosan, alginate, gelatin, zein and albumin have been employed to overcome the adverse effects of nonbiodegradable polymeric NPs such as biodegradability and toxicity [274]. [275] depicted the synthesis of polymer-based ZnONPs using thermoplastic polyurethane (TPU). TPU was first prepared from fatty acids using rapeseed oil. These TPU/ZnO NPs have shown wound healing property. Ref. [276] reported the synthesis of bio-based chitosan/gelatin/Ag@ZnO bionanocomposites wherein Ag-loaded ZnO NPs were synthesized by sol-gel method using gelatin as a template and further chitosan/gelatin/Ag@ZnO NPs were synthesized using chitosan. These NPs depicted antibacterial potential.

#### *12.3.3.2 Green synthesis of NPs from agro-industrial waste*

Various types of agro-waste materials have been exploited for green synthesis of NPs. The waste material used for synthesis are mainly biodegradable food wastes rich in organic compounds including vitamins, carotenoids, flavonoids, phenols, and other phytochemical molecules. These biomolecules participate in bio-reduction and stabilization of NPs. The NPs synthesized from waste have revealed biological activities including antimicrobial, antioxidant, anticancer, biosensors, etc. that make these materials a potent source for green synthesis and are cost effective. The biomolecules are extracted from the agro-waste materials by hot water extraction procedure from the dried and ground materials and are further used for NPs synthesis [263,277,278]. A study by Ref. [279] reported AgNPs synthesis by green approach using cocoa pod husk extract. The synthesized NPs indicated antimicrobial, antioxidant and larvicidal activities. Ref. [280] reported AuNPs synthesis using petals extracts of *Moringa oleifera*, an agroforestry waste material and depicted anticancer potential of the synthesized NPs. Ref. [172]

demonstrated green synthesis of AuNPs from watermelon (*Citrus lanatus*) rind extract. The extract contained biomolecules including cellulose, pectin, proteins, carotenoids, citrulline that provided carboxylic and hydroxyl groups for NPs synthesis. The synthesized NPs exhibited antibacterial, antioxidant and proteosome inhibitory activities. Anticancer potential of green synthesized AgNPs formulated using oak fruit hull extract was reported by Ref. [281] that indicated anticancer potential against Human breast cancer cells MCF-7.

#### 12.3.3.3 Polysaccharide-based NPs synthesis

Synthesis of NPs using polysaccharides is gaining interest in recent years owing to several advantages of this bio-based green approach including cost effectiveness, less toxicity, fewer side effects, etc. Several polysaccharides like starch, cellulose, glucan, pectin, dextrose, xanthan, carrageenan, alginate, keratin, etc., have been exploited for green synthesis of NPs. These polysaccharides are obtained from biological forms such as microorganism, algae, plants, animals [50,278]. Biodegradable gums such as gum ghatti, gum acacia, gum karaya, gum cashew, etc., are employed for green synthesis of AgNPs. These NPs have shown antimicrobial potentiality [282]. Ref. [283] demonstrated green synthesis of AgNPs using biocompatible hydroxyethyl cellulose (HEC) that showed application in tissue engineering and were biodegradable. Microbial exopolysaccharides (EPS) including curdlan, dextran, xanthan gum, gellan gum, cellulose, levan, succinoglycan, FucoPol, etc., have been employed in green synthesis of NPs due to their biocompatibility nature, cost-effectiveness, less toxicity, and biodegradability [284]. The synthesized NPs using EPS have shown anticancer, antioxidant, and antimicrobial potency [285]. Nanocomposites especially cellulose-based composite scaffolds compounded with other ingredients, such as metal NPs is gaining importance in terms of biomedical applications mainly as antimicrobial agents. A study by Ref. [286] synthesized bacterial cellulose-based silver nanocomposites using bacterial cellulose produced from *Gluconacetobacter xylinus* BKNC 19. The AgNPs were first synthesized using *Moringa oleifera* Lam leaf extracts that provided biomolecules for bio-reducing, capping and stabilization of AgNPs.

#### 12.3.3.4 Secondary metabolites and phytochemicals in green synthesis of NPS

Primary metabolites like vitamins, polysaccharides, proteins, and DNA are widely applied for green synthesis of NPs. On the contrary, secondary metabolites being more diverse in nature and can be obtained from various organisms are gaining interest for green synthesis of NPs in recent years [287]. Phytochemicals are such secondary metabolites used in green synthesis of NPs and belong to organic compounds like alcohols, phenols, terpenes, alkaloids, saponins, proteins, etc. These molecules impose medicinal value for traditional medicinal plants. These phytochemical constituents can be exploited for green synthesis of NPs for therapeutic applications rather than the entire plant extract. A review study by Ref. [78] has thrown light on the biosynthetic pathways of secondary metabolites in

plants that can be exploited for production of metallic NPs. Till date phytochemical constituents like polyphenols including flavonoids, phenolic acid, and terpenoids and organic acids and proteins have been predicted as bio-reducing and stabilizing agents for NPs synthesis. Flavonoids are reported to participate in bio-reduction of NPs by donating hydrogen atoms or electrons and are considered as main bio-reducing molecules. The −OH groups of terpenoids are also known to aid in bio-reduction of metal ions in NP synthesis.

#### *12.3.3.5 Green synthesis of NPs using vitamins*

Vitamins are a group of organic compounds essential for the normal body functioning and whose deficiencies are associated with certain diseases or disorders. Ref. [288] synthesized AgNPs and AuNPs using ascorbic acid (vitamin C) as both reducing and stabilizing agent. A study by Ref. [289] synthesized novel core (Fe, Cu)-shell (Au, Pt, Pd, and Ag) nanocrystals using vitamin C wherein Cu and Fe were reduced by vitamin C. Although no capping agent was added in this study, the core−shell structure stabilized the synthesized NPs. A review by Ref. [290] emphasized on the role of phytochemicals including vitamins (vitamin C, vitamin A) obtained from fruits and their role as capping agents in green synthesis of metallic NPs. The study also stressed on the importance of green synthesizing NPs using plant/fruit extracts rich in phytochemicals including vitamins with special reference to the health beneficial effects. A study by Ref. [291] demonstrated encapsulation of vitamins C, B9, and B12 with the help of NPs synthesized using chitosan and N,N,N-trimethyl chitosan.

### 12.3.4 Green synthesis of NPS from animal sources

A very few reports indicate animal-mediated synthesis of NPs among which silk sericin and fibroin from silkworm *Bombyx mori* are widely experimented for NP synthesis [219].

#### *12.3.4.1 Silkworm silk protein (sericin and fibroin)*

Silk fibroin and sericin are biopolymers that are biodegradable and hence advantageous in synthesizing NPs and biomedical applications. Silk fibroin and sericin have been documented in variety of biotechnological applications especially in biomedical for tissue engineering of bone, tissue and regeneration of nerve tissue, antioxidant, antimicrobial potential, etc. [292,293]. Various NPs have been synthesized with silk fibroin and silk sericin. Ref. [294] developed luminescent AgNPs from silk fibroin with antibacterial nature. Ref. [295] explored green synthesis of AuNPs/reduced graphene oxide using silk fibroin as reducing and stabilizing agent. Cd (cadmium), Se, Pd and Pt NPs have also been synthesized from silk fibroin [296]. Silk sericin has also been used as reducing and stabilizing agent in green synthesis of NPs. Ref. [297] demonstrated green synthesis of AgNPs with silk sericin exhibiting antibacterial potency.

#### 12.3.4.2 Spider silk

Spider cobweb (spider silk) has also been selected for biomedical applications for wound healing and antimicrobial activities. Ref. [298] used spider silk for synthesis of AgNPs and depicted its antimicrobial nature. Similarly, Ref. [299] demonstrated spider silk as reducing and stabilization agent for green synthesis of AuNPs.

#### 12.3.4.3 Hydrolyzed nest of paper wasp

The nests of paper wasps (*Polistes*) are rich in cellulose and proteins that can be used as reducing and stabilizing agents in green synthesis of NPs. This property has been exploited by Ref. [300] for green synthesis of AgNPs using hydrolyzed paper wasp nest. The green synthesized NPs depicted antimicrobial and anticoagulant properties.

#### 12.3.4.4 Bee honey

Bee honey rich in sugars like fructose and glucose, minerals, vitamins, proteins are mainly shown to repair and regenerate tissue. Several NPs like Ag, Au, Ce, Pd, CuO NPs have been synthesized using honey as reducing and stabilizing agent [301]. Ref. [302] synthesized AgNPs from bee honey and showed potential to treat colon cancer.

#### 12.3.4.5 Propolis

Propolis is a natural bee product with several medicinal properties such as antibacterial, antifungal, hepatoprotective, antiproliferative, antimicrobial, antioxidative, anti-inflammatory, antiviral, immunomodulatory and regenerative activities. A review study by Ref. [303] shed light on the green synthesized NPs using this product. SeNPs and AgNPs are mainly synthesized using this bee product as its extract provides natural reducing and stabilizing compounds like phenolic and flavonoid content. Nanopropolis as a nanoproduct has gained importance in pharmaceutical and biomedical applications.

#### 12.3.4.6 Bio-silica

SiNPs (Silica NPs) are researched for the green synthesis using marine algae and terrestrial plants which has been used in biomedical application. Ref. [304] demonstrated green synthesis of SiNPs using *Cynodon dactylon* L. extracts and have shown good antimicrobial potency.

#### 12.3.4.7 Chitosan

Chitosan derived from arthropods like crabs and shrimps is a natural polysaccharide. The properties of chitosan like biodegradability, nontoxicity, biocompatibility makes it an ideal source for green synthesis of NPs for biomedical application. A variety of NPs have been synthesized using chitosan including Ag, CuO, ZnNPs, etc., and have been used in biomedical application for tissue engineering, biosensors, antioxidant, antimicrobial, etc.

[305]. Ref. [306] synthesized chitosan NPs with methoxy-4-hydroxybenzaldehyde (vanillin). These chitosan NPs were further loaded with anticancer drug 5-FU and used as a drug delivery system against colon cancer using cell line HT-29.

### 12.3.5 Virus-based green synthesis of NPs

Viruses are nanoscale particles containing genes (DNA or RNA) and protective capsid proteins and envelops. These biological materials can be exploited for green synthesis of NPs. Also, intact biological particles of viruses have been used to extend biological techniques to nanocrystal production. Inorganic materials can be nucleated and assembled using viral scaffolds. The capsid protein can be genetically engineered for NPs synthesis and can be used for biomedical applications for treating cancers and for targeted drug delivery [12,307]. Artificial nanostructures like zinc sulfide (ZnS), cadmium sulfide (CdS) and silicon dioxide ($SiO_2$) have been synthesized using viruses. Ref. [308] developed AuNPs using a bacteriophage (*Salmonella serovar* Paratyphi B) for synthesis and has shown to possess antimicrobial and antibiofilm activities. A study by Ref. [309] synthesized AgNPs and AuNPs using plant pathogenic virus Squash leaf curl China virus (SLCCNV) with biomedical applications. The synthesized NPs were biocompatible and indicated their effectiveness to be used as bio-semi-conductors for biomedical applications. Ref. [318] produced NPs from a filamentous plant virus, Potato virus X for drug delivery of doxorubicin in various cancer therapies like ovarian cancer, breast cancer, and cervical cancer.

### 12.3.6 Human cells–based green synthesis of NPs

Nuclear material plays an important role in determining the progression of various diseases including cancer, thus targeting the nucleus with green synthesized NPs would be a promising approach in such diseases as NPs are known to influence the cell functioning leading to DNA damage, cytokinesis arrest and apoptosis. Although the significance of NPs to target the nucleus is documented, it still faces some challenges as it has to pass through the cell membrane and reach the cytoplasm and further cross the nuclear membrane. To overcome this drawback of NPs, certain researchers have experimented methods to synthesize NPs inside human cell nucleus itself. This method of using human cells for NP synthesis is advantageous as it does not require any additional reducing or capping agents [310]. A study by Ref. [311] illustrated AgNPs and AuNPs synthesis intracellularly in cancer and non-cancer cells. Human cervical cancer cell line (HeLa), human embryonic kidney cells (HEK293T) and Human liver carcinoma cell line (HepG2) were used for NP synthesis and it was observed that AgNPs and AuNPs were formed intercellularly with enzymes NADH and QOH-1 (quinone oxidoreductase homolog-1) participating in NPs synthesis. Ref. [312] synthesized AuNPs using human skin cells (epithelial cells). A study by Ref. [313] depicted synthesis of magnetic NPs in human stem cells.

### 12.3.7 Green synthesized NPs as antivirals against SARS-CoV-2

SARS-CoV-2, a novel coronavirus involved in the ongoing pandemic disease COVID-19 since December 2019 impacted human health in various ways and also caused increased mortality worldwide. It stimulated the researchers worldwide to discover vaccines and therapeutic drugs for fighting the infection. Researchers in the field of nanotechnology especially in nanomedicine and biosensors have taken initiative in finding nanoparticles for disease treatment and diagnosis. A study by Ref. [314] proposed the development of nanofibre filters (nanoparticle-coated air filters) for air purification to avoid the spread of virus through air. Ref. [315] hypothesized the possible mechanisms of various green synthesized AgNPs using plant materials for fighting the infection. It showed the possibility of inactivation and disintegration of viral strains by targeting the viral entry and post-entry points that are crucial for virus survival using AgNPs. This study also depicted that the antiviral drugs can be combined with green synthesized AgNPs for treating COVID-19. A study by Ref. [316] demonstrated synthesis of decoy NPs synthesized by fusing cell membranes nanovesicles obtained from human monocytes and genetically engineered cells expressing angiotensin converting enzyme II (ACE2) receptors. The synthesized nanodecoys provided protection against SARS-CoV-2 by adsorbing viruses and inflammatory cytokines. Ref. [317] depicted antiviral activity of PLGA-LPV@M NPs against SARS-CoV-2. The antiviral drug Lopinavir (LPV) was loaded in polymeric NPs (Poly (lactic-*co*-glycolic acid) nanocores (PLGA NPs). Later, macrophage (human macrophage cell line (THP-1 cells) membrane was coated on PLGA-LPV NPs giving rise to PLGA-LPV@M NPs. The synthesized NPs suppressed macrophage and neutrophils activation by neutralizing proinflammatory cytokines. This study depicts the role of macrophage biomimetic nanocarriers for treating COVID-19 and their drug delivery system.

## 12.4 Summary and conclusion

Metal/metal ions have been employed since ages in traditional medicine for treating variety of infectious and degenerative diseases. Nanotechnology is a field that deals with various kinds of NPs synthesized using physical, chemical, and biological forms. With the advent of green technology, green synthesis of metallic NPs has been widely exploited with proven advantages over chemical and physical methods of synthesis. Various NPs like Ag, Au, Zn, Cu, CuO, $TiO_2$, Pd, Pt, Zn, ZnO, Se, etc., have been synthesized via green approach using biological forms. The biological forms used for green synthesis of NPs include bacteria, fungi, algae, plants, animals, viruses and biomolecules produced by these biological forms that act as bio-reducing and stabilizing agents and thus does not require addition of chemicals. These biological agents can be used directly or their extracts can be used for NPs synthesis. The phytochemicals like phenols,

flavonoids, proteins, polysaccharides, enzymes help in bio-reduction and stabilization of the green synthesized NPs mainly due to presence of functional groups. The green synthesized NPs have been researched for treating a variety of diseases like cancer, type-2 diabetes mellitus, infections caused by pathogens, neurodegenerative diseases, etc. The green synthesized NPs are found to be biocompatible and thus are safe for consumption and are biodegradable. The green synthesized NPs are reported to bear antimicrobial, antioxidant, antiinflammatory, antidiabetic, anticancer, anticoagulant, thrombolytic activities, and thus proven beneficial in treating various diseases. Various mechanisms are involved that determines therapeutic properties of green synthesized NPs. Recently, these NPs have been developed as biosensors and bio-imaging molecules beneficial in diagnostics. Drug delivery and gene delivery systems are also being researched for use of green synthesized NPs in the system. Therefore, the green synthesized NPs can be employed in nanomedicine for diagnosis and treatment of various diseases.

## 12.5 Challenges and future outlook

Although the field of nanomedicine is gaining interest, the rising concerns on biocompatibility and hazardous nature of chemically and physically synthesized NPs limits their use in biomedical applications. With the advent of green technology, synthesizing NPs from biological forms has gained attention, however FDA has not approved the use of green synthesized NPs in biomedical applications till date [50]. The traditional knowledge on medicinal plants and their therapeutic applications have been explored by researchers in utilizing these plant extracts for green synthesis of NPs. However, these studies are mostly limited to in vitro conditions and few in vivo and very few are under clinical trials and thus are limited to laboratory conditions. Therefore, clinical trials of potent green synthesized NPs need to be undertaken for their use in therapy. As the phytochemical constituents and other biomolecules of plants, microbes and animals participate in NPs synthesis in green approach, these biomolecules need to be isolated, characterized and purified for synthesizing NPs. Virus-mediated approach for green synthesis of NPs is advantageous for drug delivery systems especially due to their smaller sizes, but yet very few reports are documented for NPs synthesis using viruses. Plant-pathogenic viruses and Bacteriophages can be explored for NPs synthesis for biomedical applications. Agro-waste is the cheapest source for green synthesis of NPs, yet is poorly explored and thus needs improvement. A few reports indicate use of human cells (cancer and non-cancer cells) for NPs synthesis intracellularly that can be a great achievement for destroying target cells especially cancer cells and virus infected cells and drug delivery. Furthermore, COVID-19 pandemic has boosted the researchers at work for developing novel drugs or repurposing drugs for immediate therapy, therefore the researchers in green synthesis of NPs need to explore more biological forms for green synthesis of NPs for biomedical applications.

## References


[1] V.J. Mohanraj, Y. Chen, Nanoparticles—a review, Trop. J. Pharmaceut. Res. 5 (1) (2006) 561–573.
[2] S. Ahmad, S. Munir, N. Zeb, A. Ullah, B. Khan, J. Ali, et al., Green nanotechnology: a review on green synthesis of silver nanoparticles—an ecofriendly approach, Int. J. Nanomed. 14 (2019) 5087.
[3] D. Zhang, X.L. Ma, Y. Gu, H. Huang, G.W. Zhang, Green synthesis of metallic nanoparticles and their potential applications to treat cancer, Front. Chem. 799 (2020).
[4] M. Wypij, T. Jedrzejewski, J. Trzcińska-Wencel, M. Ostrowski, M. Rai, P. Golińska, Green synthesized silver nanoparticles: antibacterial and anticancer activities, biocompatibility, and analyses of surface-attached proteins, Front. Microbiol. 12 (2021) 888.
[5] I. Hussain, N.B. Singh, A. Singh, H. Singh, S.C. Singh, Green synthesis of nanoparticles and its potential application, Biotechnol. Lett. 38 (4) (2016) 545–560.
[6] K. Parveen, V. Banse, L. Ledwani, Green synthesis of nanoparticles: their advantages and disadvantages, AIP Conference Proceedings 1724 (1) (April 2016) 020048 (AIP Publishing LLC).
[7] N. Pantidos, L.E. Horsfall, Biological synthesis of metallic nanoparticles by bacteria, fungi and plants, J. Nanomed. Nanotechnol. 5 (5) (2014) 1.
[8] S. Jadoun, R. Arif, N.K. Jangid, R.K. Meena, Green synthesis of nanoparticles using plant extracts: a review, Environ. Chem. Lett. 19 (1) (2021) 355–374.
[9] J. Singh, T. Dutta, K.H. Kim, M. Rawat, P. Samddar, P. Kumar, 'Green'synthesis of metals and their oxide nanoparticles: applications for environmental remediation, J. Nanobiotechnol. 16 (1) (2018) 1–24.
[10] S. Ghosh, R. Ahmad, K. Banerjee, M.F. AlAjmi, S. Rahman, Mechanistic aspects of microbe-mediated nanoparticle synthesis, Front. Microbiol. 12 (2021) 867.
[11] S. Mukherjee, S.K. Nethi, Biological synthesis of nanoparticles using bacteria, in: Nanotechnology for Agriculture, Springer, Singapore, 2019, pp. 37–51.
[12] B. Koul, A.K. Poonia, D. Yadav, J.O. Jin, Microbe-mediated biosynthesis of nanoparticles: applications and future prospects, Biomolecules 11 (6) (2021) 886.
[13] N.I. Hulkoti, T.C. Taranath, Biosynthesis of nanoparticles using microbes—a review, Colloids Surf. B Biointerfaces 121 (2014) 474–483.
[14] R.K. Das, V.L. Pachapur, L. Lonappan, M. Naghdi, R. Pulicharla, S. Maiti, et al., Biological synthesis of metallic nanoparticles: plants, animals and microbial aspects, Nanotechnol. Environ. Eng. 2 (1) (2017) 1–21.
[15] S. Iravani, Bacteria in nanoparticle synthesis: current status and future prospects, Int. Sch. Res. Notices 2014 (2014).
[16] S.I. Tsekhmistrenko, V.S. Bityutskyy, O.S. Tsekhmistrenko, L.P. Horalskyi, N.O. Tymoshok, M.Y. Spivak, Bacterial synthesis of nanoparticles: a green approach, Biosyst. Divers. 28 (1) (2020) 9–17.
[17] M. Abdollahnia, A. Makhdoumi, M. Mashreghi, H. Eshghi, Exploring the potentials of halophilic prokaryotes from a solar saltern for synthesizing nanoparticles: the case of silver and selenium, PLoS One 15 (3) (2020) e0229886.
[18] D.N. Nagar, N.N. Ghosh, J.M. Braganca, Green synthesis of selenium nanospheres and nanoneedles by halophilic archaea, Appl. Nanosci. (2022), https://doi.org/10.1007/s13204-022-02665-6.
[19] P. Srivastava, J. Braganca, S.R. Ramanan, M. Kowshik, Green synthesis of silver nanoparticles by haloarchaeon Halococcus salifodinae BK6, in: Advanced Materials Research 938, Trans Tech Publications Ltd, 2014, pp. 236–241.
[20] A. Boroumand Moghaddam, F. Namvar, M. Moniri, P. Md Tahir, S. Azizi, R. Mohamad, Nanoparticles biosynthesized by fungi and yeast: a review of their preparation, properties, and medical applications, Molecules 20 (9) (2015) 16540–16565.
[21] J. Saxena, M.M. Sharma, S. Gupta, A. Singh, Emerging role of fungi in nanoparticle synthesis and their applications, World J. Pharm. Sci. 3 (9) (2014) 1586–1613.
[22] M. Guilger-Casagrande, R.D. Lima, Synthesis of silver nanoparticles mediated by fungi: a review, Front. Bioeng. Biotechnol. 7 (2019) 287.
[23] S.A. Dahoumane, M. Mechouet, K. Wijesekera, C.D. Filipe, C. Sicard, D.A. Bazylinski, C. Jeffryes, Algae-mediated biosynthesis of inorganic nanomaterials as a promising route in nanobiotechnology—a review, Green Chem. 19 (3) (2017) 552–587.

[24] P. Khanna, A. Kaur, D. Goyal, Algae-based metallic nanoparticles: synthesis, characterization and applications, J. Microbiol. Methods 163 (2019) 105656.
[25] F. Khan, A. Shahid, H. Zhu, N. Wang, M.R. Javed, N. Ahmad, et al., Prospects of algae-based green synthesis of nanoparticles for environmental applications, Chemosphere 293 (2022) 133571.
[26] R. Chaudhary, K. Nawaz, A.K. Khan, C. Hano, B.H. Abbasi, S. Anjum, An overview of the algae-mediated biosynthesis of nanoparticles and their biomedical applications, Biomolecules 10 (11) (2020) 1498.
[27] A. Mukherjee, D. Sarkar, S. Sasmal, A review of green synthesis of metal nanoparticles using algae, Front. Microbiol. 12 (2021).
[28] V.V. Makarov, A.J. Love, O.V. Sinitsyna, S.S. Makarova, I.V. Yaminsky, M.E. Taliansky, N.O. Kalinina, "Green" nanotechnologies: synthesis of metal nanoparticles using plants, Acta Naturae (англоязычная версия) 6 (1 (20)) (2014) 35–44.
[29] P. Kuppusamy, M.M. Yusoff, G.P. Maniam, N. Govindan, Biosynthesis of metallic nanoparticles using plant derivatives and their new avenues in pharmacological applications—an updated report, Saudi Pharm. J. 24 (4) (2016) 473–484.
[30] C. Vanlalveni, S. Lallianrawna, A. Biswas, M. Selvaraj, B. Changmai, S.L. Rokhum, Green synthesis of silver nanoparticles using plant extracts and their antimicrobial activities: a review of recent literature, RSC Adv. 11 (5) (2021) 2804–2837.
[31] J.K. Patra, K.H. Baek, Green nanobiotechnology: factors affecting synthesis and characterization techniques, J. Nanomater. 2014 (2014).
[32] M.S. Jameel, A.A. Aziz, M.A. Dheyab, Green synthesis: proposed mechanism and factors influencing the synthesis of platinum nanoparticles, Green Process. Synth. 9 (1) (2020) 386–398.
[33] Q. Zhang, J. Xie, Y. Yu, J.Y. Lee, Monodispersity control in the synthesis of monometallic and bimetallic quasi-spherical gold and silver nanoparticles, Nanoscale 2 (10) (2010) 1962–1975.
[34] Q. Shou, C. Guo, L. Yang, L. Jia, C. Liu, H. Liu, Effect of pH on the single-step synthesis of gold nanoparticles using PEO–PPO–PEO triblock copolymers in aqueous media, J. Colloid Interface Sci. 363 (2) (2011) 481–489.
[35] P. Traiwatcharanon, K. Timsorn, C. Wongchoosuk, Flexible room-temperature resistive humidity sensor based on silver nanoparticles, Mater. Res. Express 4 (8) (2017) 085038.
[36] M. Ahani, M. Khatibzadeh, Green synthesis of silver nanoparticles using gallic acid as reducing and capping agent: effect of pH and gallic acid concentration on average particle size and stability, Inorg. Nano-Met. Chem. 52 (2) (2022) 234–240.
[37] A. Roy, O. Bulut, S. Some, A.K. Mandal, M.D. Yilmaz, Green synthesis of silver nanoparticles: biomolecule-nanoparticle organizations targeting antimicrobial activity, RSC Adv. 9 (5) (2019) 2673–2702.
[38] E.K. Elbeshehy, A.M. Elazzazy, G. Aggelis, Silver nanoparticles synthesis mediated by new isolates of *Bacillus* spp., nanoparticle characterization and their activity against Bean Yellow Mosaic Virus and human pathogens, Front. Microbiol. 6 (2015) 453.
[39] T. Ahmad, M. Irfan, M.A. Bustam, S. Bhattacharjee, Effect of reaction time on green synthesis of gold nanoparticles by using aqueous extract of *Elaise guineensis* (oil palm leaves), Procedia Eng. 148 (2016) 467–472.
[40] A.O. Dada, A.A. Inyinbor, E.I. Idu, O.M. Bello, A.P. Oluyori, T.A. Adelani-Akande, et al., Effect of operational parameters, characterization and antibacterial studies of green synthesis of silver nanoparticles using *Tithonia diversifolia*, PeerJ 6 (2018) e5865.
[41] O.A. Yeshchenko, I.S. Bondarchuk, V.S. Gurin, I.M. Dmitruk, A.V. Kotko, Temperature dependence of the surface plasmon resonance in gold nanoparticles, Surf. Sci. 608 (2013) 275–281.
[42] M.S. Latif, F. Kormin, M.K. Mustafa, I.I. Mohamad, M. Khan, S. Abbas, et al., Effect of temperature on the synthesis of *Centella asiatica* flavonoids ext*ract-mediated gol*d nanoparticles: UV-visible spectra analyses, AIP Conference Proceedings 2016 (1) (September 2018) 020071 (AIP Publishing LLC).
[43] H.M. Kredy, The effect of pH, temperature on the green synthesis and biochemical activities of silver nanoparticles from *Lawsonia inermis* extract, J. Pharm. Sci. Res. 10 (8) (2018) 2022–2026.
[44] L. Biswas, A. Mahtab, A.K. Verma, Pharmacokinetics and *in vivo* evaluation of nanoparticles, in: Nanoparticle Therapeutics, Academic Press, 2022, pp. 265–289.

[45] X. Li, S.C. Lee, S. Zhang, T. Akasaka, Biocompatibility and toxicity of nanobiomaterials 2014, J. Nanomater. 2015 (2015).
[46] S. Naahidi, M. Jafari, F. Edalat, K. Raymond, A. Khademhosseini, P. Chen, Biocompatibility of engineered nanoparticles for drug delivery, J. Contr. Release 166 (2) (2013) 182–194.
[47] M.J.H. Dowlath, S.A. Musthafa, S.M. Khalith, S. Varjani, S.K. Karuppannan, G.M. Ramanujam, et al., Comparison of characteristics and biocompatibility of green synthesized iron oxide nanoparticles with chemical synthesized nanoparticles, Environ. Res. 201 (2021) 111585.
[48] P. Singh, A. Garg, S. Pandit, V.R.S.S. Mokkapati, I. Mijakovic, Antimicrobial effects of biogenic nanoparticles, Nanomaterials 8 (12) (2018) 1009.
[49] A. Lateef, J.A. Elegbede, P.O. Akinola, V.A. Ajayi, Biomedical applications of green synthesized-metallic nanoparticles: a review, Pan Afr. J. Life Sci. 3 (2019) 157–182.
[50] A.K. Barui, S. Das, C.R. Patra, Biomedical applications of green-synthesized metal nanoparticles using polysaccharides, in: Functional Polysaccharides for Biomedical Applications, Woodhead Publishing, 2019, pp. 329–355.
[51] K.X. Lee, K. Shameli, Y.P. Yew, S.Y. Teow, H. Jahangirian, R. Rafiee-Moghaddam, T.J. Webster, Recent developments in the facile bio-synthesis of gold nanoparticles (AuNPs) and their biomedical applications, Int. J. Nanomed. 15 (2020) 275.
[52] Y. Zhang, W.C. Ruder, P.R. LeDuc, Artificial cells: building bioinspired systems using small-scale biology, Trends Biotechnol. 26 (1) (2008) 14–20.
[53] M. Thapa, S.R. Choudhury, Green synthesized nanoparticles: physicochemical properties and mode of antimicrobial activities, Compr. Anal. Chem. 94 (2021) 49–79.
[54] J.S. Moodley, S.B.N. Krishna, K. Pillay, P. Govender, Green synthesis of metal nanoparticles for antimicrobial activity, Novel Nanomater. (2020) 253–278.
[55] L. Wang, C. Hu, L. Shao, The antimicrobial activity of nanoparticles: present situation and prospects for the future, Int. J. Nanomed. 12 (2017) 1227.
[56] J. McCauley, A. Zivanovic, D. Skropeta, Bioassays for anticancer activities, in: Metabolomics Tools for Natural Product Discovery, Humana Press, Totowa, NJ, 2013, pp. 191–205.
[57] S. Jabeen, R. Qureshi, M. Munazir, M. Maqsood, M. Munir, S.S.H. Shah, B.Z. Rahim, Application of green synthesized silver nanoparticles in cancer treatment—a critical review, Mater. Res. Express 8 (9) (2021) 092001.
[58] A. Patel, J. Patel, Anti-cancer activity of eco-friendly gold nanoparticles against lung and liver cancer cells, in: Handbook of Lung Targeted Drug Delivery Systems, CRC Press, 2021, pp. 483–495.
[59] S.S. Salem, A. Fouda, Green synthesis of metallic nanoparticles and their prospective biotechnological applications: an overview, Biol. Trace Elem. Res. 199 (1) (2021) 344–370.
[60] H.I. Gomes, C.S. Martins, J.A. Prior, Silver nanoparticles as carriers of anticancer drugs for efficient target treatment of cancer cells, Nanomaterials 11 (4) (2021) 964.
[61] Z. Bedlovičová, I. Strapáč, M. Baláž, A. Salayová, A brief overview on antioxidant activity determination of silver nanoparticles, Molecules 25 (14) (2020) 3191.
[62] J.M. Lü, P.H. Lin, Q. Yao, C. Chen, Chemical and molecular mechanisms of antioxidants: experimental approaches and model systems, J. Cell Mol. Med. 14 (4) (2010) 840–860.
[63] L. Valgimigli, A. Baschieri, R. Amorati, Antioxidant activity of nanomaterials, J. Mater. Chem. B 6 (14) (2018) 2036–2051.
[64] Y. Liu, K. Ai, X. Ji, D. Askhatova, R. Du, L. Lu, J. Shi, Comprehensive insights into the multi-antioxidative mechanisms of melanin nanoparticles and their application to protect brain from injury in ischemic stroke, J. Am. Chem. Soc. 139 (2) (2017) 856–862.
[65] I. Khalil, W.A. Yehye, A.E. Etxeberria, A.A. Alhadi, S.M. Dezfooli, N.B.M. Julkapli, et al., Nanoantioxidants: recent trends in antioxidant delivery applications, Antioxidants 9 (1) (2019) 24.
[66] I. Ghlichloo, V. Gerriets, Nonsteroidal anti-inflammatory drugs (NSAIDs), in: StatPearls, StatPearls Publishing, Treasure Island (FL), 2022. https://www.ncbi.nlm.nih.gov/books/NBK547742.
[67] C. Tyavambiza, A.M. Elbagory, A.M. Madiehe, M. Meyer, S. Meyer, The antimicrobial and anti-inflammatory effects of silver nanoparticles synthesised from *Cotyledon orbiculata* aqueous extract, Nanomaterials 11 (5) (2021) 1343.
[68] H. Agarwal, A. Nakara, V.K. Shanmugam, Anti-inflammatory mechanism of various metal and metal oxide nanoparticles synthesized using plant extracts: a review, Biomed. Pharmacother. 109 (2019) 2561–2572.

[69] H. Agarwal, V. Shanmugam, A review on anti-inflammatory activity of green synthesized zinc oxide nanoparticle: mechanism-based approach, Bioorg. Chem. 94 (2020) 103423.
[70] D. Rehana, D. Mahendiran, R.S. Kumar, A.K. Rahiman, *In vitro* antioxidant and antidiabetic activities of zinc oxide nanoparticles synthesized using different plant extracts, Bioprocess Biosyst. Eng. 40 (6) (2017) 943–957.
[71] R.G. Saratale, H.S. Shin, G. Kumar, G. Benelli, D.S. Kim, G.D. Saratale, Exploiting antidiabetic activity of silver nanoparticles synthesized using *Punica granatum* leaves and anticancer potential against human liver cancer cells (HepG2), Artif. Cell Nanomed. Biotechnol. 46 (1) (2018) 211–222.
[72] M. Bhardwaj, P. Yadav, S. Dalal, S.K. Kataria, A review on ameliorative green nanotechnological approaches in diabetes management, Biomed. Pharmacother. 127 (2020) 110198.
[73] S. Hamdan, I. Pastar, S. Drakulich, E. Dikici, M. Tomic-Canic, S. Deo, S. Daunert, Nanotechnology-driven therapeutic interventions in wound healing: potential uses and applications, ACS Cent. Sci. 3 (3) (2017) 163–175.
[74] S. Kanimozhi, R. Durga, M. Sabithasree, A.V. Kumar, A. Sofiavizhimalar, A.A. Kadam, et al., Biogenic synthesis of silver nanoparticle using *Cissus quadrangularis* extract and its invitro study, J. King Saud Univ. Sci. 34 (4) (2022) 101930.
[75] B. Paul, B. Bhuyan, D.D. Purkayastha, S. Vadivel, S.S. Dhar, One-pot green synthesis of gold nanoparticles and studies of their anticoagulative and photocatalytic activities, Mater. Lett. 185 (2016) 143–147.
[76] B.S. Harish, K.B. Uppuluri, V. Anbazhagan, Synthesis of fibrinolytic active silver nanoparticle using wheat bran xylan as a reducing and stabilizing agent, Carbohydr. Polym. 132 (2015) 104–110.
[77] L.H. Madkour, Ecofriendly green biosynthesized of metallic nanoparticles: bio-reduction mechanism, characterization and pharmaceutical applications in biotechnology industry, Drugs Ther 3 (2017) 1–11.
[78] M. Ovais, A.T. Khalil, N.U. Islam, I. Ahmad, M. Ayaz, M. Saravanan, et al., Role of plant phytochemicals and microbial enzymes in biosynthesis of metallic nanoparticles, Appl. Microbiol. Biotechnol. 102 (16) (2018) 6799–6814.
[79] P.G. Jamkhande, N.W. Ghule, A.H. Bamer, M.G. Kalaskar, Metal nanoparticles synthesis: an overview on methods of preparation, advantages and disadvantages, and applications, J. Drug Deliv. Sci. Technol. 53 (2019) 101174.
[80] Z. Alhalili, Green synthesis of copper oxide nanoparticles CuO NPs from *Eucalyptus globoulu*s leaf extract: adsorption and design of experiments, Arab. J. Chem. 15 (5) (2022) 103739.
[81] D. Sharma, S. Kanchi, K. Bisetty, Biogenic synthesis of nanoparticles: a review, Arab. J. Chem. 12 (8) (2019) 3576–3600.
[82] R. Javed, M. Zia, S. Naz, S.O. Aisida, Q. Ao, Role of capping agents in the application of nanoparticles in biomedicine and environmental remediation: recent trends and future prospects, J. Nanobiotechnol. 18 (1) (2020) 1–15.
[83] S.J. Begum, S. Pratibha, J.M. Rawat, D. Venugopal, P. Sahu, A. Gowda, et al., Recent advances in green synthesis, characterization, and applications of bioactive metallic nanoparticles, Pharmaceuticals 15 (4) (2022) 455.
[84] H. Bahrulolum, S. Nooraei, N. Javanshir, H. Tarrahimofrad, V.S. Mirbagheri, A.J. Easton, G. Ahmadian, Green synthesis of metal nanoparticles using microorganisms and their application in the agrifood sector, J. Nanobiotechnol. 19 (1) (2021) 1–26.
[85] K.I. Alsamhary, Eco-friendly synthesis of silver nanoparticles by *Bacillus subtilis* and their antibacterial activity, Saudi J. Biol. Sci. 27 (8) (2020) 2185–2191.
[86] A. Banerjee, D. Das, R. Andler, R. Bandopadhyay, Green synthesis of silver nanoparticles using exopolysaccharides produced by *Bacillus anthracis* PFAB2 and its biocidal property, J. Polym. Environ. 29 (8) (2021) 2701–2709.
[87] S.M. Syame, A.S. Mansour, D.D. Khalaf, E.S. Ibrahim, E.S. Gaber, Green synthesis of silver nanoparticles using lactic acid bacteria: assessment of antimicrobial activity, World's Vet. J. (WVJ) 10 (2020) 625–633.
[88] Q.A. Naseer, X. Xue, X. Wang, S. Dang, S.U. Din, J. Jamil, Synthesis of silver nanoparticles using *Lactobacillus bulgaricus* and assessment of their antibacterial potential, Braz. J. Biol. 82 (2021).

[89] S. Sudarsan, M. Kumar Shankar, A. Kumar Belagal Motatis, S. Shankar, D. Krishnappa, C.D. Mohan, et al., Green synthesis of silver nanoparticles by *Cytobacillus firmus* isolated from the stem bark of *Terminalia arjuna* and their antimicrobial activity, Biomolecules 11 (2) (2021) 259.
[90] L. Muthukrishnan, M. Chellappa, A. Nanda, S. Thukkaram, G. Selvaraj, B. Muthiah, et al., Biofabrication of pigment-capped silver nanoparticles encountering antibiotic-resistant strains and their cytotoxic effect towards human epidermoid larynx carcinoma (HEp-2) cells, RSC Adv. 9 (28) (2019) 15874–15886.
[91] S. Patil, M. Sastry, A. Bharde, Size and shape directed novel green synthesis of plasmonic nanoparticles using bacterial metabolites and their anticancer effects, Front. Microbiol. 13 (2022).
[92] S.S. Pallavi, H.A. Rudayni, A. Bepari, S.K. Niazi, S. Nayaka, Green synthesis of Silver nanoparticles using *Streptomyces hirsutus* strain SNPGA-8 and their characterization, antimicrobial activity, and anticancer activity against human lung carcinoma cell line A549, Saudi J. Biol. Sci. 29 (1) (2022) 228–238.
[93] M.A. Huq, Green synthesis of silver nanoparticles using *Pseudoduganella eburnea* MAHUQ-39 and their antimicrobial mechanisms investigation against drug resistant human pathogens, Int. J. Mol. Sci. 21 (4) (2020) 1510.
[94] C.W. Johnston, M.A. Wyatt, X. Li, A. Ibrahim, J. Shuster, G. Southam, N.A. Magarvey, Gold biomineralization by a metallophore from a gold-associated microbe, Nat. Chem. Biol. 9 (4) (2013) 241–243.
[95] B. Syed, N.M. Prasad, S. Satish, Endogenic mediated synthesis of gold nanoparticles bearing bactericidal activity, J. Microsc. Ultrastruct. 4 (3) (2016) 162–166.
[96] T. Bennur, Z. Khan, R. Kshirsagar, V. Javdekar, S. Zinjarde, Biogenic gold nanoparticles from the Actinomycete *Gordonia amarae*: application in rapid sensing of copper ions, Sensor. Actuators B Chem. 233 (2016) 684–690.
[97] M. Składanowski, M. Wypij, D. Laskowski, P. Golińska, H. Dahm, M. Rai, Silver and gold nanoparticles synthesized from *Streptomyces* sp. isolated from acid forest soil with special reference to its antibacterial activity against pathogens, J. Cluster Sci. 28 (1) (2017) 59–79.
[98] M.P. Patil, M.J. Kang, I. Niyonizigiye, A. Singh, J.O. Kim, Y.B. Seo, G.D. Kim, Extracellular synthesis of gold nanoparticles using the marine bacterium *Paracoccus haeundaensis* BC74171T and evaluation of their antioxidant activity and antiproliferative effect on normal and cancer cell lines, Colloids Surf. B Biointerfaces 183 (2019) 110455.
[99] R.K. Thakur, P. Shirkot, Exploration of Western Himalayan region for identification of gold nanoparticles synthesizing bacteria, bioRxiv (2017) 164103.
[100] P. Yong, N.A. Rowson, J.P.G. Farr, I.R. Harris, L.E. Macaskie, Bioaccumulation of palladium by *Desulfovibrio desulfuricans*, J. Chem. Technol. Biotechnol. 77 (5) (2002) 593–601.
[101] M. Schlüter, T. Hentzel, C. Suarez, M. Koch, W.G. Lorenz, L. Böhm, et al., Synthesis of novel palladium (0) nanocatalysts by microorganisms from heavy-metal-influenced high-alpine sites for dehalogenation of polychlorinated dioxins, Chemosphere 117 (2014) 462–470.
[102] M.D. Yates, R.D. Cusick, B.E. Logan, Extracellular palladium nanoparticle production using Geobacter sulfurreducens, ACS Sustain. Chem. Eng. 1 (9) (2013) 1165–1171.
[103] J.B. Omajali, I.P. Mikheenko, M.L. Merroun, J. Wood, L.E. Macaskie, Characterization of intracellular palladium nanoparticles synthesized by *Desulfovibrio desulfuricans* and *Bacillus benzeovorans*, J. Nanopart. Res. 17 (6) (2015) 1–17.
[104] Q. Lv, B. Zhang, X. Xing, Y. Zhao, R. Cai, W. Wang, Q. Gu, Biosynthesis of copper nanoparticles using *Shewanella loihica* PV-4 with antibacterial activity: novel approach and mechanisms investigation, J. Hazard Mater. 347 (2018) 141–149.
[105] M. Noman, T. Ahmed, S. Hussain, M.B.K. Niazi, M. Shahid, F. Song, Biogenic copper nanoparticles synthesized by using a copper-resistant strain *Shigella flexneri* SNT22 reduced the translocation of cadmium from soil to wheat plants, J. Hazard Mater. 398 (2020) 123175.
[106] B.T. Abd-Elhalim, G. RF, A.T. Kh A, H. AA, Biosynthesis of Copper nanoparticles using bacterial supernatant optimized with certain agro-industrial byproducts, Novel Res. Microbiol. J. 3 (6) (2019) 558–578.

[107] M.S. John, J.A. Nagoth, M. Zannotti, R. Giovannetti, A. Mancini, K.P. Ramasamy, et al., Biogenic synthesis of copper nanoparticles using bacterial strains isolated from an antarctic consortium associated to a psychrophilic marine ciliate: characterization and potential application as antimicrobial agents, Mar. Drugs 19 (5) (2021) 263.
[108] N. Ghasemi, F. Jamali-Sheini, R. Zekavati, CuO and Ag/CuO nanoparticles: biosynthesis and antibacterial properties, Mater. Lett. 196 (2017) 78–82.
[109] K. Siddique, M. Shahid, T. Shahzad, F. Mahmood, H. Nadeem, M. Saif ur Rehman, et al., Comparative efficacy of biogenic zinc oxide nanoparticles synthesized by *Pseudochrobactrum* sp. C5 and chemically synthesized zinc oxide nanoparticles for catalytic degradation of dyes and wastewater treatment, Environ. Sci. Pollut. Control Ser. 28 (22) (2021) 28307–28318.
[110] Z.S. Mahdi, F. Talebnia Roshan, M. Nikzad, H. Ezoji, Biosynthesis of zinc oxide nanoparticles using bacteria: a study on the characterization and application for electrochemical determination of bisphenol A, Inorg. Nano-Met. Chem. 51 (9) (2021) 1249–1257.
[111] G.K. Ağçeli, H. Hammachi, S.P. Kodal, N. Cihangir, Z. Aksu, A novel approach to synthesize $TiO_2$ nanoparticles: biosynthesis by using *Streptomyces* sp. HC1, J. Inorg. Organomet. Polym. Mater. 30 (8) (2020) 3221–3229.
[112] M. Taran, M. Rad, M. Alavi, Biosynthesis of $TiO_2$ and ZnO nanoparticles by *Halomonas elongata* IBRC-M 10214 in different conditions of medium, Bioimpacts 8 (2) (2018) 81.
[113] K. Pollmann, J. Raff, M. Merroun, K. Fahmy, S. Selenska-Pobell, Metal binding by bacteria from uranium mining waste piles and its technological applications, Biotechnol. Adv. 24 (1) (2006) 58–68.
[114] V. Ahluwalia, J. Kumar, R. Sisodia, N.A. Shakil, S. Walia, Green synthesis of silver nanoparticles by *Trichoderma harzianum* and their bio-efficacy evaluation against *Staphylococcus aureus* and *Klebsiella pneumonia*, Ind. Crops Prod. 55 (2014) 202–206.
[115] R.M. Elamawi, R.E. Al-Harbi, A.A. Hendi, Biosynthesis and characterization of silver nanoparticles using *Trichoderma longibrachiatum* and their effect on phytopathogenic fungi, Egypt. J. Biol. Pest Control 28 (1) (2018) 1–11.
[116] S. Hamedi, M. Ghaseminezhad, S. Shokrollahzadeh, S.A. Shojaosadati, Controlled biosynthesis of silver nanoparticles using nitrate reductase enzyme induction of filamentous fungus and their antibacterial evaluation, Artif. Cell Nanomed. Biotechnol. 45 (8) (2017) 1588–1596.
[117] K. AbdelRahim, S.Y. Mahmoud, A.M. Ali, K.S. Almaary, A.E.Z.M. Mustafa, S.M. Husseiny, Extracellular biosynthesis of silver nanoparticles using *Rhizopus stolonifer*, Saudi J. Biol. Sci. 24 (1) (2017) 208–216.
[118] A. Shahzad, H. Saeed, M. Iqtedar, S.Z. Hussain, A. Kaleem, R. Abdullah, et al., Size-controlled production of silver nanoparticles by *Aspergillus fumigatus* BTCB10: likely antibacterial and cytotoxic effects, J. Nanomater. 2019 (2019).
[119] S.J. Ashrafi, M.F. Rastegar, M. Ashrafi, F. Yazdian, R. Pourrahim, A.K. Suresh, Influence of external factors on the production and morphology of biogenic silver nanocrystallites, J. Nanosci. Nanotechnol. 13 (3) (2013) 2295–2301.
[120] G.K. Rose, R. Soni, P. Rishi, S.K. Soni, Optimization of the biological synthesis of silver nanoparticles using *Penicillium oxalicum* GRS-1 and their antimicrobial effects against common food-borne pathogens, Green Process. Synth. 8 (1) (2019) 144–156.
[121] K.S. Almaary, S.R. Sayed, O.H. Abd-Elkader, T.M. Dawoud, N.F. El Orabi, A.M. Elgorban, Complete green synthesis of silver-nanoparticles applying seed-borne *Penicillium duclauxii*, Saudi J. Biol. Sci. 27 (5) (2020) 1333–1339.
[122] D. Wang, B. Xue, L. Wang, Y. Zhang, L. Liu, Y. Zhou, Fungus-mediated green synthesis of nano-silver using *Aspergillus sydowii* and its antifungal/antiproliferative activities, Sci. Rep. 11 (1) (2021) 1–9.
[123] Z.P. Qiao, M.Y. Wang, J.F. Liu, Q.Z. Wang, Green synthesis of silver nanoparticles using a novel endophytic fungus *Letendraea* sp. WZ07: characterization and evaluation of antioxidant, antibacterial and catalytic activities (3-in-1 system), Inorg. Chem. Commun. 138 (2022) 109301.
[124] A. Sharma, A. Sagar, J. Rana, R. Rani, Green synthesis of silver nanoparticles and its antibacterial activity using fungus *Talaromyces purpureogenus* isolated from Taxus baccata Linn, Micro Nano Syst. Lett. 10 (1) (2022) 1–12.

[125] C.G. Joshi, A. Danagoudar, J. Poyya, A.K. Kudva, B.L. Dhananjaya, Biogenic synthesis of gold nanoparticles by marine endophytic fungus-*Cladosporium cladosporioides* isolated from seaweed and evaluation of their antioxidant and antimicrobial properties, Process Biochem. 63 (2017) 137–144.
[126] P. Clarance, B. Luvankar, J. Sales, A. Khusro, P. Agastian, J.C. Tack, et al., Green synthesis and characterization of gold nanoparticles using endophytic fungi *Fusarium solani* and its *in-vitro* anticancer and biomedical applications, Saudi J. Biol. Sci. 27 (2) (2020) 706–712.
[127] Z. Molnár, V. Bódai, G. Szakacs, B. Erdélyi, Z. Fogarassy, G. Sáfrán, et al., Green synthesis of gold nanoparticles by thermophilic filamentous fungi, Sci. Rep. 8 (1) (2018) 1–12.
[128] K. Gupta, T.S. Chundawat, Zinc oxide nanoparticles synthesized using *Fusarium oxysporum* to enhance bioethanol production from rice-straw, Biomass Bioenergy 143 (2020) 105840.
[129] J.L. Sharma, V. Dhayal, R.K. Sharma, White-rot fungus mediated green synthesis of zinc oxide nanoparticles and their impregnation on cellulose to develop environmental friendly antimicrobial fibers, 3 Biotech 11 (6) (2021) 1–10.
[130] S. Noor, Z. Shah, A. Javed, A. Ali, S.B. Hussain, S. Zafar, et al., A fungal based synthesis method for copper nanoparticles with the determination of anticancer, antidiabetic and antibacterial activities, J. Microbiol. Methods 174 (2020) 105966.
[131] M.A.A. Abboud, A Novel Biological Approach to Copper Nanoparticles Synthesis: Characterization and its Application against Phytopathogenic Fungi, 2021.
[132] V.F. Consolo, A. Torres-Nicolini, V.A. Alvarez, Mycosinthetized Ag, CuO and ZnO nanoparticles from a promising *Trichoderma harzianum* strain and their antifungal potential against important phytopathogens, Sci. Rep. 10 (1) (2020) 1–9.
[133] E. Castro-Longoria, S.D. Moreno-Velasquez, A.R. Vilchis-Nestor, E. Arenas-Berumen, M. Avalos-Borja, Production of platinum nanoparticles and nanoaggregates using *Neurospora crassa*, J. Microbiol. Biotechnol. 22 (7) (2012) 1000–1004.
[134] K. Gupta, T.S. Chundawat, Bio-inspired synthesis of platinum nanoparticles from fungus *Fusarium oxysporum*: its characteristics, potential antimicrobial, antioxidant and photocatalytic activities, Mater. Res. Express 6 (10) (2019) 1050d6.
[135] G. Rajakumar, A.A. Rahuman, S.M. Roopan, V.G. Khanna, G. Elango, C. Kamaraj, et al., Fungus-mediated biosynthesis and characterization of TiO2 nanoparticles and their activity against pathogenic bacteria, Spectrochim. Acta Mol. Biomol. Spectrosc. 91 (2012) 23–29.
[136] M. Şahin, A.Y. Demir, T.Y. Koç, M. Güllüce, Extracellular biosynthesis and characterization of titanium dioxide nanoparticles ($TiO_2$) by using *Aspergillus* sp. TK4, Anatol. J. Biol. 1 (1) (2020) 8–11.
[137] S. Rehman, R. Jermy, S.M. Asiri, M.A. Shah, R. Farooq, V. Ravinayagam, et al., Using *Fomitopsis pinicola* for bioinspired synthesis of titanium dioxide and silver nanoparticles, targeting biomedical applications, RSC Adv. 10 (53) (2020) 32137–32147.
[138] S. Mohana, S. Sumathi, Multi-functional biological effects of palladium nanoparticles synthesized using *Agaricus bisporus*, J. Cluster Sci. 31 (2) (2020) 391–400.
[139] T. Kathiraven, A. Sundaramanickam, N. Shanmugam, T. Balasubramanian, Green synthesis of silver nanoparticles using marine algae *Caulerpa racemosa* and their antibacterial activity against some human pathogens, Appl. Nanosci. 5 (4) (2015) 499–504.
[140] S. Husain, M. Sardar, T. Fatma, Screening of cyanobacterial extracts for synthesis of silver nanoparticles, World J. Microbiol. Biotechnol. 31 (8) (2015) 1279–1283.
[141] N.E.A. El-Naggar, M.H. Hussein, S.A. Shaaban-Dessuuki, S.R. Dalal, Production, extraction and characterization of *Chlorella vulgaris* soluble polysaccharides and their applications in AgNPs biosynthesis and biostimulation of plant growth, Sci. Rep. 10 (1) (2020) 1–19.
[142] J. Jena, N. Pradhan, B.P. Dash, P.K. Panda, B.K. Mishra, Pigment mediated biogenic synthesis of silver nanoparticles using diatom *Amphora* sp. and its antimicrobial activity, J. Saudi Chem. Soc. 19 (6) (2015) 661–666.
[143] R.A. Hamouda, M.H. Hussein, R.A. Abo-Elmagd, S.S. Bawazir, Synthesis and biological characterization of silver nanoparticles derived from the cyanobacterium *Oscillatoria limnetica*, Sci. Rep. 9 (1) (2019) 1–17.
[144] N. González-Ballesteros, M.C. Rodríguez-Argüelles, M. Lastra-Valdor, G. González-Mediero, S. Rey-Cao, M. Grimaldi, et al., Synthesis of silver and gold nanoparticles by *Sargassum muticum*

biomolecules and evaluation of their antioxidant activity and antibacterial properties, J. Nanostruct. Chem. 10 (4) (2020) 317–330.
[145] P. Balaraman, B. Balasubramanian, D. Kaliannan, M. Durai, H. Kamyab, S. Park, et al., Phycosynthesis of silver nanoparticles mediated from marine algae *Sargassum myriocystum* and its potential biological and environmental applications, Waste Biomass Valorization 11 (10) (2020) 5255–5271.
[146] M. Ramakrishna, D. Rajesh Babu, R.M. Gengan, S. Chandra, G. Nageswara Rao, Green synthesis of gold nanoparticles using marine algae and evaluation of their catalytic activity, J. Nanostruct. Chem. 6 (1) (2016) 1–13.
[147] N. Abdel-Raouf, N.M. Al-Enazi, I.B. Ibraheem, Green biosynthesis of gold nanoparticles using *Galaxaura elongata* and characterization of their antibacterial activity, Arab. J. Chem. 10 (2017) S3029–S3039.
[148] N.M. El-Deeb, S.M. Khattab, M.A. Abu-Youssef, A. Badr, Green synthesis of novel stable biogenic gold nanoparticles for breast cancer therapeutics via the induction of extrinsic and intrinsic pathways, Sci. Rep. 12 (1) (2022) 1–18.
[149] H.P. Borase, C.D. Patil, R.K. Suryawanshi, S.H. Koli, B.V. Mohite, G. Benelli, S.V. Patil, Mechanistic approach for fabrication of gold nanoparticles by Nitzschia diatom and their antibacterial activity, Bioprocess Biosyst. Eng. 40 (10) (2017) 1437–1446.
[150] A. Arya, K. Gupta, T.S. Chundawat, D. Vaya, Biogenic synthesis of copper and silver nanoparticles using green alga Botryococcus braunii and its antimicrobial activity, Bioinorg. Chem. Appl. 2018 (2018).
[151] H.Y. El-Kassas, M.A.E.A. Okbah, Phytotoxic effects of seaweed mediated copper nanoparticles against the harmful alga: *Lyngbya majuscula*, J. Genet. Eng. Biotechnol. 15 (1) (2017) 41–48.
[152] K. Araya-Castro, T.C. Chao, B. Durán-Vinet, C. Cisternas, G. Ciudad, O. Rubilar, Green synthesis of copper oxide nanoparticles using protein fractions from an aqueous extract of Brown Algae *Macrocystis pyrifera*, Processes 9 (1) (2020) 78.
[153] E.F. El-Belely, M.M. Farag, H.A. Said, A.S. Amin, E. Azab, A.A. Gobouri, A. Fouda, Green synthesis of zinc oxide nanoparticles (ZnO-NPs) using *Arthrospira platensis* (class: Cyanophyceae) and evaluation of their biomedical activities, Nanomaterials 11 (1) (2021) 95.
[154] T. Khalafi, F. Buazar, K. Ghanemi, Phycosynthesis and enhanced photocatalytic activity of zinc oxide nanoparticles toward organosulfur pollutants, Sci. Rep. 9 (1) (2019) 1–10.
[155] Z. Sanaeimehr, I. Javadi, F. Namvar, Antiangiogenic and antiapoptotic effects of green-synthesized zinc oxide nanoparticles using *Sargassum muticum* algae extraction, Cancer Nanotechnol. 9 (1) (2018) 1–16.
[156] H. Sonbol, F. Ameen, S. AlYahya, A. Almansob, S. Alwakeel, *Padina boryana* mediated green synthesis of crystalline palladium nanoparticles as potential nanodrug against multidrug resistant bacteria and cancer cells, Sci. Rep. 11 (1) (2021) 1–19.
[157] V.S. Ramkumar, A. Pugazhendhi, S. Prakash, N.K. Ahila, G. Vinoj, S. Selvam, et al., Synthesis of platinum nanoparticles using seaweed *Padina gymnospora* and their catalytic activity as PVP/PtNPs nanocomposite towards biological applications, Biomed. Pharmacother. 92 (2017) 479–490.
[158] M. Sharma, K. Behl, S. Nigam, M. Joshi, $TiO_2$-GO nanocomposite for photocatalysis and environmental applications: a green synthesis approach, Vacuum 156 (2018) 434–439.
[159] S.J. bakht Dalir, H. Djahaniani, F. Nabati, M. Hekmati, Characterization and the evaluation of antimicrobial activities of silver nanoparticles biosynthesized from *Carya illinoinensis* leaf extract, Heliyon 6 (3) (2020) e03624.
[160] A. Rautela, J. Rani, Green synthesis of silver nanoparticles from *Tectona grandis* seeds extract: characterization and mechanism of antimicrobial action on different microorganisms, J. Anal. Sci. Technol. 10 (1) (2019) 1–10.
[161] S. Kulkarni, M. Jadhav, P. Raikar, D.A. Barretto, S.K. Vootla, U.S. Raikar, Green synthesized multifunctional $Ag@Fe_2O_3$ nanocomposites for effective antibacterial, antifungal and anticancer properties, New J. Chem. 41 (17) (2017) 9513–9520.
[162] S. Samuggam, S.V. Chinni, P. Mutusamy, S.C. Gopinath, P. Anbu, V. Venugopal, et al., Green synthesis and characterization of silver nanoparticles using *Spondias mombin* extract and their antimicrobial activity against biofilm-producing bacteria, Molecules 26 (9) (2021) 2681.

[163] A. Baraka, S. Dickson, M. Gobara, G.S. El-Sayyad, M. Zorainy, M.I. Awaad, et al., Synthesis of silver nanoparticles using natural pigments extracted from Alfalfa leaves and its use for antimicrobial activity, Chem. Pap. 71 (11) (2017) 2271–2281.
[164] H. Mahmoodi Esfanddarani, A. Abbasi Kajani, A.K. Bordbar, Green synthesis of silver nanoparticles using flower extract of *Malva sylvestris* and investigation of their antibacterial activity, IET Nanobiotechnol. 12 (4) (2018) 412–416.
[165] S. Mathew, C.P. Victorio, J. Sidhi, B.T. BH, Biosynthesis of silver nanoparticle using flowers of *Calotropis gigantea* (L.) WT Aiton and activity against pathogenic bacteria, Arab. J. Chem. 13 (12) (2020) 9139–9144.
[166] S. Chinnappan, S. Kandasamy, S. Arumugam, K.K. Seralathan, S. Thangaswamy, G. Muthusamy, Biomimetic synthesis of silver nanoparticles using flower extract of *Bauhinia purpurea* and its antibacterial activity against clinical pathogens, Environ. Sci. Pollut. Control Ser. 25 (1) (2018) 963–969.
[167] M.G. González-Pedroza, L. Argueta-Figueroa, R. García-Contreras, Y. Jiménez-Martínez, E. Martínez-Martínez, S.A. Navarro-Marchal, et al., Silver nanoparticles from *Annona muricata* peel and leaf extracts as a potential potent, biocompatible and low cost antitumor tool, Nanomaterials 11 (5) (2021) 1273.
[168] M. Ponnanikajamideen, S. Rajeshkumar, M. Vanaja, G. Annadurai, In vivo type 2 diabetes and wound-healing effects of antioxidant gold nanoparticles synthesized using the insulin plant *Chamaecostus cuspidatus* in albino rats, Can. J. Diabetes 43 (2) (2019) 82–89.
[169] D.A. Lomelí-Rosales, A. Zamudio-Ojeda, O.K. Reyes-Maldonado, M.E. López-Reyes, G.C. Basulto-Padilla, E.J. Lopez-Naranjo, et al., Green synthesis of gold and silver nanoparticles using leaf extract of *Capsicum chinense* plant, Molecules 27 (5) (2022) 1692.
[170] K.P. Shejawal, D.S. Randive, S.D. Bhinge, M.A. Bhutkar, S.S. Todkar, A.S. Mulla, Jadhav, Tomato: their characterization and cytotoxicity against COLO320DM, HT29 and Hella cell, J. Mater. Sci. Mater. Med. 32 (2) (2021) 1–12.
[171] N.M. Santos, A.S. Gomes, D.G. Cavalcante, L.F. Santos, S.R. Teixeira, F.C. Cabrera, A.E. Job, Green synthesis of colloidal gold nanoparticles using latex from *Hevea brasiliensis* and evaluation of their *in vitro* cytotoxicity and genotoxicity, IET Nanobiotechnol. 13 (3) (2019) 307–315.
[172] J.K. Patra, K.H. Baek, Novel green synthesis of gold nanoparticles using *Citrullus lanatus* rind and investigation of proteasome inhibitory activity, antibacterial, and antioxidant potential, Int. J. Nanomed. 10 (2015) 7253.
[173] A. Happy, M. Soumya, S.V. Kumar, S. Rajeshkumar, R.D. Sheba, T. Lakshmi, V.D. Nallaswamy, Phyto-assisted synthesis of zinc oxide nanoparticles using *Cassia alata* and its antibacterial activity against *Escherichia coli*, Biochem. Biophys. Rep. 17 (2019) 208–211.
[174] J. Santhoshkumar, S.V. Kumar, S. Rajeshkumar, Synthesis of zinc oxide nanoparticles using plant leaf extract against urinary tract infection pathogen, Resour. Effic. Technol. 3 (4) (2017) 459–465.
[175] N.K. Rajendran, B.P. George, N.N. Houreld, H. Abrahamse, Synthesis of zinc oxide nanoparticles using *Rubus fairholmianus* root extract and their activity against pathogenic bacteria, Molecules 26 (10) (2021) 3029.
[176] M.S. Jadhav, S. Kulkarni, P. Raikar, D.A. Barretto, S.K. Vootla, U.S. Raikar, Green biosynthesis of CuO & Ag–CuO nanoparticles from *Malus domestica* leaf extract and evaluation of antibacterial, antioxidant and DNA cleavage activities, New J. Chem. 42 (1) (2018) 204–213.
[177] S. Wu, S. Rajeshkumar, M. Madasamy, V. Mahendran, Green synthesis of copper nanoparticles using *Cissus vitiginea* and its antioxidant and antibacterial activity against urinary tract infection pathogens, Artif. Cell Nanomed. Biotechnol. 48 (1) (2020) 1153–1158.
[178] S.M. Hunagund, V.R. Desai, J.S. Kadadevarmath, D.A. Barretto, S. Vootla, A.H. Sidarai, Biogenic and chemogenic synthesis of $TiO_2$ NPs via hydrothermal route and their antibacterial activities, RSC Adv. 6 (99) (2016) 97438–97444.
[179] M. Altaf, M.T. Zeyad, M.A. Hashmi, S. Manoharadas, S.A. Hussain, M.S.A. Abuhasil, M.A.M. Almuzaini, Effective inhibition and eradication of pathogenic biofilms by titanium dioxide nanoparticles synthesized using *Carum copticum* extract, RSC Adv. 11 (31) (2021) 19248–19257.
[180] B.K. Thakur, A. Kumar, D. Kumar, Green synthesis of titanium dioxide nanoparticles using *Azadirachta indica* leaf extract and evaluation of their antibacterial activity, South Afr. J. Bot. 124 (2019) 223–227.

[181] N. Rabiee, M. Bagherzadeh, M. Kiani, A.M. Ghadiri, *Rosmarinus officinalis* directed palladium nanoparticle synthesis: investigation of potential anti-bacterial, anti-fungal and Mizoroki-Heck catalytic activities, Adv. Powder Technol. 31 (4) (2020) 1402–1411.
[182] S. Vinodhini, B.S.M. Vithiya, T.A.A. Prasad, Green synthesis of palladium nanoparticles using aqueous plant extracts and its biomedical applications, J. King Saud Univ. Sci. 34 (4) (2022) 102017.
[183] T.V. Surendra, S.M. Roopan, M.V. Arasu, N.A. Al-Dhabi, G.M. Rayalu, RSM optimized *Moringa oleifera* peel extract for green synthesis of *M. oleifera* capped palladium nanoparticles with antibacterial and hemolytic property, J. Photochem. Photobiol. B Biol. 162 (2016) 550–557.
[184] R. Dobrucka, A. Romaniuk-Drapała, M. Kaczmarek, Evaluation of biological synthesized platinum nanoparticles using *Ononidis radix* extract on the cell lung carcinoma A549, Biomed. Microdevices 21 (3) (2019) 1–10.
[185] V. Kshtriya, B. Koshti, N. Gour, Green synthesized nanoparticles: classification, synthesis, characterization, and applications, Compr. Anal. Chem. 94 (2021) 173–222.
[186] C.P. Devatha, A.K. Thalla, Green synthesis of nanomaterials, in: Synthesis of Inorganic Nanomaterials, Woodhead Publishing, 2018, pp. 169–184.
[187] K. Akhtar, S.A. Khan, S.B. Khan, A.M. Asiri, Scanning electron microscopy: principle and applications in nanomaterials characterization, in: Handbook of Materials Characterization, Springer, Cham, 2018, pp. 113–145.
[188] R. Yang, S. He, J. Yi, Q. Hu, Nano-scale pore structure and fractal dimension of organic-rich Wufeng-Longmaxi shale from Jiaoshiba area, Sichuan Basin: investigations using FE-SEM, gas adsorption and helium pycnometry, Mar. Petrol. Geol. 70 (2016) 27–45.
[189] M. Joshi, A. Bhattacharyya, S.W. Ali, Characterization Techniques for Nanotechnology Applications in Textiles, 2008.
[190] M. Noruzi, Biosynthesis of gold nanoparticles using plant extracts, Bioprocess Biosyst. Eng. 38 (1) (2015) 1–14.
[191] D. Titus, E.J.J. Samuel, S.M. Roopan, Nanoparticle characterization techniques, in: Green Synthesis, Characterization and Applications of Nanoparticles, Elsevier, 2019, pp. 303–319.
[192] A. Zuber, M. Purdey, E. Schartner, C. Forbes, B. Van der Hoek, D. Giles, et al., Detection of gold nanoparticles with different sizes using absorption and fluorescence based method, Sensor. Actuators B Chem. 227 (2016) 117–127.
[193] M. Taha, M. Hassan, S. Essa, Y. Tartor, Use of Fourier transform infrared spectroscopy (FTIR) spectroscopy for rapid and accurate identification of yeasts isolated from human and animals, Int. J. Vet. Sci. Med. 1 (1) (2013) 15–20.
[194] G.B. Reddy, K.G. Mangatayaru, D.M. Reddy, S.B.N. Krishna, N. Golla, Biosynthesis and characterization methods of copper nanoparticles and their applications in the agricultural sector, in: Copper Nanostructures: Next-Generation of Agrochemicals for Sustainable Agroecosystems, Elsevier, 2022, pp. 45–80.
[195] S. Jaast, A. Grewal, Green synthesis of silver nanoparticles, characterization and evaluation of their photocatalytic dye degradation activity, Curr. Res. Green Sustain. Chem. 4 (2021) 100195.
[196] I. Khan, K. Saeed, I. Khan, Nanoparticles: properties, applications and toxicities, Arab. J. Chem. 12 (7) (2019) 908–931.
[197] A.V. Tugarova, P.V. Mamchenkova, Y.A. Dyatlova, A.A. Kamnev, FTIR and Raman spectroscopic studies of selenium nanoparticles synthesised by the bacterium *Azospirillum thiophilum*, Spectrochim. Acta Mol. Biomol. Spectrosc. 192 (2018) 458–463.
[198] J. Iqbal, B.A. Abbasi, T. Yaseen, S.A. Zahra, A. Shahbaz, S.A. Shah, et al., Green synthesis of zinc oxide nanoparticles using *Elaeagnus angustifolia* L. leaf extracts and their multiple *in vitro* biological applications, Sci. Rep. 11 (1) (2021) 1–13.
[199] S.K. Sivan, S.S. Shankar, A. Kandambath Padinjareveetil, R. Pilankatta, V.S. Kumar, B. Mathew, et al., Fabrication of a greener $TiO_2$@gum arabic-carbon paste electrode for the electrochemical detection of $Pb^{2+}$ ions in plastic toys, ACS Omega 5 (39) (2020) 25390–25399.
[200] R. Xu, Progress in nanoparticles characterization: sizing and zeta potential measurement, Particuology 6 (2) (2008) 112–115.

[201] C.F. Holder, R.E. Schaak, Tutorial on powder X-ray diffraction for characterizing nanoscale materials, ACS Nano 13 (7) (2019) 7359–7365.
[202] M. Khan, P. Karuppiah, H.Z. Alkhathlan, M. Kuniyil, M. Khan, S.F. Adil, M.R. Shaik, Green synthesis of silver nanoparticles using *Juniperus procera* extract: their characterization, and biological activity, Crystals 12 (3) (2022) 420.
[203] N. Hutchinson, Y. Wu, Y. Wang, M. Kanungo, A. DeBruine, E. Kroll, et al., Green synthesis of gold nanoparticles using upland cress and their biochemical characterization and assessment, Nanomaterials 12 (2021) 28.
[204] D.R. Baer, Guide to making XPS measurements on nanoparticles, J. Vac. Sci. Technol. Vac. Surf. Films 38 (3) (2020) 031201.
[205] G.R. Salunke, S. Ghosh, R.S. Kumar, S. Khade, P. Vashisth, T. Kale, et al., Rapid efficient synthesis and characterization of silver, gold, and bimetallic nanoparticles from the medicinal plant *Plumbago zeylanica* and their application in biofilm control, Int. J. Nanomed. 9 (2014) 2635.
[206] J. Stetefeld, S.A. McKenna, T.R. Patel, Dynamic light scattering: a practical guide and applications in biomedical sciences, Biophys. Rev. 8 (4) (2016) 409–427.
[207] M.S. Alwhibi, D.A. Soliman, M.A. Awad, A.B. Alangery, H. Al Dehaish, Y.A. Alwasel, Green synthesis of silver nanoparticles: characterization and its potential biomedical applications, Green Process. Synth. 10 (1) (2021) 412–420.
[208] K. Dulta, P. Chauhan, K. Thakur, P.K. Chauhan, Green synthesis characterization of silver oxide nanoparticles using Bergenia ciliata rhizome extract, AIP Conference Proceedings 2357 (1) (May 2022) 050009 (AIP Publishing LLC).
[209] A.W. Bauer, Antibiotic susceptibility testing by a standardized single disc method, Am. J. Clin. Pathol. 45 (1966) 149–158.
[210] G. Meroni, J.F. Soares Filipe, P.A. Martino, *In vitro* antibacterial activity of biological-derived silver nanoparticles: preliminary data, Vet. Sci. 7 (1) (2020) 12.
[211] D. Garibo, H.A. Borbón-Nuñez, J.N.D. de León, E. García Mendoza, I. Estrada, Y. Toledano-Magaña, et al., Green synthesis of silver nanoparticles using *Lysiloma acapulcensis* exhibit high-antimicrobial activity, Sci. Rep. 10 (1) (2020) 1–11.
[212] CLSI, Performance Standards for Antimicrobial Susceptibility Testing; Twenty-Second Informational Supplement, The Clinical and Laboratory Standards Institute, Wayne, PA, 2012.
[213] S.M. Hunagund, V.R. Desai, D.A. Barretto, M.S. Pujar, J.S. Kadadevarmath, S. Vootla, A.H. Sidarai, Photocatalysis effect of a novel green synthesis gadolinium doped titanium dioxide nanoparticles on their biological activities, J. Photochem. Photobiol. Chem. 346 (2017) 159–167.
[214] Clinical and Laboratory Standards Institute, Performance Standards for Antimicrobial Susceptibility Testing, CLSI supplement M100, 2017.
[215] H.M. Ibrahim, Green synthesis and characterization of silver nanoparticles using banana peel extract and their antimicrobial activity against representative microorganisms, J. Radiat. Res. Appl. Sci. 8 (3) (2015) 265–275.
[216] S. Renganathan, G.P.D. Geoprincy, P. Kalainila, Green synthesis of ecofriendly nanoparticles and their medical applications, in: V. Sivasubramaniam (Ed.), Environmental Sustainability Using Green Technologies, first ed., 2016, pp. 79–102.
[217] C. Bankier, Y. Cheong, S. Mahalingam, M. Edirisinghe, G. Ren, E. Cloutman-Green, L. Ciric, A comparison of methods to assess the antimicrobial activity of nanoparticle combinations on bacterial cells, PLoS One 13 (2) (2018) e0192093.
[218] S.S.D. Kumar, N.N. Houreld, E.M. Kroukamp, H. Abrahamse, Cellular imaging and bactericidal mechanism of green-synthesized silver nanoparticles against human pathogenic bacteria, J. Photochem. Photobiol. B Biol. 178 (2018) 259–269.
[219] B. Das, S.K. Dash, D. Mandal, T. Ghosh, S. Chattopadhyay, S. Tripathy, et al., Green synthesized silver nanoparticles destroy multidrug resistant bacteria via reactive oxygen species mediated membrane damage, Arab. J. Chem. 10 (6) (2017) 862–876.
[220] H. Li, Q. Chen, J. Zhao, K. Urmila, Enhancing the antimicrobial activity of natural extraction using the synthetic ultrasmall metal nanoparticles, Sci. Rep. 5 (1) (2015) 1–13.

[221] F. Armas, S. Pacor, E. Ferrari, F. Guida, T.A. Pertinhez, A.A. Romani, et al., Design, antimicrobial activity and mechanism of action of Arg-rich ultra-short cationic lipopeptides, PLoS One 14 (2) (2019) e0212447.
[222] P. Tippayawat, N. Phromviyo, P. Boueroy, A. Chompoosor, Green synthesis of silver nanoparticles in aloe vera plant extract prepared by a hydrothermal method and their synergistic antibacterial activity, PeerJ 4 (2016) e2589.
[223] A. Anwar, A. Masri, K. Rao, K. Rajendran, N.A. Khan, M.R. Shah, R. Siddiqui, Antimicrobial activities of green synthesized gums-stabilized nanoparticles loaded with flavonoids, Sci. Rep. 9 (1) (2019) 1–12.
[224] R. Vazquez-Muñoz, A. Meza-Villezcas, P.G.J. Fournier, E. Soria-Castro, K. Juarez-Moreno, A.L. Gallego-Hernández, et al., Enhancement of antibiotics antimicrobial activity due to the silver nanoparticles impact on the cell membrane, PLoS One 14 (11) (2019) e0224904.
[225] F.K. Alsammarraie, W. Wang, P. Zhou, A. Mustapha, M. Lin, Green synthesis of silver nanoparticles using turmeric extracts and investigation of their antibacterial activities, Colloids Surf. B Biointerfaces 171 (2018) 398–405.
[226] S. Chowdhury, A. Basu, S. Kundu, Green synthesis of protein capped silver nanoparticles from phytopathogenic fungus *Macrophomina phaseolina* (Tassi) Goid with antimicrobial properties against multidrug-resistant bacteria, Nanoscale Res. Lett. 9 (1) (2014) 1–11.
[227] D. Gerlier, N. Thomasset, Use of MTT colorimetric assay to measure cell activation, J. Immunol. Methods 94 (1–2) (1986) 57–63.
[228] S. Rajeshkumar, Anticancer activity of eco-friendly gold nanoparticles against lung and liver cancer cells, J. Genet. Eng. Biotechnol. 14 (1) (2016) 195–202.
[229] N.E.A. El-Naggar, M.H. Hussein, A.A. El-Sawah, Bio-fabrication of silver nanoparticles by phycocyanin, characterization, *in vitro* anticancer activity against breast cancer cell line and *in vivo* cytotxicity, Sci. Rep. 7 (1) (2017) 1–20.
[230] D. Acharya, S. Satapathy, P. Somu, U.K. Parida, G. Mishra, Apoptotic effect and anticancer activity of biosynthesized silver nanoparticles from marine algae *Chaetomorpha linum* extract against human colon cancer cell HCT-116, Biol. Trace Elem. Res. 199 (5) (2021) 1812–1822.
[231] M.M.R. Mollick, D. Rana, S.K. Dash, S. Chattopadhyay, B. Bhowmick, D. Maity, et al., Studies on green synthesized silver nanoparticles using *Abelmoschus esculentus* (L.) pulp extract having anticancer (*in vitro*) and antimicrobial applications, Arab. J. Chem. 12 (8) (2019) 2572–2584.
[232] N.K. Sahoo, M. Sahu, C.P. Pullaiah, K.S. Muralikrishna, *In vitro* anticancer activity of *Eclipta alba* whole plant extract on colon cancer cell HCT-116, BMC Complement. Med. Ther. 20 (1) (2020) 1–8.
[233] P. Kumari, A. Gupta, Assays to assess the proliferative behavior of cancer cells, in: Protocol Handbook for Cancer Biology, Academic Press, 2021, pp. 23–41.
[234] Z. Xu, Q. Feng, M. Wang, H. Zhao, Y. Lin, S. Zhou, Green biosynthesized silver nanoparticles with aqueous extracts of *Ginkgo biloba* induce apoptosis via mitochondrial pathway in cervical cancer cells, Front. Oncol. (2020) 2282.
[235] G.M. Sulaiman, A.T. Tawfeeq, A.S. Naji, Biosynthesis, characterization of magnetic iron oxide nanoparticles and evaluations of the cytotoxicity and DNA damage of human breast carcinoma cell lines, Artif. Cell Nanomed. Biotechnol. 46 (6) (2018) 1215–1229.
[236] N.P. Singh, M.T. McCoy, R.R. Tice, E.L. Schneider, A simple technique for quantitation of low levels of DNA damage in individual cells, Exp. Cell Res. 175 (1) (1988) 184–191.
[237] A.R. Collins, M. Ai-Guo, S.J. Duthie, The kinetics of repair of oxidative DNA damage (strand breaks and oxidised pyrimidines) in human cells, Mutat. Res. DNA Repair 336 (1) (1995) 69–77.
[238] S. Şimşek, A.A. Şüküroğlu, D. Yetkin, B. Özbek, D. Battal, R. Genç, DNA-damage and cell cycle arrest initiated anti-cancer potency of super tiny carbon dots on MCF7 cell line, Sci. Rep. 10 (1) (2020) 1–14.
[239] A. Elnady, N.M. Sorour, R.N. Abbas, Characterization, cytotoxicity, and genotoxicity properties of novel biomediated nanosized-silver by Egyptian *Streptomyces roseolus* for safe antimicrobial applications, World J. Microbiol. Biotechnol. 38 (3) (2022) 1–17.

[240] M. Singh, M. Kumar, S. Manikandan, N. Chandrasekaran, A. Mukherjee, A.K. Kumaraguru, Drug delivery system for controlled cancer therapy using physico-chemically stabilized bioconjugated gold nanoparticles synthesized from marine macroalgae, *Padina gymnospora*, J. Nanomed. Nanotechnol. (S5) (2014) 1.
[241] D. Wu, Z. Wang, M. Lin, Y. Shang, F. Wang, J. Zhou, et al., *In vitro* and *in vivo* antitumor activity of Cucurbitacin C, a novel natural product from cucumber, Front. Pharmacol. 10 (2019) 1287.
[242] D. Acharya, S. Satapathy, D.T.K. Dora, G. Mishra, Green synthesis of silver nanoparticles using *Enteromorpha compressa* and its *in vitro* anticancer potential against human colon cancer cells, Indian Assoc. Biomed. Sci. (IABMS) 39 (4) (2019) 587–594.
[243] E.S. Al-Sheddi, N.N. Farshori, M.M. Al-Oqail, S.M. Al-Massarani, Q. Saquib, R. Wahab, et al., Anticancer potential of green synthesized silver nanoparticles using extract of Nepeta deflersiana against human cervical cancer cells (HeLA), Bioinorg. Chem. Appl. 2018 (2018).
[244] I.G. Munteanu, C. Apetrei, Analytical methods used in determining antioxidant activity: a review, Int. J. Mol. Sci. 22 (7) (2021) 3380.
[245] F. Pilaquinga, J. Morey, L. Fernandez, P. Espinoza-Montero, M. Moncada-Basualto, J. Pozo-Martinez, et al., Determination of antioxidant activity by oxygen radical absorbance capacity (ORAC-FL), cellular antioxidant activity (CAA), electrochemical and microbiological analyses of silver nanoparticles using the aqueous leaf extract of *Solanum mammosum* L, Int. J. Nanomed. 16 (2021) 5879.
[246] S. Ansar, H. Tabassum, N.S. Aladwan, M. Naiman Ali, B. Almaarik, S. AlMahrouqi, et al., Eco friendly silver nanoparticles synthesis by *Brassica oleracea* and its antibacterial, anticancer and antioxidant properties, Sci. Rep. 10 (1) (2020) 1–12.
[247] H. Čížová, A. Lojek, L. Kubala, M. Číž, The effect of intestinal ischemia duration on changes in plasma antioxidant defense status in rats, Physiol. Res. 53 (2004) 523–531.
[248] A.H. Labulo, O.A. David, A.D. Terna, Green synthesis and characterization of silver nanoparticles using *Morinda lucida* leaf extract and evaluation of its antioxidant and antimicrobial activity, Chem. Pap. (2022) 1–13.
[249] J. Mussin, V. Robles-Botero, R. Casañas-Pimentel, F. Rojas, L. Angiolella, S. Martín-Martínez, G. Giusiano, Antimicrobial and cytotoxic activity of green synthesis silver nanoparticles targeting skin and soft tissue infectious agents, Sci. Rep. 11 (1) (2021) 1–12.
[250] A. Sudha, J. Jeyakanthan, P. Srinivasan, Green synthesis of silver nanoparticles using *Lippia nodiflora* aerial extract and evaluation of their antioxidant, antibacterial and cytotoxic effects, Resour. Effic. Technol. 3 (4) (2017) 506–515.
[251] A.O. Akintola, B.D. Kehinde, P.B. Ayoola, A.G. Adewoyin, O.T. Adedosu, J.F. Ajayi, S.B. Ogunsona, Antioxidant properties of silver nanoparticles biosynthesized from methanolic leaf extract of Blighia sapida, IOP Conference Series: Materials Science and Engineering 805 (1) (March 2020) 012004 (IOP Publishing).
[252] B. Babu, S. Palanisamy, M. Vinosha, R. Anjali, P. Kumar, B. Pandi, et al., Bioengineered gold nanoparticles from marine seaweed *Acanthophora spicifera* for pharmaceutical uses: antioxidant, antibacterial, and anticancer activities, Bioproc. Biosyst. Eng. 43 (12) (2020) 2231–2242.
[253] A.R. Phull, Q. Abbas, A. Ali, H. Raza, M. Zia, I.U. Haq, Antioxidant, cytotoxic and antimicrobial activities of green synthesized silver nanoparticles from crude extract of *Bergenia ciliata*, Future J. Pharm. Sci. 2 (1) (2016) 31–36.
[254] S.K. Das, S. Behera, J.K. Patra, H. Thatoi, Green synthesis of sliver nanoparticles using *Avicennia officinalis* and *Xylocarpus granatum* extracts and *in vitro* evaluation of antioxidant, antidiabetic and anti-inflammatory activities, J. Cluster Sci. 30 (4) (2019) 1103–1113.
[255] P. Sneha, S. Sheela, D.B. Manickam, *In-vitro* studies of bio-silver nanoparticles in cytotoxicity and anti-inflammatory, J. Complement. Med. Altern. Healthc. 7 (4) (2018) 01–10.
[256] P. Chirumamilla, S. Vankudoth, S.B. Dharavath, R. Dasari, S. Taduri, *In vitro* anti-inflammatory activity of green synthesized silver nanoparticles and leaf methanolic extract of Solanum khasianum Clarke, Proc. Natl. Acad. Sci. India B Biol. Sci. (2022) 1–7.

[257] L.Y. Yan, B.B. Qiu, T.T. Li, D.D. Wu, J.H. Zhu, D.B. Zhao, Green synthesis of silver nanoparticles from *Lonicera japonica* leaf extract and their anti-inflammatory and antibacterial effects, Micro. Nano Lett. 15 (2020) 90–95.
[258] P.B.E. Kedi, F.E.A. Meva, L. Kotsedi, E.L. Nguemfo, C.B. Zangueu, A.A. Ntoumba, et al., Eco-friendly synthesis, characterization, *in vitro* and *in vivo* anti-inflammatory activity of silver nanoparticle-mediated *Selaginella myosurus* aqueous extract, Int. J. Nanomed. 13 (2018) 8537.
[259] R.P. Pereira, R. Jadhav, A. Baghela, D.A. Barretto, In vitro assessment of Probiotic potential of *Saccharomyces cerevisiae* DABRP5 isolated from bollo batter, a traditional Goan fermented food, Probiotics Antimicrob. Proteins 13 (3) (2021) 796–808.
[260] V. Varadharaj, A. Ramaswamy, R. Sakthivel, R. Subbaiya, H. Barabadi, M. Chandrasekaran, M. Saravanan, Antidiabetic and antioxidant activity of green synthesized starch nanoparticles: an *in vitro* study, J. Cluster Sci. 31 (6) (2020) 1257–1266.
[261] U. Hossain, A.K. Das, S. Ghosh, P.C. Sil, An overview on the role of bioactive α-glucosidase inhibitors in ameliorating diabetic complications, Food Chem. Toxicol. 145 (2020) 111738.
[262] K. Balan, W. Qing, Y. Wang, X. Liu, T. Palvannan, Y. Wang, et al., Antidiabetic activity of silver nanoparticles from green synthesis using *Lonicera japonica* leaf extract, Rsc Adv. 6 (46) (2016) 40162–40168.
[263] I.A. Adelere, A. Lateef, A novel approach to the green synthesis of metallic nanoparticles: the use of agro-wastes, enzymes, and pigments, Nanotechnol. Rev. 5 (6) (2016) 567–587.
[264] J.A. Elegbede, A. Lateef, M.A. Azeez, T.B. Asafa, T.A. Yekeen, I.C. Oladipo, et al., Biofabrication of gold nanoparticles using xylanases through valorization of corncob by *Aspergillus niger* and *Trichoderma longibrachiatum*: antimicrobial, antioxidant, anticoagulant and thrombolytic activities, Waste Biomass Valorization 11 (3) (2020) 781–791.
[265] A.S. Grewal, K. Kumar, S. Redhu, S. Bhardwaj, Microwave assisted synthesis: a green chemistry approach, Int. Res. J. Pharmaceut. Appl. Sci. 3 (5) (2013) 278–285.
[266] C. Mellinas, A. Jiménez, M.D.C. Garrigós, Microwave-assisted green synthesis and antioxidant activity of selenium nanoparticles using *Theobroma cacao* L. bean shell extract, Molecules 24 (22) (2019) 4048.
[267] C. Mallikarjunaswamy, V. Lakshmi Ranganatha, R. Ramu, G. Nagaraju, Facile microwave-assisted green synthesis of ZnO nanoparticles: application to photodegradation, antibacterial and antioxidant, J. Mater. Sci. Mater. Electron. 31 (2) (2020) 1004–1021.
[268] D.L. Su, P.J. Li, M. Ning, G.Y. Li, Y. Shan, Microwave assisted green synthesis of pectin based silver nanoparticles and their antibacterial and antifungal activities, Mater. Lett. 244 (2019) 35–38.
[269] I. Jahan, F. Erci, I. Isildak, Microwave-assisted green synthesis of non-cytotoxic silver nanoparticles using the aqueous extract of *Rosa santana* (rose) petals and their antimicrobial activity, Anal. Lett. 52 (12) (2019) 1860–1873.
[270] A. Muthuvel, N.M. Said, M. Jothibas, K. Gurushankar, V. Mohana, Microwave-assisted green synthesis of nanoscaled titanium oxide: photocatalyst, antibacterial and antioxidant properties, J. Mater. Sci. Mater. Electron. 32 (18) (2021) 23522–23539.
[271] V.N. Anjana, M. Joseph, S. Francis, A. Joseph, E.P. Koshy, B. Mathew, Microwave assisted green synthesis of silver nanoparticles for optical, catalytic, biological and electrochemical applications, Artif. Cell Nanomed. Biotechnol. 49 (1) (2021) 438–449.
[272] N.S. Al-Radadi, Microwave assisted green synthesis of Fe@Au core-shell NPs magnetic to enhance olive oil efficiency on eradication of *Helicobacter pylori* (life preserver), Arab. J. Chem. (2022) 103685.
[273] K. Karthik, M. Shashank, V. Revathi, T. Tatarchuk, Facile microwave-assisted green synthesis of NiO nanoparticles from *Andrographis paniculata* leaf extract and evaluation of their photocatalytic and anticancer activities, Mol. Cryst. Liq. Cryst. (2019).
[274] A. Gagliardi, E. Giuliano, E. Venkateswararao, M. Fresta, S. Bulotta, V. Awasthi, D. Cosco, Biodegradable polymeric nanoparticles for drug delivery to solid tumors, Front. Pharmacol. 17 (2021).
[275] A. Bužarovska, S. Dinescu, A.D. Lazar, M. Serban, G.G. Pircalabioru, M. Costache, et al., Nanocomposite foams based on flexible biobased thermoplastic polyurethane and ZnO nanoparticles as potential wound dressing materials, Mater. Sci. Eng. C 104 (2019) 109893.

[276] S. Murali, S. Kumar, J. Koh, S. Seena, P. Singh, A. Ramalho, A.J. Sobral, Bio-based chitosan/gelatin/Ag@ZnO bionanocomposites: synthesis and mechanical and antibacterial properties, Cellulose 26 (9) (2019) 5347–5361.
[277] R.G. Saratale, G.D. Saratale, H.S. Shin, J.M. Jacob, A. Pugazhendhi, M. Bhaisare, G. Kumar, New insights on the green synthesis of metallic nanoparticles using plant and waste biomaterials: current knowledge, their agricultural and environmental applications, Environ. Sci. Pollut. Control Ser. 25 (11) (2018) 10164–10183.
[278] F. Ortega, F. Versino, O.V. López, M.A. García, Biobased composites from agro-industrial wastes and by-products, Emerg. Mater. (2021) 1–49.
[279] A. Lateef, M.A. Azeez, T.B. Asafa, T.A. Yekeen, A. Akinboro, I.C. Oladipo, et al., Cocoa pod husk extract-mediated biosynthesis of silver nanoparticles: its antimicrobial, antioxidant and larvicidal activities, J. Nanostruct. Chem. 6 (2) (2016) 159–169.
[280] K. Anand, R.M. Gengan, A. Phulukdaree, A. Chuturgoon, Agroforestry waste *Moringa oleifera* petals mediated green synthesis of gold nanoparticles and their anti-cancer and catalytic activity, J. Ind. Eng. Chem. 21 (2015) 1105–1111.
[281] R. Heydari, M. Rashidipour, Green synthesis of silver nanoparticles using extract of oak fruit hull (Jaft): synthesis and *in vitro* cytotoxic effect on MCF-7 cells, Int. J. Breast Cancer 2015 (2015).
[282] T. Khan, H. Jalal, K. Karam, M.A. Khan, Biodegradable gum: a green source for silver nanoparticles, in: Green Synthesis of Silver Nanomaterials, Elsevier, 2022, pp. 189–217.
[283] F.H. Zulkifli, F.S.J. Hussain, S.S. Zeyohannes, M.S.B.A. Rasad, M.M. Yusuff, A facile synthesis method of hydroxyethyl cellulose-silver nanoparticle scaffolds for skin tissue engineering applications, Mater. Sci. Eng. C 79 (2017) 151–160.
[284] C.E. Escárcega-González, J.A. Garza-Cervantes, A. Vázquez-Rodríguez, J.R. Morones-Ramírez, Bacterial exopolysaccharides as reducing and/or stabilizing agents during synthesis of metal nanoparticles with biomedical applications, Int. J. Polym. Sci. 2018 (2018).
[285] G. Sathiyanarayanan, K. Dineshkumar, Y.H. Yang, Microbial exopolysaccharide-mediated synthesis and stabilization of metal nanoparticles, Crit. Rev. Microbiol. 43 (6) (2017) 731–752.
[286] S. Audtarat, P. Hongsachart, T. Dasri, S. Chio-Srichan, S. Soontaranon, W. Wongsinlatam, S. Sompech, Green synthesis of silver nanoparticles loaded into bacterial cellulose for antimicrobial application, Nanocomposites (2022) 1–13.
[287] L.P. Silva, T.M. Pereira, C.C. Bonatto, Frontiers and perspectives in the green synthesis of silver nanoparticles, in: Green Synthesis, Characterization and Applications of Nanoparticles, Elsevier, 2019, pp. 137–164.
[288] L. Malassis, R. Dreyfus, R.J. Murphy, L.A. Hough, B. Donnio, C.B. Murray, One-step green synthesis of gold and silver nanoparticles with ascorbic acid and their versatile surface post-functionalization, RSC Adv. 6 (39) (2016) 33092–33100.
[289] M.N. Nadagouda, R.S. Varma, A greener synthesis of core (Fe, Cu)-shell (Au, Pt, Pd, and Ag) nanocrystals using aqueous vitamin C, Cryst. Growth Des. 7 (12) (2007) 2582–2587.
[290] H. Kumar, K. Bhardwaj, D.S. Dhanjal, E. Nepovimova, F. Şen, H. Regassa, et al., Fruit extract mediated green synthesis of metallic nanoparticles: a new avenue in pomology applications, Int. J. Mol. Sci. 21 (22) (2020) 8458.
[291] D. de Britto, M.R. de Moura, F.A. Aouada, F.G. Pinola, L.M. Lundstedt, O.B. Assis, L.H. Mattoso, Entrapment characteristics of hydrosoluble vitamins loaded into chitosan and N,N,N-trimethyl chitosan nanoparticles, Macromol. Res. 22 (12) (2014) 1261–1267.
[292] S.K. Vootla, C.C. Su, S.I. Masanakatti, Self-assembled nanoparticles prepared from Tasar *Antherea mylitta* silk sericin, in: Biomedical Applications of Natural Proteins, Springer, New Delhi, 2015, pp. 65–77.
[293] D. Gh, D. Kong, J. Gautrot, S.K. Vootla, Fabrication and characterization of conductive Conjugated polymer-coated Antheraea mylitta silk fibroin fibers for biomedical applications, Macromol. Biosci. 17 (7) (2017) 1600443.
[294] X. Wang, W. Gao, S. Xu, W. Xu, Luminescent fibers: in situ synthesis of silver nanoclusters on silk via ultraviolet light-induced reduction and their antibacterial activity, Chem. Eng. J. 210 (2012) 585–589.

[295] S. Xu, L. Yong, P. Wu, One-pot, green, rapid synthesis of flowerlike gold nanoparticles/reduced graphene oxide composite with regenerated silk fibroin as efficient oxygen reduction electrocatalysts, ACS Appl. Mater. Interfaces 5 (3) (2013) 654–662.
[296] A. Lateef, S.A. Ojo, J.A. Elegbede, The emerging roles of arthropods and their metabolites in the green synthesis of metallic nanoparticles, Nanotechnol. Rev. 5 (6) (2016) 601–622.
[297] P. Aramwit, N. Bang, J. Ratanavaraporn, S. Ekgasit, Green synthesis of silk sericin-capped silver nanoparticles and their potent anti-bacterial activity, Nanoscale Res. Lett. 9 (1) (2014) 1–7.
[298] A. Lateef, S.A. Ojo, M.A. Azeez, T.B. Asafa, T.A. Yekeen, A. Akinboro, et al., Cobweb as novel biomaterial for the green and eco-friendly synthesis of silver nanoparticles, Appl. Nanosci. 6 (6) (2016) 863–874.
[299] S.P. Vinay, G. Nagaraju, C.P. Chandrappa, N. Chandrasekhar, Hydrothermal synthesis of gold nanoparticles using spider cobweb as novel biomaterial: application to photocatalytic, Chem. Phys. Lett. 748 (2020) 137402.
[300] A. Lateef, M.A. Akande, S.A. Ojo, B.I. Folarin, E.B. Gueguim-Kana, L.S. Beukes, Paper wasp nest-mediated biosynthesis of silver nanoparticles for antimicrobial, catalytic, anticoagulant, and thrombolytic applications, 3 Biotech 6 (2) (2016) 1–10.
[301] E.R. Balasooriya, C.D. Jayasinghe, U.A. Jayawardena, R.W.D. Ruwanthika, R. Mendis de Silva, P.V. Udagama, Honey mediated green synthesis of nanoparticles: new era of safe nanotechnology, J. Nanomater. 2017 (2017).
[302] N.M. El-Deeb, I.M. El-Sherbiny, M.R. El-Aassara, E.E. Hafez, Novel trend in colon cancer therapy using silver nanoparticles synthesized by honey bee, J. Nanomed. Nanotechnol. 6 (2) (2015) 265.
[303] B. Barsola, P. Kumari, Green synthesis of nano-propolis and nanoparticles (Se and Ag) from ethanolic extract of propolis, their biochemical characterization: a review, Green Process. Synth. 11 (1) (2022) 659–673.
[304] R.H. Babu, P. Yugandhar, N. Savithramma, Synthesis, characterization and antimicrobial studies of bio silica nanoparticles prepared from *Cynodon dactylon* L.: a green approach, Bull. Mater. Sci. 41 (3) (2018) 1–8.
[305] K. Divya, M.S. Jisha, Chitosan nanoparticles preparation and applications, Environ. Chem. Lett. 16 (1) (2018) 101–112.
[306] P.W. Li, G. Wang, Z.M. Yang, W. Duan, Z. Peng, L.X. Kong, Q.H. Wang, Development of drug-loaded chitosan–vanillin nanoparticles and its cytotoxicity against HT-29 cells, Drug Deliv. 23 (1) (2016) 30–35.
[307] S.Y. Lee, J.S. Lim, M.T. Harris, Synthesis and application of virus-based hybrid nanomaterials, Biotechnol. Bioeng. 109 (1) (2012) 16–30.
[308] S.S. Ahiwale, A.V. Bankar, S. Tagunde, B.P. Kapadnis, A bacteriophage mediated gold nanoparticles synthesis and their anti-biofilm activity, Indian J. Microbiol. 57 (2) (2017) 188–194.
[309] R.M. Thangavelu, R. Ganapathy, P. Ramasamy, K. Krishnan, Fabrication of virus metal hybrid nanomaterials: an ideal reference for bio semiconductor, Arab. J. Chem. 13 (1) (2020) 2750–2765.
[310] B. Kang, M.A. Mackey, M.A. El-Sayed, Nuclear targeting of gold nanoparticles in cancer cells induces DNA damage, causing cytokinesis arrest and apoptosis, J. Am. Chem. Soc. 132 (5) (2010) 1517–1519.
[311] W.A. El-Said, H.Y. Cho, C.H. Yea, J.W. Choi, Synthesis of metal nanoparticles inside living human cells based on the intracellular formation process, Adv. Mater. 26 (6) (2014) 910–918.
[312] E. Larios-Rodriguez, C. Rangel-Ayon, S.J. Castillo, G. Zavala, R. Herrera-Urbina, Bio-synthesis of gold nanoparticles by human epithelial cells, in vivo, Nanotechnology 22 (35) (2011) 355601.
[313] A. Van de Walle, A.P. Sangnier, A. Abou-Hassan, A. Curcio, M. Hémadi, N. Menguy, et al., Biosynthesis of magnetic nanoparticles from nano-degradation products revealed in human stem cells, Proc. Natl. Acad. Sci. USA 116 (10) (2019) 4044–4053.
[314] A.A. Jazie, A.J. Albaaji, S.A. Abed, A review on recent trends of antiviral nanoparticles and airborne filters: special insight on COVID-19 virus, Air Qual. Atmos. Health 14 (11) (2021) 1811–1824.
[315] C. Karthik, K.A. Punnaivalavan, S.P. Prabha, D.G. Caroline, Multifarious global flora fabricated phytosynthesis of silver nanoparticles: a green nanoweapon for antiviral approach including SARS-CoV-2, Int. Nano Lett. (2022) 1–32.

[316] L. Rao, S. Xia, W. Xu, R. Tian, G. Yu, C. Gu, et al., Decoy nanoparticles protect against COVID-19 by concurrently adsorbing viruses and inflammatory cytokines, Proc. Natl. Acad. Sci. USA 117 (44) (2020) 27141–27147.
[317] Q. Tan, L. He, X. Meng, W. Wang, H. Pan, W. Yin, et al., Macrophage biomimetic nanocarriers for anti-inflammation and targeted antiviral treatment in COVID-19, J. Nanobiotechnol. 19 (1) (2021) 1–16.
[318] D.H. Le, K.L. Lee, S. Shukla, U. Commandeur, N.F. Steinmetz, Potato virus X, a filamentous plant viral nanoparticle for doxorubicin delivery in cancer therapy, Nanoscale 9 (6) (2017) 2348–2357.